Power Control and Resource Allocation for QoS-Constrained Wireless Networks

Ziqiang Feng

Computer Laboratory
University of Cambridge

This dissertation is submitted for the degree of
Doctor of Philosophy

Churchill College October 2017

Power Control and Resource Allocation for QoS-Constrained Wireless Networks

Ziqiang Feng

Developments such as machine-to-machine communications and multimedia services are placing growing demands on high-speed reliable transmissions and limited wireless spectrum resources. Although multiple-input multiple-output (MIMO) systems have shown the ability to provide reliable transmissions in fading channels, it is not practical for single-antenna devices to support MIMO system due to cost and hardware limitations. Cooperative communication allows single-antenna devices to share their spectrum resources and form a virtual MIMO system where their quality of service (QoS) may be improved via cooperation. Most cooperative communication solutions are based on fixed spectrum access schemes and thus cannot further improve spectrum efficiency. In order to support more users in the existing spectrum, we consider dynamic spectrum access schemes and cognitive radio techniques in this dissertation.

Our work includes the modelling, characterization and optimization of QoS-constrained cooperative networks and cognitive radio networks. QoS constraints such as delay and data rate are modelled. To solve power control and channel resource allocation problems, dynamic power control, matching theory and multi-armed bandit algorithms are employed in our investigations. In this dissertation, we first consider a cluster-based cooperative wireless network utilizing a centralized cooperation model. The dynamic power control and optimization problem is analyzed in this scenario. We then consider a cooperative cognitive radio network utilizing an opportunistic spectrum access model. Distributed spectrum access algorithms are proposed to help secondary users utilize vacant channels of primary users in order to optimize the total utility of the network. Finally, a noncooperative cognitive radio network utilizing the opportunistic spectrum access model is analyzed. In this model, primary users do not communicate with secondary users. Therefore, secondary users are required to find vacant channels on which to transmit. Multi-armed bandit algorithms are proposed to help secondary users predict the availability of licensed channels.

In summary, in this dissertation we consider both cooperative communication networks and cognitive radio networks with QoS constraints. Efficient power control and channel resource allocation schemes have been proposed for optimization problems in different scenarios.

Declaration

I hereby declare that except where specific reference is made to the work of others, the contents of this dissertation are original and have not been submitted in whole or in part for consideration for any other degree or qualification in this, or any other university. This dissertation is my own work and contains nothing which is the outcome of work done in collaboration with others, except as specified in the text and Acknowledgements. This dissertation contains fewer than 60,000 words including appendices, bibliography, footnotes, tables and equations and has fewer than 150 figures.

Ziqiang Feng
October 2017

Acknowledgements

First and foremost, I would like to thank my supervisor, Dr Ian Wassell, for his kind support and guidance throughout my PhD study. His patience, enthusiasm and encouragement have been a source of great inspiration to me. I also thank him for giving me the freedom to pursue my own research interests while keeping me on the right track. This work would not have been possible without his invaluable advice.

My sincere thanks go to my friends and labmates that have made my life memorable and enjoyable at Cambridge. Thanks to Hongfei Li, Shaoran Hu, Xiaoming Yu and Bingyan Yang, for the wonderful time and happiness we shared. Thanks to Chao Gao, Yu Wang, Xing Ding, Yang Liu, David Turner and Oliver Chick, for their kind help and valuable discussions in the research group.

I am also grateful to the Cambridge Overseas Trust, the China Scholarship Council and the Computer Laboratory, for sponsoring my research in the past four years.

Finally, I am greatly indebted to my family, who have always supported me and believed in me. I would like to thank my mom and dad, for their love and encouragement in my life since the day I was born. I would like to thank my wife, Menglin, for her great sacrifice and support during my PhD. I wouldn't have made it this far if it hadn't been for her.

Table of contents

List of figures

List of tables

List of acronyms

ACK	Acknowledgement
ACK-A	Acknowledgement of Acceptance
ACK-R	Acknowledgement of Refusal
ADC	Analog to Digital Converter
AE	Active Elimination
ARQ	Automatic Repeat Request
AT	Algorithm Termination
AWGN	Additive White Gaussian Noise
BER	Bit Error Rate
BP	Broadcast Phase
CAR	Channel Access Request
CDF	Cumulative Distribution Function
CP	Cooperation Phase
CR	Cognitive Radio
CRN	Cognitive Radio Network
CRWSN	Cognitive Radio Wireless Sensor Network
CSI	Channel State Information
D2D	Device-to-Device

DAC	Digital to Analog Converter
DM	Distributed Matching
DPC	Dynamic Power Control
DPCO	Dynamic Power Control and Optimization
FDM	Fast Distributed Matching
FIFO	First-In First-Out
IFA	Intermediate Frequency Amplifier
IR	Improved Reject
JCSPC	Joint Channel Sensing and Power Control
LIFO	Last-In First-Out
LNA	Low Noise Amplifier
LO	Local Oscillator
MIMO	Multiple-Input Multiple-Output
MISO	Multiple-Input Single-Output
PA	Power Amplifier
PAC	Probably Approximately Correct
PB	Priority-Based
PER	Packet Error Rate
PMF	Probability Mass Function
PR	Passive Rejection
PU	Primary User
QoS	Quality of Service
RA	Random Access
RCA	Random Channel Access

RD	Ready for Data
RFD	Reduced-Function Device
SISO	Single-Input Single-Output
SNR	Signal-to-Noise Ratio
SR	Simple Reject
STBC	Space-Time Block Code
SU	Secondary User
SVD	Singular Value Decomposition
TD	Threshold Detection
TDD	Time Division Duplex
UCB	Upper Confidence Bound
UPDA	User-Proposing Deferred Acceptance
UWB	Ultra-Wide-Band
WSN	Wireless Sensor Network

Chapter 1

Introduction

Developments such as machine-to-machine communications and multimedia services are placing growing demands for high data rate transmissions and are putting pressure on limited wireless spectrum resources. In order to improve the transmission quality and spectrum efficiency, innovative techniques such as cooperative communication [1] and cognitive radio [2] have been proposed.

1.1 Cooperative Communication

Multiple-input multiple-output (MIMO) systems have shown the ability to provide reliable transmissions in fading channels by exploiting spatial diversity with multiple antennas [3]. However, it is not practical for single-antenna devices to support MIMO systems due to cost and hardware limitations [4]. Cooperative communication allows single-antenna devices to share their spectrum resources and form a virtual MIMO system where their quality of service (QoS) may be improved via cooperation [5–7]. There are two network models proposed based on the concept of cooperative communication [1]:

1. **Centralized Cooperation Model:** In the centralized cooperation model, the cooperative transmission is controlled by the cluster heads. In the multi-hop architecture, all devices communicate through a cluster head. Each cluster head cooperatively transmits the data with multiple cooperative devices to the next cluster which provides cooperative gains compared to the noncooperative transmission. In this model, power control and cooperative node selection algorithms in general aim to optimize the total power consumption without violating QoS constraints.

2. **Decentralized Cooperation Model:** In the decentralized cooperation model, additional control information and channel parameters are carried in the transmission data.

Devices in the network are responsible for inferring the channel conditions and the transmission schedules through the additional information to form a random cooperative cluster. In this model, it is important to have efficient clustering protocols for reliable transmissions.

Both the centralized and decentralize models require cluster-based cooperation to form a virtual MIMO system. In the cluster-based virtual MIMO system, the cluster-to-cluster transmission in the time domain is divided into two phases, the broadcast phase and the cooperation phase. In the broadcast phase, the cluster head broadcasts its data within the cluster. In the cooperation phase, the cooperative devices decode the received data and forward it to the next cluster.

In this dissertation, we mainly focus on the centralized cooperation model and propose efficient algorithms for optimal power control and cooperative node selection subject to the data rate and channel capacity constraints. Although cooperative communication provides spatial diversity for single-antenna devices, most cooperative communication solutions are based on fixed spectrum access scheme and thus cannot further improve spectrum efficiency. In order to support more users in the existing spectrum, we also consider dynamic spectrum access schemes and cognitive radio techniques in this dissertation.

1.2 Cognitive Radio Networks

Traditional fixed spectrum access schemes face spectrum scarcity due to the limited availability of wireless spectrum and the increasing number of high data rate wireless devices. On the other hand, a large portion of the assigned spectrum experiences low utilization according to spectrum utilization measurements [8, 9]. In a cognitive radio network, a part of the spectrum is allocated to one or more primary users that have a higher priority to use the spectrum. In contrast to the fixed spectrum access scheme, spectrum resources are not allocated for exclusive use by the primary users. Secondary users, who have a lower priority compared to primary users, can exploit the allocated spectrum as long as they do not cause severe interference to primary users. In order to guarantee the performance of the primary users and support the dynamic spectrum access scheme, secondary users are required to monitor the spectrum usage using cognitive radio techniques. Such approaches may help secondary users detect vacant spectrum not being used by primary users or estimate the interference level at the primary user's receiver. Different cognitive radio techniques may have different cognitive capabilities available to monitor the spectrum. Depending on the assumptions made about the cognitive capabilities of secondary users, there are two common models employed in cognitive radio networks [10, 11]:

1. **Concurrent Spectrum Access Model:** In the concurrent spectrum access model, secondary users are allowed to transmit their data concurrently with primary users without causing severe interference to primary users. Secondary users equipped with cognitive radios should be able to monitor the spectrum and predict the interference power level at a particular location. In order to manage the interference power level and keep it below the interference threshold, secondary users can transmit their data over a wide bandwidth with low power density using ultra-wide-band (UWB) technology. In the concurrent spectrum access model, since the interference constraints are quite restrictive, in most cases, this means that secondary users are limited to short range communications.

2. **Opportunistic Spectrum Access Model:** In the opportunistic spectrum access model, secondary users seek transmission opportunities by detecting spectrum holes [12], and in particular secondary users can only transmit data on identified spectrum holes. Meanwhile, secondary users should monitor the spectrum and vacate it whenever the primary users become active. The utilization of spectrum is improved by opportunistic spectrum access in the spectrum holes [13]. In this model, secondary users should be able to detect and predict the activity of primary users.

In this dissertation, we mainly focus on the opportunistic spectrum access model of cognitive radio networks. We consider both the cooperative and noncooperative scenarios. In the cooperative scenario, primary users lease their vacant spectrum to secondary users to help secondary transmissions. Secondary users send their data transmission requirements to primary users once they detect spectrum holes and primary users allocate their vacant spectrum to secondary users to improve the network throughput and spectrum efficiency. In the noncooperative scenario, we assume no cooperation between primary users and secondary users. Secondary users are responsible for monitoring the spectrum and to avoid interfering excessively with primary users. The data of secondary users is opportunistically transmitted in spectrum holes.

1.3 Main Contributions and Dissertation Outline

This dissertation focuses on the design of efficient power control and resource allocation algorithms for QoS-constrained wireless networks for cooperative communication and cognitive radio techniques:

- In Chapter 2, the concept of QoS constraints such as wireless channel capacity and end-to-end delay are discussed in detail. We also introduce some methods on power control and resource allocation of wireless networks to facilitate understanding our work. These concepts and methods are used in the various scenarios presented in this study.

- In Chapter 3, we consider a cluster-based cooperative wireless network utilizing the centralized cooperation model. In this network, cooperative devices in each cluster help the cluster head to transmit its data to the next cluster. With the QoS constraints on single-hop outage capacity and multi-hop delay, we propose a dynamic power control algorithm that can minimize the total power consumption without violating the QoS constraints. To reduce the computational complexity of the dynamic power control algorithm, an approximate algorithm is proposed. The performance of the dynamic power control algorithm and the approximate algorithm are evaluated by simulation results. Most of the results in this chapter are published in the IEEE International Conference on Communications (ICC) 2016 conference proceedings [14].

- In Chapter 4, a cooperative cognitive radio network utilizing the opportunistic spectrum access model is studied. In this cognitive radio network, secondary users can send their data transmission requests to the primary users. Primary users allocate their vacant channels to secondary users to help secondary transmissions. Different secondary users may have different QoS requirement. In order to maximize the network throughput under the QoS constraints, we propose a distributed channel allocation algorithm based on matching theory. The proposed algorithm can match up the secondary users to the vacant channels of primary users which can meet the QoS requirements. We prove that the proposed algorithm has near-optimal performance and has a much lower computational complexity than the centralized solution. Most of the results in this chapter are published in the IEEE Global Communications Conference (GLOBECOM) 2016 conference proceedings [15].

- In Chapter 5, we investigate a noncooperative cognitive radio network utilizing the opportunistic spectrum access model. In this scenario, primary users do not communicate with secondary users. Secondary users are required to monitor the channels of primary users and opportunistically transmit their data through vacant channels. Since one secondary user can only sense part of the spectrum due to cost and hardware limitation, we propose a cooperative sensing method where secondary users share their sensing results and predict the primary users behaviour by utilizing the historical sensing results. In particular, three probably approximately correct (PAC) algorithms are proposed to predict the primary users behaviour and channel availability. All the algorithms can terminate in a finite time with a finite error rate. The performance of these algorithms are investigated via simulation results. Some of the results in this chapter are published in the Wireless Days (WD) 2017 conference proceedings [16].

- In Chapter 6, we summarize the main results of the dissertation and discuss future research directions.

Chapter 2

Background

2.1 Wireless Channel Capacity

In information theory, the channel capacity is the maximum data rate that can be reliably transmitted over a particular wireless channel assuming no constraints on delay [17]. Understanding different wireless channel models and their capacity are key factors for solving power control and resource allocation problems in wireless networks. In the following sections, the wireless channel models for single-input single-output (SISO) and for multiple-input multiple-output (MIMO) systems are presented.

2.1.1 SISO Channel Capacity

A block-fading SISO channel model with time-varying gain and additive white Gaussian noise (AWGN) is given in Fig. 2.1 [18].

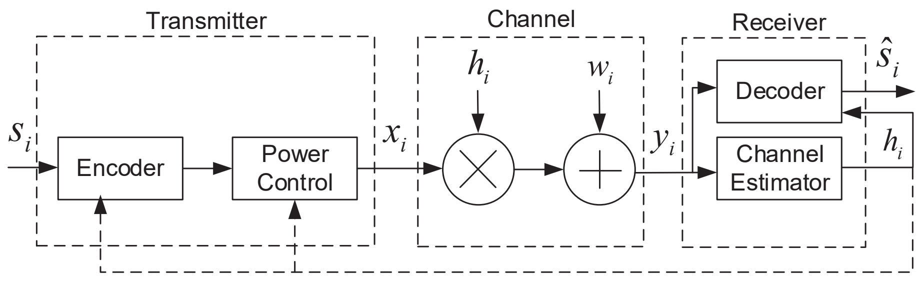

Fig. 2.1 A SISO channel model.

At time block i, the message s_i is encoded into the codeword x_i and transmitted over the time-varying channel with channel amplitude gain h_i and additive white Gaussian noise

(AWGN) w_i. In the block-fading channel model, channel amplitude h_i, also called the channel state information (CSI), is constant over some number of transmitted data blocks and changes as an independent and identically distributed (i.i.d.) process over time. The received signal y_i at time block i of the block-fading SISO channel is given by

$$y_i = h_i x_i + w_i. \tag{2.1}$$

Let P_i denote the average transmit signal power at time block i. The instantaneous signal-to-noise ratio (SNR) at time block i is then given by

$$\gamma_i = \frac{P_i |h_i|^2}{N_0 B} = \frac{P_i g_i}{N_0 B}, \tag{2.2}$$

where $\frac{N_0}{2}$ is the noise power spectral density of w_i, $g_i = |h_i|^2$ is the channel power gain and B is the received signal bandwidth. According to Shannon's theory [19], the instantaneous channel capacity of the block-fading channel at time block i is given by

$$C_i = B \log_2 (1 + \gamma_i). \tag{2.3}$$

In the block-fading SISO channel model, the CSI is assumed to be known at the receiver. The transmitter may obtain the CSI from the receiver if a feedback link exists between the transmitter and the receiver. We also assume that both the transmitter and receiver know the distribution of CSI. There are two channel capacity definitions that we are interested in, namely the ergodic capacity and the outage capacity.

Ergodic Capacity of SISO Channel Model

The ergodic capacity of a block-fading SISO channel is defined as the channel capacity averaged over the distribution of the instantaneous SNR γ [20]. Let $f(\gamma) = \Pr(\gamma_i = \gamma)$ denote the probability density function (PDF) of the SNR at the receiver. According to Equation (2.3), the ergodic capacity is expressed as

$$C_{erg}^{SISO} = \mathrm{E}_\gamma [B \log_2 (1+\gamma)] = \int_0^\infty B \log_2 (1+\gamma) f(\gamma) d\gamma. \tag{2.4}$$

Let $f(g) = \Pr(g_i = g)$ denote the PDF of the channel power gain. With the average power constraint $\mathrm{E}[P] \le \bar{P}$ where $\bar{P}$ is the power constraint, the channel capacity depends upon the assumptions concerning the transmitter CSI.

When no CSI is available at the transmitter, constant maximum power is allocated at any time to maximize the channel capacity. The ergodic capacity is thus given by

$$C_{erg}^{SISO} = \mathrm{E}_g \left[B\log_2 \left(1 + \frac{g\bar{P}}{N_0 B} \right) \right] = \int_0^\infty B\log_2 \left(1 + \frac{g\bar{P}}{N_0 B} \right) f(g)\, dg. \tag{2.5}$$

If perfect CSI is available at the transmitter, power is allocated adaptively according to the channel condition. With the average power constraint $\bar{P}$, the ergodic capacity is expressed as

$$C_{erg}^{SISO} = \max_{\mathrm{E}[P] \leq \bar{P}} \mathrm{E}_g \left[B\log_2 \left(1 + \frac{gP}{N_0 B} \right) \right]. \tag{2.6}$$

According to [18], the capacity in Equation (2.6) can be achieved if the message is properly encoded and decoded according to the CSI. The optimal power allocation strategy for Equation (2.6) is called the water-filling strategy and is given by

$$\frac{P}{N_0 B} = \left(\frac{1}{g_0} - \frac{1}{g} \right)^+, \tag{2.7}$$

where $(x)^+ = \max(0, x)$ and g_0 is found from the power constraint

$$\int_{g_0}^\infty \left(\frac{1}{g_0} - \frac{1}{g} \right) f(g)\, dg = \frac{\bar{P}}{N_0 B}. \tag{2.8}$$

From Equation (2.7), we know that the transmitter allocates more power to the good channel blocks and less power to bad channel blocks. The ergodic capacity based on the optimal power allocation is given by

$$C_{erg}^{SISO} = \int_{g_0}^\infty B\log_2 \left(\frac{g}{g_0} \right) f(g)\, dg. \tag{2.9}$$

More work on the ergodic capacity can be found in [21] and [22].

Outage Capacity of SISO Channel Model

The outage capacity is considered in slow-fading channels, where SNR γ remains constant over a long period of time before changing to a new value. When there is no CSI available at the transmitter, the transmission data rate is fixed and independent of the instantaneous SNR at the receiver. Therefore, messages received with poor SNR may be decoded incorrectly. Specifically, the outage capacity is defined as a fixed transmission data rate with minimum

SNR requirement which is expressed as

$$C_{out}^{SISO} = B\log_2(1+\gamma_{out}), \tag{2.10}$$

where γ_{out} is the minimum SNR requirement. Any bits received having an SNR lower than γ_{out} cannot be decoded correctly with a sufficiently high probability. The outage probability p_{out} is thus defined as $p_{out} = \Pr(\gamma < \gamma_{out})$. Given the definitions of outage capacity and outage probability, the average data rate that can be correctly received over time is obtained by

$$\bar{C}_{out}^{SISO} = (1-p_{out})C_{out}^{SISO} = (1-p_{out})B\log_2(1+\gamma_{out}). \tag{2.11}$$

For a Rayleigh fading channel with average SNR $\bar{\gamma} = 10$, the outage capacity versus outage probability is given in Fig. 2.2.

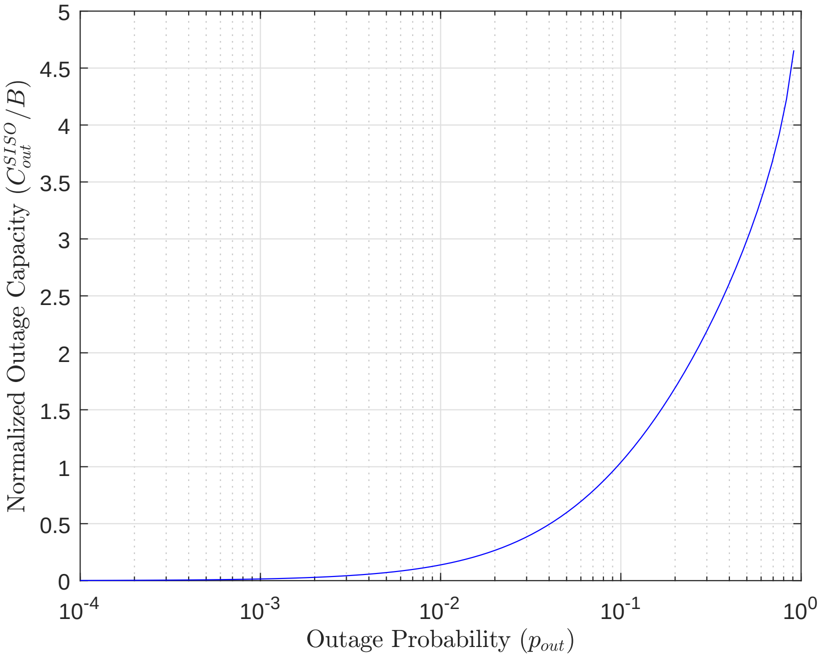

Fig. 2.2 Normalized outage capacity versus outage probability.

As shown in Fig. 2.2, the outage capacity increases as the outage probability increases. However, large outage capacity also has high outage probability and a high error rate in decoding received messages. Therefore, the average outage capacity in Equation (2.11) is used to represent the average data rate.

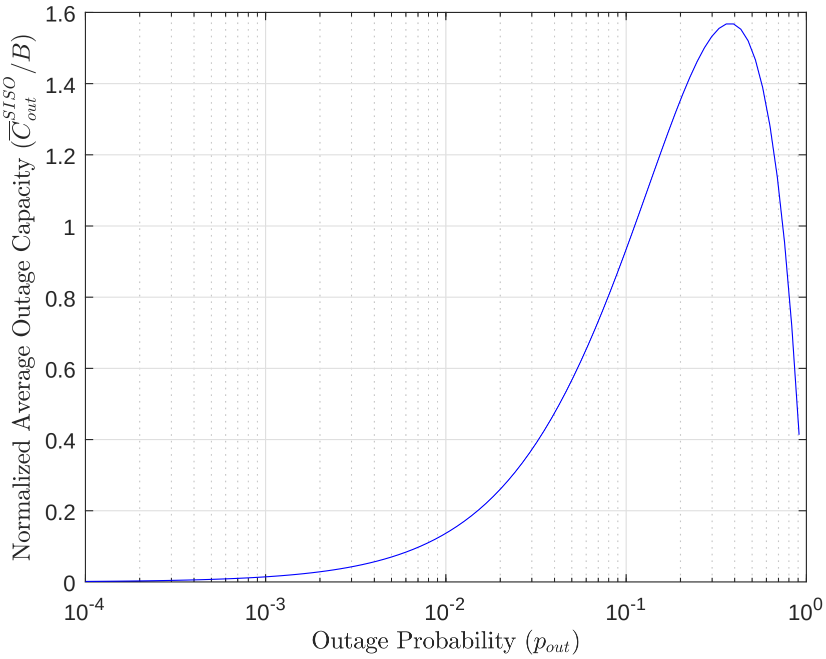

Fig. 2.3 Normalized average outage capacity versus outage probability.

The average outage capacity versus outage probability is given in Fig. 2.3. We see that the average data rate can be maximized by finding the outage probability that maximizes the average outage capacity. Existing work concerning the outage capacity can be found in [23] and [24].

2.1.2 MIMO Channel Capacity

A block-fading MIMO channel model with time-varying gain and additive white Gaussian noise (AWGN) is given in Fig. 2.4 [25]. We assume that the MIMO system has n_t transmit

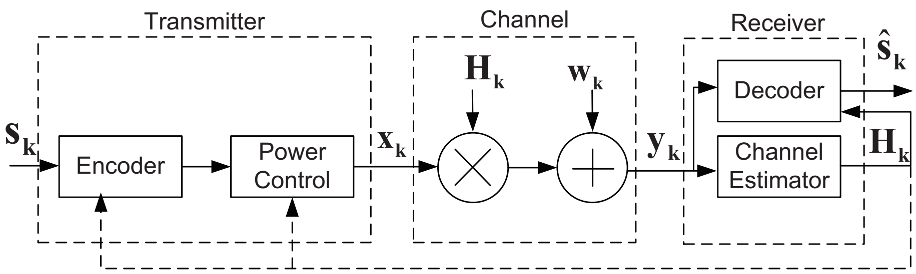

Fig. 2.4 A MIMO channel model.

antennas and n_r receive antennas. $\mathbf{H_k}$ is an $n_r \times n_t$ MIMO channel matrix, in which the element $h_{i,j}^{(k)}$ is the channel amplitude gain from transmit antenna j to receive antenna i at time block k. The received signal $\mathbf{y_k}$ at time block k of the MIMO channel model is given by [26]

$$\mathbf{y_k} = \mathbf{H_k x_k} + \mathbf{w_k} \tag{2.12}$$

where $\mathbf{y_k}$ is an $n_r \times 1$ vector of the received symbols, $\mathbf{x_k}$ is an $n_t \times 1$ vector of the transmitted symbols and $\mathbf{w_k}$ is an $n_r \times 1$ vector of noise. Elements in $\mathbf{w_k}$ are assumed to be additive white Gaussian noise (AWGN) and i.i.d. complex Gaussian variables with zero mean and unit variance for normalization. Let $P_k = \mathbf{x_k^H x_k}$ denote the average transmit signal power at time block k where $\mathbf{x_k^H}$ is the conjugate transpose of $\mathbf{x_k}$.

In the block-fading MIMO channel model, the CSI is assumed to be known at the receiver. A feedback link between the transmitter and the receiver may exist for the transmitter to obtain the instantaneous CSI from the receiver. Both the transmitter and receiver are assumed to know the distribution of CSI. The ergodic capacity and the outage capacity are given respectively in the following sections.

Ergodic Capacity of MIMO Channel Model

We assume that the transmitter is subject to an average power constraint of $\mathrm{E}\left[\mathbf{x^H x}\right] \leq \bar{P}$. By definition, the ergodic capacity depends upon the assumptions made concerning the transmitter CSI [27].

With no CSI available at the transmitter, the optimum transmit strategy is to transmit in all spatial directions with equal power allocated in each transmit antenna [28, 29]. Thus the ergodic capacity is given by

$$C_{erg}^{MIMO} = \mathrm{E}_{\mathbf{H}} \left[B \log_2 \left| \mathbf{I}_{n_r} + \frac{\bar{P}\mathbf{HH^H}}{n_t N_0 B} \right| \right], \tag{2.13}$$

where $|\mathbf{X}|$ is the determinant of matrix $\mathbf{X}$. Further analyses of MIMO systems and MIMO channel models can be found in [28].

We assume that $n_t \geq n_r$ in the MIMO channel model. Thus $\mathbf{HH^H}$ is a $n_r \times n_r$ random non-negative definite matrix with real, non-negative eigenvalues. The n_r eigenvalues $(\lambda_1, \lambda_2, \ldots, \lambda_{n_r})$ of $\mathbf{HH^H}$ can be obtained from the singular value decomposition (SVD) of matrix $\mathbf{H}$. Thus, the capacity in Equation (2.13) can be expressed as

$$C_{erg}^{MIMO} = \mathrm{E}_{\lambda} \left[\sum_{i=1}^{n_r} B \log_2 \left(1 + \frac{\bar{P}\lambda_i}{n_t N_0 B} \right) \right]. \tag{2.14}$$

For the case of perfect CSI available at the transmitter, the ergodic capacity with power constraint $\sum_{i=1}^{n_r} \mathrm{E}[P_i] \leq \bar{P}$ is given by

$$C_{erg}^{MIMO} = \max_{\mathrm{E}[P] \leq \bar{P}} \mathrm{E}_{\lambda} \left[\sum_{i=1}^{n_r} B \log_2 \left(1 + \frac{P_i \lambda_i}{N_0 B} \right) \right]. \tag{2.15}$$

The adaptive power allocation strategy based on the water-filling policy is given in [26] as

$$\frac{P_i}{N_0 B} = \left[\frac{1}{\lambda_0} - \frac{1}{\lambda_i} \right]^{+}, \tag{2.16}$$

where λ_0 satisfies the power constraint

$$\sum_{i=1}^{n_r} \mathrm{E} \left[\left(\frac{1}{\lambda_0} - \frac{1}{\lambda_i} \right)^{+} \right] = \frac{\bar{P}}{N_0 B}. \tag{2.17}$$

Outage Capacity of MIMO Channel Model

In slow-fading MIMO channels, $\mathbf{H}$ is random but remains constant over a long period of time. With no CSI at the transmitter, the transmission data rate (outage capacity) C_{out}^{MIMO} is fixed and the receiver may incorrectly decode the messages having poor SNR. In this case, the transmit power is equally allocated to all transmit antennas. The outage probability of MIMO channel is defined as

$$p_{out} = \Pr \left(B \log_2 \left| \mathbf{I}_{n_r} + \frac{\bar{P} \mathbf{H} \mathbf{H}^{\mathbf{H}}}{n_t N_0 B} \right| < C_{out}^{MIMO} \right). \tag{2.18}$$

We are interested in the outage performance of MIMO channels at different values of SNR. Consider the i.i.d. Rayleigh fading channel as an example. At very low SNR, the conjecture is given in [26] that only one transmit antenna should be used. On the other hand, for high SNR cases, MIMO channels with i.i.d. Rayleigh fading are expected to yield a diversity gain of $n_t n_r$ in the outage performance. Similar to the SISO channel model, we are also interested in minimizing the outage probability and maximizing the average outage capacity of MIMO channel models. We will discuss these problems in detail in the following chapters.

2.2 Delay Analysis

In wireless networks, the end-to-end packet delay D generally consists four parts [30]:

1. **Transmission delay** $D^{(t)}$ is the time required for a packet's bits to be transmitted at the transmitter. $D^{(t)}$ is a function of the packet's length and the transmission data rate.

2. **Propagation delay** $D^{(p)}$ is the time required for a packet to travel from the source to the destination. $D^{(p)}$ is a function of the distance between the source and the destination.

3. **Signal processing delay** $D^{(s)}$ is the time for a packet to be processed at the receiver. $D^{(s)}$ is related to the hardware performance of the receiver.

4. **Queueing delay** $D^{(q)}$ is the time required for a packet to wait in the queue (buffer) until it can be sent by the transmitter. $D^{(q)}$ is related to the congestion level of the transmitter.

Thus, the end-to-end packet delay is expressed as

$$D = D^{(t)} + D^{(p)} + D^{(s)} + D^{(q)}. \tag{2.19}$$

Since the propagation delay and the processing delay are not strongly related to the infrastructure of wireless networks and are generally very small compared to the transmission delay and queueing delay, the end-to-end packet delay is usually expressed as

$$D = D^{(t)} + D^{(q)}. \tag{2.20}$$

In order to estimate the queueing delay and transmission delay of a packet, we analyze the queueing delay using queueing theory.

2.2.1 Queueing Theory

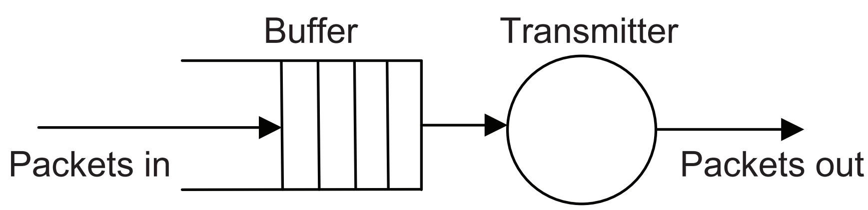

Fig. 2.5 A basic queueing model of a wireless source.

Queueing theory [31] has been widely used for decades to analyze the delay in wireless networks. A basic queueing model of a wireless source node is shown in Fig. 2.5. The queueing model consists of a buffer and a transmitter. The queueing model is characterized by four components [32]:

1. **Arrival process** describes how packets arrive at the buffer. The input process generally uses random variables to represent the number of arriving packets in a time interval.

2. **Service mechanism** describes how packets are transmitted at the transmitter. Random variables are used to describe the transmission time (delay) and the rate of a packet.

3. **System capacity** is the maximum number of packets that can wait at a time in the buffer.

4. **Queue discipline** is the rule to choose the packets from the buffer when the transmitter becomes free. The queue discipline can be "first-in, first-out" (FIFO), "last-in, first-out" (LIFO), "priority-based" (PB), etc.

In queueing theory, Kendall's notation [33] ($A/S/c$) is widely used to describe a queueing model where A denotes the arrival process, S the service mechanism and c the number of servers (transmitters). For example, using M for Poisson or exponential and D for deterministic, $M/D/1$ means that packets arrive according to a Poisson process and are transmitted by a single transmitter with deterministic (fixed) time.

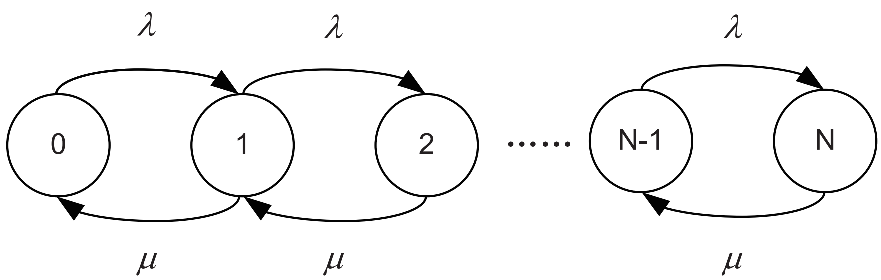

Fig. 2.6 State space diagram of $M/D/1$ queueing model.

By definition, an $M/D/1$ queueing model with FIFO discipline and infinite buffer size is a stochastic process whose state space is the set $\{0, 1, 2, \ldots\}$ where the value is the number of packets in the source node. We use λ to denote the packets arrival rate and μ to denote the packets service (transmission) rate. The state space diagram is shown is Fig. 2.6.

2.2.2 Delay Model with Queueing theory

The queueing model with a Poisson arrival process can be considered as a Markov process. It is clear that the arrival rate λ should be less than the service rate μ to make the model stable. With a stable model condition, the average number of packets in the source node, namely the queue length L, is given by the Pollaczek-Khinchin formula [34, 35]

$$L = \rho + \frac{\rho^2 + \lambda^2 \sigma^2}{2(1-\rho)} \tag{2.21}$$

where $\rho = \frac{\lambda}{\mu}$ is the load factor and σ^2 is the variance of the packet service (transmission) time ($\frac{1}{\mu}$).

In the $M/D/1$ queueing model, the service time is constant and thus the total number of packets in the source node is given by

$$L = \rho + \frac{\rho^2}{2(1-\rho)}. \tag{2.22}$$

The average waiting time of a packet in the source node is defined by $W = W^{(q)} + W^{(t)}$ where $W^{(q)}$ is the average waiting time in the queue (buffer) and $W^{(t)} = \mu^{-1}$ is the packet transmission rate. According to Little's Law [32], we have

$$L = \lambda W. \tag{2.23}$$

Thus, the average time waiting time of a packet in the source node is given by

$$W = \frac{1}{\mu} + \frac{\rho}{2\mu(1-\rho)}. \tag{2.24}$$

2.3 QoS Constraints

With the increasing number of delay and loss sensitive applications, it is important for wireless networks to provide reliable performance and to utilize limited wireless resources efficiently.

The quality of service (QoS) of a wireless application is a measurement of the performance of the application. Different applications may have different QoS requirements. There are typically four of QoS requirements that are given as follows:

1. **Delay requirement** is the maximum time allowed for a packet of data to travel from the transmitter to the receiver. The delay requirement is usually expressed as the end-to-end time delay.

2. **Throughput requirement** is the minimum amount of data required to be transmitted from the transmitter to the receiver in some specified unit of time. The throughput requirement is usually expressed as the required data rate.

3. **Error rate requirement** is the maximum fraction of packets that can be lost during the transmission from the transmitter to the receiver. The error rate requirement is usually expressed as the required bit error rate (BER) or the packet error rate (PER).

4. **Jitter requirement** is the maximum variation in the delay of the received packets. The jitter requirement is usually expressed as the difference between the maximum and the minimum end-to-end delay.

There are two types of QoS requirements, namely the hard requirements and the soft requirements [36]. For applications such as real-time industrial control systems, it is critical to guarantee the delay and error rate requirements of the packet transmissions. The QoS requirements of such applications are stringent and thus called the hard QoS requirements. On the other hand, applications such as multimedia streaming, web surfing and video services can tolerate a small probability of QoS violation. The QoS requirements of these applications can be flexible and are thus called the soft QoS requirements.

In this dissertation, we consider the soft QoS requirements in most scenarios as it is easy to define and is applicable to many applications. The QoS requirements of the delay, throughput and error rate are considered in various scenarios.

2.4 Power Control Analysis

2.4.1 Power Consumption Analysis

We now consider the power consumption of the transmitter and the receiver in detail. According to [37], the block diagrams of a typical transmitter and a receiver are given in Fig. 2.7 and Fig. 2.8 respectively.

For simplicity, we omit some blocks in the block diagrams such as the source coding block, the modulation block and so on. We first consider the power consumption of the transmitter.

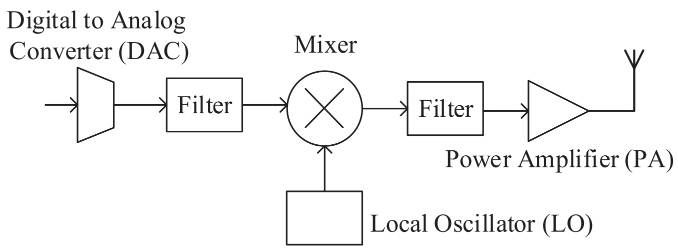

Fig. 2.7 A transmitter block diagram.

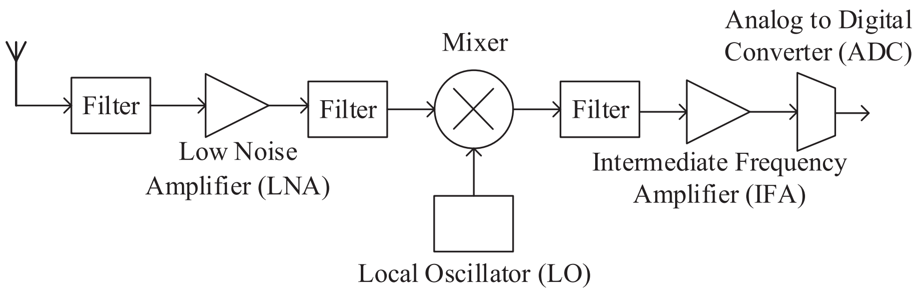

Fig. 2.8 A receiver block diagram.

The total power consumption of the transmitter is dominated by two parts: the power consumption during transmission owing to the power amplifier (PA) P_{PA} and the power consumption owing to the remaining circuits, $P_{Tx,cir}$. The transmission power consumption P_{PA} is related to the transmission power P_t and can be expressed as

$$P_t = \lambda P_{AP}, \tag{2.25}$$

where λ is the power amplifier efficiency constant related to the drain efficiency [38] and the peak-to-average ratio [39]. The circuit power consumption contains the power consumption of the rest parts of the transmitter which is expressed as

$$P_{Tx,cir} = P_{DAC} + P_{mixer} + P_{LO} + P_{filter}, \tag{2.26}$$

where P_{DAC}, P_{mixer}, P_{LO} and P_{filter} are the power consumption of the digital to analog converter (DAC), the mixer, the local oscillator (LO) and the filter, respectively.

The total power consumption of the receiver can be expressed as

$$P_{Rx,cir} = P_{ADC} + P_{IFA} + P_{mixer} + P_{filter} + P_{LO} + P_{LNA}, \tag{2.27}$$

where P_{ADC}, P_{IFA} and P_{LNA} are the power consumption of the analog to digital converter (ADC), the intermediate frequency amplifier (IFA) and the low noise amplifier (LNA), respectively.

In general, we mainly consider the power consumption of the transmitter in different wireless scenarios. For simplicity, we assume that the power amplifier efficiency is $\lambda = 1$ in this dissertation. Thus the total power consumption of the transmitter is given by

$$P_{Tx,total} = P_{AP} + P_{Tx,cir} = P_t + P_{Tx,cir}. \tag{2.28}$$

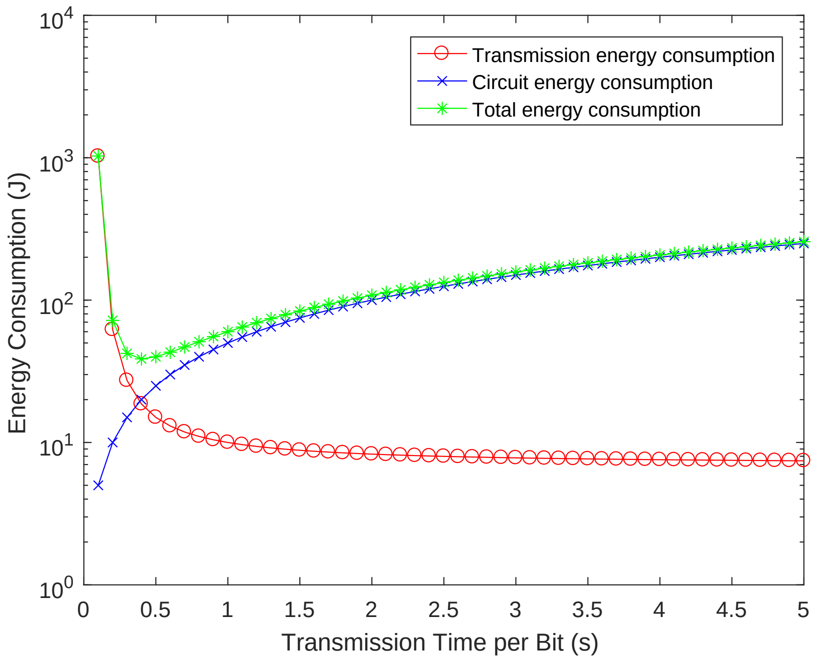

Fig. 2.9 The tradeoff between the transmission energy and the circuit energy consumption with different transmission time per bit.

In a non-cooperative wireless network, given a data packet with a specified length in bits, it is obvious that the transmission time increases with the increasing transmission time per bit (namely the reciprocal of the data rate). Thus, the transmission energy consumption decreases while the circuit energy consumption increases with the increasing transmission time per bit. In [40, 41], the authors show that there is a tradeoff between the transmission energy consumption and the circuit energy consumption with different transmission times per bit. An example is given in Fig. 2.9.

In a cooperative wireless network, cooperative communication provides spatial diversity for single-antenna devices. Therefore, the transmission energy required by a specified data

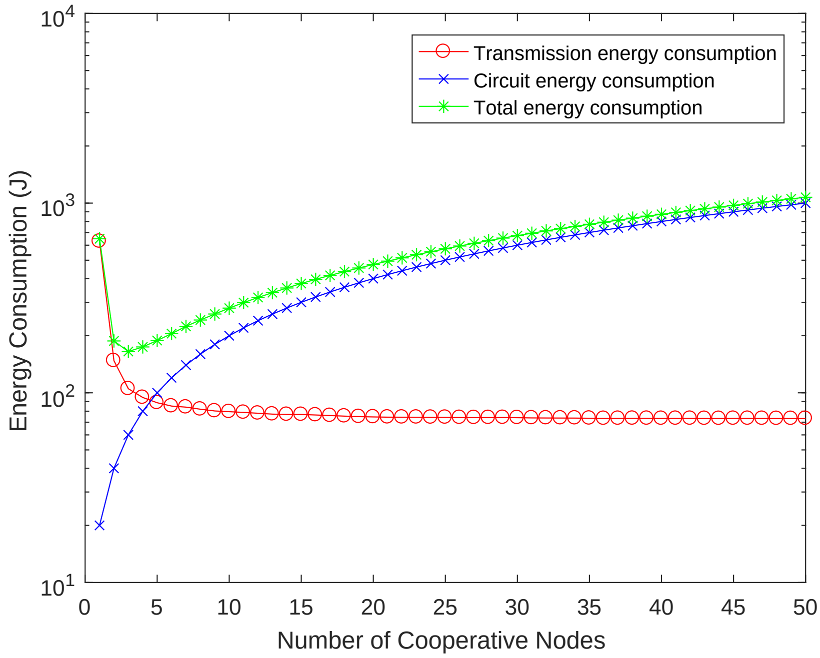

Fig. 2.10 The tradeoff between the transmission energy and the circuit energy consumption with different number of cooperative nodes.

rate decreases with the increasing number of cooperative nodes. However, the circuit energy consumption increases with the increasing number of cooperative nodes. Thus, there is a tradeoff between the transmission energy consumption and the circuit power consumption with different numbers of cooperative nodes. This kind of tradeoff is analyzed in detail in [37, 42, 43]. An example is given in Fig. 2.10.

2.4.2 Power Control Methods

In general, adjusting transmission power level is an effective way to provide QoS-constrained data transmission via fading channels. Increasing the transmission power level in a timely manner can avoid the temporary communication failure caused by deep fades. On the other hand, the energy consumption in wireless communication is considered as an important issue due to the limited energy supply of wireless devices. Therefore, power control is a key factor to maximize the lifetime of the wireless devices while maintaining the QoS requirements of the wireless applications.

Classic power control methods such as the water-filling power control and the channel inversion power control have been considered to improve the wireless system performance in fading channels.

The water-filling power control has been proved to be the optimal power control strategy to maximize the ergodic channel capacity. The applications of the water-filling power control and its variants are given in [44–46]. The optimal ergodic channel capacity of the SISO channel is given in Equation (2.9). Although the water-filling power control is optimal, it requires perfect CSI on both the transmitter side and the receiver side.

The channel inversion power control is a suboptimal strategy compared to the water-filling strategy. However, it has much simple encoder and decoder designs. The effectiveness of channel inversion power control and its variants have been studied in [47–49]. Consider a SISO channel. With the channel state information (CSI), the channel inversion power control inverts the channel fading and thus maintains a constant received power at the receiver. Let γ be the instantaneous SNR and $f(\gamma) = \Pr(\gamma_i = \gamma)$ denote the probability density function (PDF) of the SNR at the receiver. The fading channel capacity with channel inversion is given by

$$C^{SISO}_{channel-inversion} = B\log_2(1+\gamma_0), \tag{2.29}$$

where γ_0 satisfies $\int \left(\frac{\gamma_0}{\gamma}\right) f(\gamma)d\gamma = 1$. In the Rayleigh fading models, γ_0 is zero and thus the channel capacity with channel inversion is zero. It is shown in [50] that the channel inversion power control results in large channel capacity loss in deep fades. Therefore, the channel inversion power control is not suitable for all channel fading models.

Although the water-filling power control and the channel inversion power control are theoretically effective in some fading models, it still requires perfect channel state information (CSI) which is hard to obtain in practice. Therefore, many existing works focus on analyzing and improving the system performance with imperfect CSI [51–55].

2.5 Resource Allocation Methods

2.5.1 The Assignment Problem

The assignment problem is a combinatorial optimization problem of finding the optimal assignment of a set of resources to a set of users, such as assignment of workers to jobs, machines to tasks and so on [56]. In wireless communications, allocating wireless resources such as channels or transmission powers to users can be formulated as an assignment problem.

An instance of a wireless channel allocation problem that is formulated as an assignment problem is generally described as follows:

There are a number of users and a number of channels in the wireless network. Each user can only access a channel at a time and achieves some utilities (e.g., channel throughput or transmission power consumption). The total utility of the network varies with different assignments of channels to users. At any time a channel can hold no more than one user. We aim at finding an assignment that can optimize the total utility (e.g., maximize the total channel throughput or minimize the total transmission power) of the network.

The mathematical statement of the channel allocation problem to maximize the total channel capacity is given as follows:

We assume that there are M users denoted by $\mathbf{U} = \{U_1, U_2, \ldots, U_M\}$ and N channels denoted by $\mathbf{CH} = \{CH_1, CH_2, \ldots, CH_N\}$ in the wireless network. Let the $M \times N$ matrix Π be the assignment matrix where the element $\pi_{i,j} = 1$ means that channel CH_j is assigned to user U_i and $\pi_{i,j} = 0$ otherwise. We define the $M \times N$ matrix Ψ as the utility matrix where the element $\psi_{i,j}$ is the channel capacity of user U_i at channel CH_j. The channel assignment problem is given by:

$$\begin{aligned} \Pi^* = \arg\max_{\Pi} & \left(\sum_{i=0}^{M} \sum_{j=0}^{N} \pi_{i,j} \psi_{i,j} \right) \\ \text{s.t.} \quad & \sum_{j=0}^{N} \pi_{i,j} \leq 1, \forall i \in \{1, 2, \ldots, M\} \\ & \sum_{i=0}^{M} \pi_{i,j} \leq 1, \forall j \in \{1, 2, \ldots, N\} \end{aligned} \tag{2.30}$$

The Hungarian algorithm can be used to find the optimal assignment of the problem in Equation (2.30). The details of the Hungarian algorithm is given in the next section.

2.5.2 The Hungarian Algorithm

The Hungarian algorithm is a combinatorial optimization algorithm for the assignment problem. Variations of the Hungarian algorithm have been used to solve the resource allocation problems in wireless networks [57–59].

Consider the channel allocation problem in Section 2.5.1 as an example. We will now show how the Hungarian algorithm works. We further assume that $M = N = n$ for the channel allocation problem. Given the utility matrix Ψ, there are five steps to complete the Hungarian algorithm which are described as follows:

1. Find the row minimum in each row. Subtract the row minimum from each row.

2. Find the column minimum in each column. Subtract the column minimum from each column.

3. Cover all zeros with a minimum number of horizontal and vertical lines.

4. Check the number of the horizontal and vertical lines. If the number of the lines is greater or equal than the number of rows or columns, the algorithm terminates. Output the set of zeros where each row or column has only one zero selected as the optimal assignment. Otherwise go to Step 5.

5. Find the smallest element that is not covered in Step 3. Subtract it from each uncovered row and add it to each covered column. Repeat Step 3 and Step 4.

The implementation of the Hungarian algorithm for the channel allocation problem is given in Algorithm 2.1.

Examples and proof of the efficiency of the Hungarian algorithms can be found in [60] and [61].

2.5.3 The Matching Algorithm

Auction algorithms are widely used to solve the resource allocation problems in wireless networks [62–64]. Matching algorithms are typical variations of auction algorithms that can find the best matching of two sets of agents where agents can either be wireless resources or users in the wireless communication scenarios.

We consider the channel allocation problem in Section 2.5.1 as an example. We first introduce a two-sided matching model [65, 66]. We then prove that the channel allocation problem can be formulated as a two-sided matching problem of users and channels. Let the set of users **U** and the set of channels **CH** be the two sets of agents of the two-sided matching model. We assume that each user U_i has a strict preference relation $\succ_{u,i}$ over the set of channels **CH** and the option to stay unmatched which is denoted by $\emptyset$. The channel CH_j is acceptable to user U_i if $CH_j \succ_{u,i} \emptyset$. Similarly, we define the strict preference relation $\succ_{ch,j}$ of CH_j over the set of users **U** and $\emptyset$. We assume that a channel can be assigned to one user at a time and vice versa.

A matching $\mathscr{M}$ is a mapping of channels and users. A matching is individually rational if (i) no user is matched to a channel that is unacceptable to it and vice versa, (ii) no user is matched with more than one channel and vice versa. We can also define a matching as a function $\mathscr{M}$: $\mathbf{U} \cup \mathbf{CH} \rightarrow \mathbf{U} \cup \mathbf{CH} \cup \emptyset$ such that for all $U_i \in \mathbf{U}$ and $CH_j \in \mathbf{CH}$:

1. $\mathscr{M}(U_i) \notin \mathbf{CH} \Rightarrow \mathscr{M}(U_i) = \emptyset$, for all $U_i \in \mathbf{U}$.

2. $\mathscr{M}\left(CH_j\right) \notin \mathbf{U} \Rightarrow \mathscr{M}\left(CH_j\right) = \emptyset$, for all $CH_j \in \mathbf{CH}$.

3. $\mathscr{M}(U_i) = CH_j \Leftrightarrow \mathscr{M}\left(CH_j\right) = U_i$, for all $U_i \in \mathbf{U}$ and $CH_j \in \mathbf{CH}$.

Algorithm 2.1 Implementation of the Hungarian algorithm

Input n, Ψ.
Initialization: for any $\pi_{i,j} \in \Pi$, let $\pi_{i,j} = 0$. Define an $n \times n$ matrix Ω to mark the zero element s during the execution of the algorithm. For any $\omega_{i,j} \in \Omega$, let $\omega_{i,j} = 0$. Define $\lambda = 0$ to indicate the termination of the algorithm. The algorithm terminates when we have $\lambda \geq n$.
for $1 \leq i \leq n$ **do**
  Find $\psi_{i,\min} = \min\limits_{j=1,2,\ldots,n} \left(\psi_{i,j}\right)$. Subtract $\psi_{i,\min}$ from each $\psi_{i,j}$ in row i.
end for
for $1 \leq j \leq n$ **do**
  Find $\psi_{\min,j} = \min\limits_{i=1,2,\ldots,n} \left(\psi_{i,j}\right)$. Subtract $\psi_{\min,j}$ from each $\psi_{i,j}$ in column j.
end for
while $\lambda < n$ **do**
  for $1 \leq i \leq n$ **do**
    if $\psi_{i,j} = 0, \forall j \in \{1,2,\ldots,n\}$ and $\omega_{i,j} = 0$ **then**
      Let $\omega_{i,j} = \omega_{i,j} + 1$, for any $\psi_{i,j} = 0, \forall j \in \{1,2,\ldots,n\}$. $\lambda = \lambda + 1$.
    end if
  end for
  for $1 \leq j \leq n$ **do**
    if $\psi_{i,j} = 0, \forall i \in \{1,2,\ldots,n\}$ and $\omega_{i,j} = 0$. **then**
      Let $\omega_{i,j} = \omega_{i,j} + 1$, for any $\psi_{i,j} = 0, \forall i \in \{1,2,\ldots,n\}$. $\lambda = \lambda + 1$.
    end if
  end for
  if $\lambda \geq n$ **then**
    Let $\pi_{i,j} = 1$ for any set of zeros where each row or column has only one zero selected.
  else
    Find $\psi_{\min} = \min\limits_{i,j} \left(\psi_{i,j}\right), \forall i,j \in \{1,2,\ldots,n\}, \omega_{i,j} = 0$.
    for $1 \leq i \leq n$ **do**
      if $\omega_{i,j} = 0, \forall j \in \{1,2,\ldots,n\}$ **then**
        $\psi_{i,j} = \psi_{i,j} - \psi_{\min}, \forall j \in \{1,2,\ldots,n\}$.
      end if
    end for
    for $1 \leq j \leq n$ **do**
      if $\omega_{i,j} = 1, \exists i \in \{1,2,\ldots,n\}$ **then**
        $\psi_{i,j} = \psi_{i,j} + \psi_{\min}, \forall i \in \{1,2,\ldots,n\}$.
      end if
    end for
    Let $\lambda = 0$ and $\omega_{i,j} = 0, \forall \omega_{i,j} \in \Omega$.
  end if
end while

We define a blocking pair to a matching $\mathscr{M}$ as a channel-user pair that prefer to be matched with each other rather than being matched by $\mathscr{M}$. A matching is stable if it is individually rational and contains no blocking pairs.

Let the utility matrix Φ decide the preference order of users over channels and channels over users. Given user U_i, channel CH_j and channel CH_k, we say that for the preference order of user U_i, $CH_j \succ_{u,i} CH_k$ if and only if $\psi_{i,j} > \psi_{i,k}$. Similar definitions are given for the preference order of channels over users. The users and channels build their preference lists based on the utility matrix Φ. According to the definition of matching, it is obvious that a matching corresponds to a valid assignment matrix Π. Therefore, the problem in Equation (2.30) is equal to find a matching that can maximize the total utility of the network.

We then propose to use the user-proposing deferred acceptance (UPDA) algorithm. It has been proved that the UPDA algorithm gives a stable matching and every user prefers this stable matching over any other stable matching. The stable matching given by the UPDA algorithm is referred as user-optimal stable matching. The proof of the above theorem can be found in [67].

The UPDA algorithm is described as follows: In step 1, each user U_i requests the best channel on its preference list. Each channel CH_j keeps the best user and rejects the other users. In step k, users that are rejected at step $k-1$ request their current best channels that have not yet rejected them. The channels that receive requests from users keep the best users on their preference list and reject the other users. The algorithm terminates when there are no further channel request. Each channel is matched to the user (if any) that it will keep until the last step. The other channels and users remain unmatched.

2.6 Summary

The wireless channel capacity model and the network delay model are two key factors for power control and resource allocation in a QoS-constrained wireless network. In this chapter, we have presented some background information concerning the wireless channel capacity, a delay analysis of wireless networks and the definition of various QoS metrics to facilitate understanding our work. We also introduce some methods that we will employ later when considering power control and resource allocation of wireless networks. In the following chapters, cooperative and noncooperative models of PUs and SUs in CRNs are proposed and analyzed. When QoS constraints such as delay and data rate are considered, queueing theory and outage capacity are used to analyze the performance of the wireless network.

Chapter 3

Dynamic Power Control and Optimization for QoS-Constrained Wireless Networks

3.1 Introduction

Energy efficiency is considered to be a major challenge in wireless sensor networks (WSNs) where sensors are assumed to be able to work for years without battery replacement [68]. On the other hand, wireless applications with QoS requirements on delay and data rate require reliable transmissions such as those used for industrial control [69] and environment monitoring. It has been proved that MIMO system consumes less energy for data transmission in fading channels compared with a SISO system [3]. However, sensor nodes are low-power, low-cost, single-antenna devices. It is thus difficult to build a MIMO system for WSNs. Cooperative communication is considered as a promising method to achieve MIMO communication among single-antenna devices [70].

In a cluster-based cooperative wireless sensor network, data can be transmitted from cluster to cluster using virtual MIMO technique [42] where cooperative nodes in each cluster use their resources to help the transmissions of the cluster heads. It has been proved in [37] that cooperative communication and the virtual MIMO system is energy-efficient for long-distance single-hop transmission. In [71], a multi-hop cooperative MIMO network is analyzed. A transmission scheme that can minimize the end-to-end outage probability is proposed. However, simply reducing the outage probability may not achieve the maximum average outage capacity [17]. Furthermore, reducing the end-to-end outage probability may increase the power consumption of the WSN.

In this chapter, we investigate the outage capacity and power control problem for the centralized cooperation model of a cooperative wireless network. Specifically, a cluster-based cooperative wireless sensor network is considered where cluster nodes cooperatively transmit with the cluster head to improve the transmission reliability and energy efficiency. In contrast to much existing work, we focus on minimizing the power consumption of the transmitters in each cluster of the WSN without violating the QoS constraints. We not only investigate the performance of cooperative transmissions in multi-hop scenario but also solve the power control and optimization problems with QoS constraints. Most of the results in this chapter are published in the IEEE International Conference on Communications (ICC) 2016 conference proceedings [14].

The rest of the chapter is organized as follows: Section 3.2 describes the system model of the multi-hop cluster-based WSN, the single-hop transmission scheme and the definition of the outage capacity. In Section 3.3, we express the QoS constraints on delay and data rate in detail. In Section 3.4, we first propose the dynamic power control and optimization (DPCO) scheme. We further propose an approximate algorithm to reduce the computational complexity and storage cost of the DPCO scheme. Simulation results are given in Section 3.5. Finally, we conclude the chapter in Section 3.6.

3.2 System Model

We consider a multi-hop cluster-based WSN as shown in Fig. 3.1. The transmission between two adjacent clusters is defined as a single-hop transmission. In our model, we assume that sensors are grouped into N clusters where each cluster contains one cluster head. For each transmission, some sensors are assigned to cooperatively transmit with the cluster head to improve the transmission reliability. We also assume that the cluster head is located near the center of the cluster and sensors in each cluster are uniformly deployed. A practical scenario of this model is the star network topology of IEEE 802.15.4 wireless network [72] where full-function devices and reduced-function devices (RFD) are assumed to be the cluster heads and normal sensor nodes, respectively. The clustering and routing protocols of the multi-hop cluster-based wireless networks are beyond the scope of this chapter. However, efficient protocols such as HEED [73] and LEACH [74] can be used.

The single-hop transmission has two phases, namely the broadcast phase (BP) and the cooperation phase (CP) as given in Fig. 3.2. The time duration of the two phases are α and $1-\alpha$ respectively. The total time duration of each transmission slot is normalized to be 1. Before the transmission start, the cluster head in the transmitter cluster first figures out the number of cooperative nodes and the transmission power allocation in the BP (P_{bp}) and

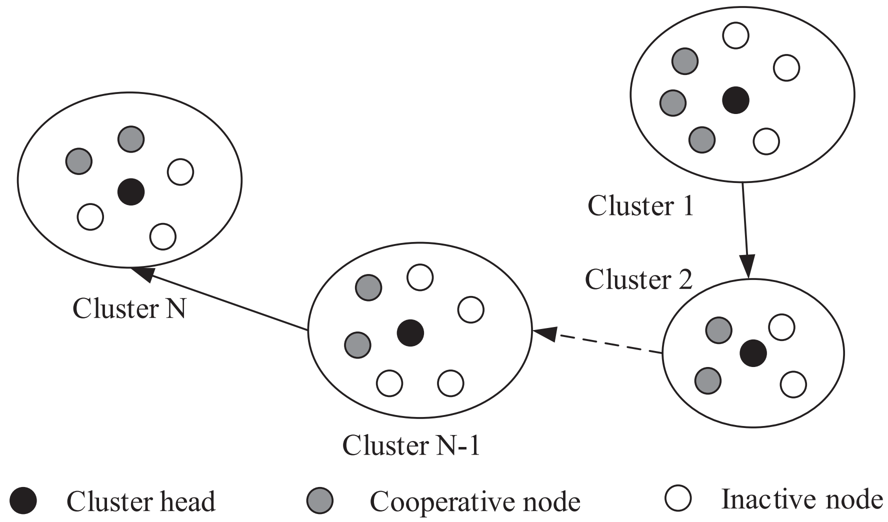

Fig. 3.1 Multi-hop cluster-based CRN.

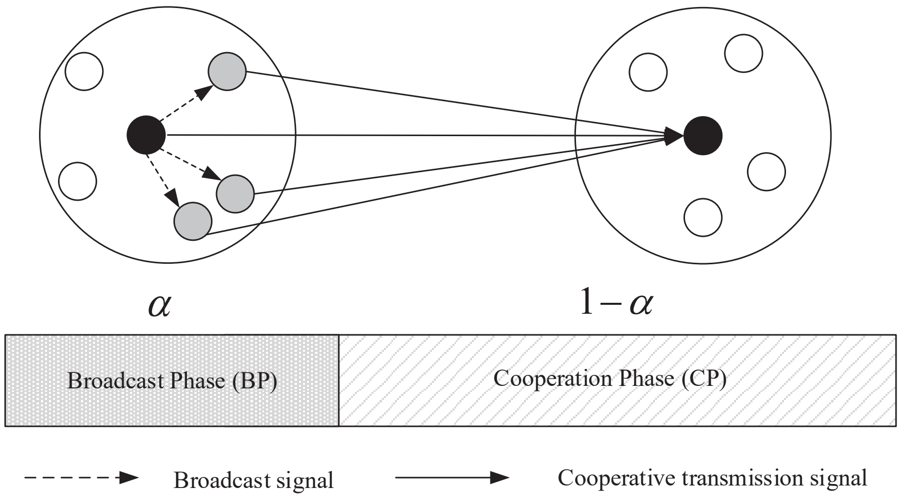

Fig. 3.2 Transmission scheme.

CP (P_{cp}). Then, these configurations are carried in the control message and sent to other cooperative nodes along with the transmission data in the BP.

1. **Broadcast Phase:** In the BP, the cluster head broadcasts the cluster configurations to the other sensor nodes in the cluster with a transmission power P_{bp}. Sensors that successfully decoded the data are selected to cooperatively transmit with the cluster head in the next CP. It is assumed that the number of cooperative nodes is proportional to P_{bp}. Thus, the cluster head can control the number of cooperative nodes by adjusting P_{bp}.

2. **Cooperation Phase:** In the CP, the cooperative nodes and the cluster head jointly transmit the data to the cluster head in the receiver cluster using orthogonal space-time block codes (STBC). We assume that no CSI is available at the transmitter cluster. Let n_t denote the number of sensors transmitting data in the CP. The transmission power P_{cp} is equally allocated among the cluster head and cooperative nodes for optimal network performance.

We only consider long-range transmission between adjacent clusters since cooperative transmission is more energy-efficient in that case [37]. The channels in the BP and the CP are modeled using an AWGN channel and a slow flat Rayleigh fading channel with AWGN respectively, since the inter-cluster distance of sensors is much larger than the intra-cluster distance of sensors. Let $\psi = \beta d^{-\theta}$ denote the inter-cluster path loss where d is the distance between two adjacent clusters, β is the path loss constant related to the channel and θ is the path loss exponent. Consider the transmission between cluster m and cluster $m+1$, the received signal at the the cluster head of cluster $m+1$ is given by the multiple-input single-output (MISO) channel model as

$$\mathbf{y_m} = \sqrt{\psi}\mathbf{h}\mathbf{x_m} + \mathbf{n_m}, \tag{3.1}$$

where elements in the $1 \times n_t$ channel vector $\mathbf{h}$ are i.i.d. complex Gaussian random variables with zero mean and unit variance for normalization. $\mathbf{x_m}$ is the $n_t \times l$ transmitted signal where l is the length of the STBC. $\mathbf{n_m} \sim N\left(0, \sigma^2\right)$ is the $1 \times l$ AWGN at the receiver.

Since no CSI is available at the transmitter cluster, all sensors transmit with equal transmission power $\frac{P_{cp}}{n_t}$. The outage capacity C_{out} of the CP is given by

$$C_{out} = B(1-\alpha)\log_2(1+\gamma_{out}), \tag{3.2}$$

where B is the channel bandwidth and γ_{out} is the minimum SNR for successful message decoding at the receiver. Let γ denote the instantaneous SNR at the receiver and $p_{out} =$

$\Pr(\gamma < \gamma_{out})$ denote the outage probability. Based on the MISO channel model in Equation (3.1), γ is given by

$$\gamma = \frac{\psi P_{cp} \|\mathbf{h}\|_F^2}{n_t \sigma^2} \tag{3.3}$$

where $\|\mathbf{h}\|_F^2$ is the squared Frobenius norm of the $1 \times n_t$ channel vector $\mathbf{h}$. According to the definition of $\mathbf{h}$, $\|\mathbf{h}\|_F^2 \sim \chi^2(2n_t)$ is a chi-square variable with $2n_t$ degrees of freedom. Given p_{out}, we have

$$\gamma_{out} = \frac{\psi P_{cp} F^{-1}(p_{out} | 2n_t)}{n_t \sigma^2} \tag{3.4}$$

where $F^{-1}(p|n)$ is the inverse chi-square cumulative distribution function (CDF) with probability p and n degrees of freedom.

The average outage capacity is given as

$$\bar{C}_{out} = B(1-\alpha)(1-p_{out})\log_2(1+\gamma_{out}). \tag{3.5}$$

3.3 Multi-Hop QoS Constraint

In the multi-hop transmission model, the QoS constraints (R, D) are considered where R is the average transmission data rate and D is the average end-to-end delay. We assume that the packet arrival rate is far less than the packet transmission rate. Therefore, the queueing delay $D^{(q)}$ is negligible compared to the transmission delay $D^{(t)}$ and we only consider the transmission delay for the average end-to-end delay analysis. An automatic repeat request (ARQ) mechanism [75] is used for cluster-to-cluster communication where the senders retransmit their data to the next cluster if they do not receive an acknowledgement (ACK) before the timeout expires.

The number of packet retransmissions k in the $N-1$ hops network follows a general distribution with the probability mass function (PMF) given as

$$\Pr(X = k) = \binom{k+N-2}{k} \prod_{i=1}^{N-1} p_{out,i}^{a_i}(1-p_{out,i}) \tag{3.6}$$

where $p_{out,i}$ is the outage probability of the single-hop transmission between cluster i and cluster $i+1$, a_i is a non-negative integer with $\sum_{i=1}^{N-1} a_i = k$ and $\binom{k+N-2}{k}$ is the binomial coefficient expressed as

$$\begin{pmatrix} k+N-2 \\ k \end{pmatrix} = \frac{(k+N-2)!}{k!\,(N-2)!} = \frac{(k+N-2)\,(k+N-3)\ldots(N-1)}{k!} \tag{3.7}$$

For simplicity, we assume that the cluster-to-cluster channels are MISO channels with i.i.d. parameters and identical configurations. Therefore, the outage probability of any single-hop transmission is assumed to be p_{out} and the number of packet retransmissions k in the $N-1$ hops network follows the negative binomial distribution with the PMF expressed as

$$\Pr(k;N-1,p_{out}) = \begin{pmatrix} k+N-2 \\ k \end{pmatrix} p_{out}^{k}\,(1-p_{out})^{N-1}. \tag{3.8}$$

Considering the QoS constraints on the average transmission data rate, we must have $R \leq \bar{C}_{out} < C_{out}$ for network stability. For one packet transmission with L (bits) length, the maximum packet transmission delay is thus given by

$$\tau = \frac{L}{R}. \tag{3.9}$$

The following proposition is given to characterize the end-to-end packet delay of the network:

Proposition 3.3.1. *The maximum average end-to-end delay of the $N-1$ hops is given by:*

$$\bar{D} = \mathrm{E}\left[(k+N-1)\,\tau\right] = \frac{(N-1)\,L}{(1-p_{out})\,R}. \tag{3.10}$$

Proof. We first prove that $\mathrm{E}[k] = \frac{(N-1)p_{out}}{1-p_{out}}$. Since k follows the negative binomial distribution, we calculate the mean value of k based on the negative binomial distribution PMF in Equation (3.8) as

$$\begin{aligned}
\mathrm{E}[k] &= \sum_{k=0}^{\infty} k \Pr(k; N-1, p_{out}) \\
&= \sum_{k=0}^{\infty} \frac{k(k+N-2)!}{k!(N-2)!} p_{out}^{k} (1-p_{out})^{N-1} \\
&= \frac{(N-1)p_{out}}{1-p_{out}} \sum_{k=1}^{\infty} \frac{(k+N-2)!}{(k-1)!(N-1)!} p_{out}^{k-1} (1-p_{out})^{N} \\
&= \frac{(N-1)p_{out}}{1-p_{out}} \sum_{k=0}^{\infty} \frac{(k+N-1)!}{k!(N-1)!} p_{out}^{k} (1-p_{out})^{N} \\
&= \frac{(N-1)p_{out}}{1-p_{out}} \sum_{k=0}^{\infty} \Pr(k; N, p_{out}) \\
&= \frac{(N-1)p_{out}}{1-p_{out}}
\end{aligned} \tag{3.11}$$

Since N is constant and the maximum packet transmission delay for one packet transmission τ is given by Equation (3.9), the maximum average end-to-end delay of the $N-1$ hops is thus given by

$$\bar{D} = \mathrm{E}[(k+N-1)\tau] = \left(\frac{(N-1)p_{out}}{(1-p_{out})} + N - 1\right)\frac{L}{R} = \frac{(N-1)L}{(1-p_{out})R}. \tag{3.12}$$

□

Considering the QoS constraints on the average end-to-end delay, we must have

$$\bar{D} = \frac{(N-1)L}{(1-p_{out})R} \leq D \tag{3.13}$$

and thus

$$p_{out} \leq 1 - \frac{(N-1)L}{RD} \tag{3.14}$$

where $RD > (N-1)L$ is required since $0 < p_{out} < 1$. If we have $RD \leq (N-1)L$, it is impossible for reliable transmission under the QoS constraints (R, D).

Consider the transmission data rate in the CP (R_{cp}) and the BP (R_{bp}). In order to have reliable transmissions, we must have

$$R \leq R_{bp} \leq R_{cp} \leq \bar{C}_{out}. \tag{3.15}$$

Now the QoS constraints are expressed by the outage probability constraint in Equation (3.14) and the average outage capacity constraint in Equation (3.15). We first show that the average outage capacity can always be maximized under QoS constraints where $RD > (N-1)L$.

Proposition 3.3.2. *For any QoS constraints where $RD > (N-1)L$, there exists p^*_{out} that can maximize $\bar{C}_{out}$, which can be denoted as follows:*

$$\begin{aligned} &\bar{C}^*_{out} = \max_{p_{out}} \{B(1-\alpha)(1-p_{out})\log_2(1+\gamma_{out})\}, \\ &\text{s.t.} \quad \bar{C}_{out} \geq R, 0 < p_{out} \leq 1 - \tfrac{(N-1)L}{RD}. \end{aligned} \tag{3.16}$$

Proof. From Equation (3.4) we know that $F^{-1}(p_{out}|2n_t)$ increases with p_{out} for any n_t. Given $p_{out} \in \left(0, 1-\frac{(N-1)L}{RD}\right]$, we have

$$\lim_{p_{out}\to 0} \bar{C}_{out} = 0 \tag{3.17}$$

and

$$\lim_{p_{out}\to p^{\max}_{out}} \bar{C}_{out} = \frac{B(1-\alpha)(N-1)L}{RD}\log_2\left(1+\frac{\psi\xi P_{cp}}{n_t\sigma^2}\right) \tag{3.18}$$

where $p^{\max}_{out} = 1-\frac{(N-1)L}{RD}$ and $\xi = F^{-1}(p^{\max}_{out}|2n_t)$. Since $\lim_{p_{out}\to p^{\max}_{out}} \bar{C}_{out} > 0$ and Equation (3.2) is continuous for $p_{out} \in \left(0, 1-\frac{(N-1)L}{RD}\right]$, there exists p^*_{out} that maximizes $\bar{C}_{out}$ according to the extreme value theorem. □

3.4 Dynamic Power Control and Optimization

Let P_{bp} and P_{cp} be the transmission power consumption in the BP and the CP respectively. The total power consumption in each hop is given by

$$P_t = \alpha P_{bp} + (1-\alpha)P_{cp} + n_t P_c, \tag{3.19}$$

where P_c is the average circuit power consumption of each sensor node.

In the BP, we assume the channel is AWGN with free space path loss $\phi = \zeta r^{-2}$ where ζ is the free space path loss constant and r is the intra-cluster transmission range. The transmission data rate R_{bp} is given by

$$R_{bp} = \alpha B\log_2\left(1+\frac{\phi P_{bp}}{\sigma^2}\right) = \alpha B\log_2\left(1+\frac{\zeta P_{bp}}{r^2\sigma^2}\right). \tag{3.20}$$

Given the transmission data rate $R_{bp} = \bar{C}_{out}$, the transmission power P_{bp} is expressed as

$$P_{bp} = \frac{r^2\sigma^2}{\zeta}\left(2^{\frac{R_{bp}}{\alpha B}} - 1\right) = \frac{r^2\sigma^2}{\zeta}\left(2^{\frac{\bar{C}_{out}}{\alpha B}} - 1\right). \tag{3.21}$$

Let $r_{\max}$ denote the maximum intra-cluster transmission range and n is the total number of sensors in each cluster. We assume that the cluster head is located in the center of the cluster and sensors are uniformly distributed in each cluster. The approximate number of sensors that can successfully receive and decode the message in the BP is given by

$$n_t = \left(\frac{r}{r_{\max}}\right)^2 n = \frac{\zeta P_{bp} n}{r_{max}^2\sigma^2}\left(2^{\frac{R_{bp}}{\alpha B}} - 1\right)^{-1} = \frac{\zeta P_{bp} n}{r_{max}^2\sigma^2}\left(2^{\frac{\bar{C}_{out}}{\alpha B}} - 1\right)^{-1}. \tag{3.22}$$

In the CP, the channel is assumed to be a slow flat Rayleigh fading channel. Given the transmission data rate $R_{cp} = \bar{C}_{out}$, the transmission power P_{cp} is given by

$$P_{cp} = \frac{\gamma_{out} n_t \sigma^2}{\psi F^{-1}\left(p_{out}\,|2n_t\right)} = \frac{2^{\frac{\bar{C}_{out}}{B(1-\alpha)(1-p_{out})}} - 1}{\psi F^{-1}\left(p_{out}\,|2n_t\right)} n_t \sigma^2. \tag{3.23}$$

3.4.1 Dynamic Power Control Algorithm

Given the QoS constraints (R, D) where $RD > (N-1)L$, we aim to find the optimal value of P_{cp} and P_{bp} that minimize the total power consumption P_t. Given $R_{bp} = \bar{C}_{out}$, n_t is directly correlated to P_{bp} as shown in Equation (3.22). Thus, P_{bp} and n_t are jointly optimized. Given $R_{cp} = \bar{C}_{out}$ and n_t, for any $p_{out} \in \left(0, 1 - \frac{(N-1)L}{RD}\right]$, $\bar{C}_{out}$ increases with $P_{cp|n_t}$ where $P_{cp|n_t}$ denotes the P_{cp} for any specific n_t. Under the QoS constraints, $P_{cp|n_t}$ is optimized when $p_{out} = p_{out}^*$ and $\bar{C}_{out} = \bar{C}_{out}^* = R$. The power optimization problem is denoted as

$$\left\{P_{cp|n_t^*}^*, n_t^*\right\} = \arg\min_{P_{cp|n_t}, n_t} P_t\left(P_{cp|n_t}, n_t\right). \tag{3.24}$$

Note that $P_{cp|n_t^*}^*$ is related to n_t^*. However, in order to determine n_t^*, we need to figure out $P_{cp|n_t}^*$ for every possible n_t. $P_{cp|n_t}$ and n_t are interrelated with each other in the optimization problem.

We first find the conditional optimal $P_{cp|n_t}^*$ for all possible n_t, which is expressed as

$$\begin{aligned} P_{cp|n_t}^* &= \arg\min_{P_{cp|n_t}} P_t\left(P_{cp|n_t}\,|n_t\right), 1 \le n_t \le n \\ \text{s.t.} \quad & 0 \le P_{cp|n_t} \le P_{cp}^{\max} \end{aligned} \tag{3.25}$$

where $P_{cp}^{\max}$ is the maximum transmission power in the CP. Then we determine n_t^* as

$$n_t^* = \arg\min_{n_t} P_t\left(n_t \left| P_{cp|n_t}^* \right.\right), 1 \le n_t \le n. \tag{3.26}$$

Given n_t^* and $\bar{C}_{out}^* = R$, $P_{bp|n_t^*}^*$ can be obtained from Equation (3.21) and Equation (3.22) as

$$P_{bp|n_t^*}^* = \frac{n_t^* r_{\max}^2 \sigma^2}{\zeta n}\left(2^{\frac{R}{\alpha B}} - 1\right). \tag{3.27}$$

The minimum total power consumption under QoS constraints is expressed by:

$$P_t^* = \alpha P_{bp|n_t^*}^* + (1-\alpha) P_{cp|n_t^*}^* + n_t^* P_c. \tag{3.28}$$

We know that there is no closed-form solution for $P_{cp|n_t}^*$ in Equation (3.25) due to the complexity of $F^{-1}\left(p_{out}\left|2n_t\right.\right)$. However, we can still find a good estimate of $P_{cp|n_t}^*$ using the dynamic power control (DPC) algorithm as shown in Algorithm 3.1.

Proposition 3.4.1. *Given n_t and the maximum number of iterations I in the DPC algorithm, $P_{cp|n_t,i}$ converges to $P_{cp|n_t}^*$ with a sufficient small difference δ in $O(1)$ iterations.*

Proof. If $0 < P_{cp|n_t,I} < P_{cp}^{\max}$, $P_{cp|n_t}^*$ must fall into one of the M equally divided intervals of $\left[0, P_{cp}^{\max}\right]$ where M is a parameter that determines the value of π_0, namely the convergence speed of the DPC algorithm. In the DPC algorithm, π_i will not halve its value until $\eta_{i-1}\eta_i = -1$. We have M iterations at most before π_i halves its value. After the first time π_i halves its value, π_i can only stay unchanged for two iterations at most. We define δ as

$$\delta = \frac{\pi_0}{2^V} = \frac{P_{cp}^{\max}}{2^V M} \tag{3.29}$$

where V is a positive integer to adjust the value of δ. After π_i halves its value, we have $\left|P_{cp|n_t,i} - P_{cp|n_t}^*\right| \le \pi_i$. Let $V = \left\lfloor \frac{I-M}{2} \right\rfloor$ where $\lfloor x \rfloor$ is the greatest preceding integer of x. We have $\left|P_{cp|n_t,I} - P_{cp|n_t}^*\right| \le \delta$ in I iterations. □

3.4.2 Outage Capacity Approximation

The DPC algorithm has high computational complexity since there in no closed-form solution for Equation (3.16). Every time a new value of $P_{cp|n_t,i-1}$ is given in Algorithm 3.1, the DPC algorithm has to find out the maximum average outage capacity $\bar{C}_{out,i}^*$ using a brute-force search. Furthermore, in order to solve Equation (3.4) and Equation (3.16), we need to store the inverse chi-square table in the wireless node which occupies a lot of storage space.

Algorithm 3.1 DPC algorithm

Input: M, η_0, $P_{cp}^{\max}$
Initialization: $P_t^{opt} = \infty$
for $1 \le n_t \le n$ **do**
  $P_{cp|n_t,0} = P_{cp}^{\max}$, $\eta_0 = 1$, $\pi_0 = \frac{P_{cp}^{\max}}{M}, M \in Z^+$
  for $1 \le i \le I$ **do**
    1) According to Equation (3.16), calculate $\bar{C}_{out,i}^*$ using $P_{cp|n_t,i-1}$.
    2) $\eta_i = sgn\left(\bar{C}_{out,i}^* - R\right)$ where $sgn(\cdot)$ is the signum function.
    3) $\pi_i = \min\left\{\frac{3+\eta_{i-1}\eta_i}{4}, 1\right\}\pi_{i-1}$.
    4) $\hat{P}_{cp|n_t,i} = P_{cp|n_t,i-1} - \eta_i \pi_i$.
    5) $P_{cp|n_t,i} = \max\left\{\min\left\{\hat{P}_{cp|n_t,i}, P_{cp}^{\max}\right\}, 0\right\}$.
    if $P_{cp|n_t,i} = P_{cp}^{\max}$ **then**
      break the current for loop
    end if
  end for
  Calculate P_t^* using $P_{cp|n_t,I}$ and n_t.
  if $0 < P_{cp|n_t,I} < P_{cp}^{\max}$ and $P_t^* < P_t^{opt}$ **then**
    $P_t^{opt} = P_t^*$, $n_t^* = n_t$, $P_{cp|n_t^*}^* = P_{cp|n_t,I}$
  end if
end for
if $P_{cp|n_t^*}^* = P_{cp}^{\max}$ **then**
  QoS constraints cannot be fulfilled.
end if

Therefore, we are motivated to find out a suboptimal algorithm that can solve the problem with less computational complexity and storage space. Inspired by the work in [76], we propose a closed-form approximation for the slow flat Rayleigh fading MISO channel.

We first calculate the mean value of γ in Equation (3.3). Since $\|\mathbf{h}\|_F^2$ follows a chi-square distribution, we have

$$\mu_\gamma = \mathrm{E}[\gamma] = \frac{\psi P_{cp}}{n_t \sigma^2} \mathrm{E}\left[\|\mathbf{h}\|_F^2\right] = \frac{2\psi P_{cp}}{\sigma^2}. \tag{3.30}$$

The variance of γ is thus given as

$$\sigma_\gamma^2 = \mathrm{var}[\gamma] = \left(\frac{\psi P_{cp}}{n_t \sigma^2}\right)^2 \mathrm{var}\left(\|\mathbf{h}\|_F^2\right) = \frac{1}{n_t}\left(\frac{2\psi P_{cp}}{\sigma^2}\right)^2. \tag{3.31}$$

Using a Taylor series, we expand Equation (3.2) at μ_γ and have

$$C_{out}(\gamma) = B(1-\alpha)\log_2\left(1+\mu_\gamma\right) - \sum_{k=1}^{\infty} \frac{B(1-\alpha)}{k\ln 2}\left(\frac{\mu_\gamma - \gamma}{1+\mu_\gamma}\right)^k. \tag{3.32}$$

We now calculate the mean value of the outage capacity μ_C. The second-order approximation for μ_C is given by

$$\mu_C = \mathrm{E}[C_{out}] \approx B(1-\alpha)\log_2\left(1+\mu_\gamma\right) - \frac{B(1-\alpha)}{2\ln 2}\left(\frac{\sigma_\gamma}{1+\mu_\gamma}\right)^2. \tag{3.33}$$

By expanding C_{out}^2 in a Taylor series at μ_γ, we have the second-order approximation for σ_C^2 given as

$$\sigma_C^2 = \mathrm{E}\left[C_{out}^2\right] - (\mathrm{E}[C_{out}])^2 \approx \left(\frac{B(1-\alpha)}{\ln 2}\right)^2 \left(\frac{\sigma_\gamma^2}{\left(1+\mu_\gamma\right)^2} - \frac{\sigma_\gamma^4}{4\left(1+\mu_\gamma\right)^4}\right). \tag{3.34}$$

We use a Gaussian approximation and assume that the approximate channel capacity $\tilde{C}_{out}$ follows a normal distribution with a mean μ_C and standard deviation σ_C. The approximate outage probability $\tilde{p}_{out}$ is defined as

$$\tilde{p}_{out} = \Pr\left(C < \tilde{C}_{out}\right) = \frac{1}{2} + \frac{1}{2}\mathrm{erf}\left(\frac{\tilde{C}_{out} - \mu_C}{\sqrt{2}\sigma_C}\right), \tag{3.35}$$

where $\mathrm{erf}(\cdot)$ is the error function. Therefore the approximate outage channel capacity is given by

$$\tilde{C}_{out} = \mu_C + \sqrt{2}\sigma_C \mathrm{erf}^{-1}(2\tilde{p}_{out} - 1), \tag{3.36}$$

where $\mathrm{erf}^{-1}(\cdot)$ is the inverse error function, which can also be defined in terms of the Maclaurin series.

$$\mathrm{erf}^{-1}(z) = \frac{\sqrt{\pi}}{2}\left(z + \frac{\pi}{12}z^3 + \frac{7\pi^2}{480}z^5 + \cdots\right). \tag{3.37}$$

By using the definition in Equation (3.37), the approximate average outage capacity $\hat{C}_{out}$ is given by

$$\hat{C}_{out} = B(1 - \tilde{p}_{out})\tilde{C}_{out} \approx \frac{B(1-\tilde{p})}{2}\left(\mu_C + \sqrt{\frac{\pi}{2}}\sigma_C\left(\tilde{p} + \frac{\pi}{12}\tilde{p}^3 + \frac{7\pi^2}{480}\tilde{p}^5\right)\right), \tag{3.38}$$

where $\tilde{p} = 2\tilde{p}_{out} - 1$.

Based on the channel approximation, we proposed an approximate dynamic power control (ADPC) algorithm. In the ADPC algorithm, we simply substitute $\hat{C}_{out}$ for $\bar{C}_{out}$ and $\tilde{p}_{out}$ for p_{out} respectively. The optimization of $\hat{C}_{out}$ is denoted as

$$\begin{aligned} &\hat{C}^*_{out} = \max_{\tilde{p}_{out}}\left(B(1-\tilde{p}_{out})\tilde{C}_{out}\right) \approx \max_{\tilde{p}}\left(\tfrac{B(1-\tilde{p})}{2}\left(\mu_C + \sqrt{\tfrac{\pi}{2}}\sigma_C\left(\tilde{p} + \tfrac{\pi}{12}\tilde{p}^3 + \tfrac{7\pi^2}{480}\tilde{p}^5\right)\right)\right) \\ &\text{s.t.} \quad \hat{C}^*_{out} \geq R, -1 < \tilde{p} \leq 1 - \tfrac{2(N-1)L}{RD}. \end{aligned} \tag{3.39}$$

Compared with Equation (3.16), it is clear that Equation (3.39) is a polynomial function on $\tilde{p}$ and thus has a closed-form solution for the optimization of $\hat{C}_{out}$. The solution to Equation (3.39) is straightforward, so the ADPC algorithm can significantly reduce the computational complexity and storage cost.

3.5 Simulation Results

In this section, simulation results are given to show the efficiency of the DPC and the ADPC algorithm. We also show that the ADPC algorithm provides accurate channel estimations. The parameters used in the simulation are given in Table 3.1.

We first investigate the performance of the DPC and the ADPC algorithm. In Fig. 3.3, we show that in the DPC algorithm $P_{ct|n_t}$ converges to its optimal value $P^*_{ct|n_t}$ with a suffi-

Table 3.1 Parameters for simulation

Symbol	Description	Value
α	Fraction of time	0.25
β	Path loss constant	1
θ	Path loss exponent	2
ζ	Free space path loss constant	1
n	Number of sensors per cluster	10
d	Transmission distance	100 m
B	Channel bandwidth	1 MHz
$r_{\max}$	Cluster range	10 m
σ^2	Noise power	5 μW
$P_{cp}^{\max}$	Maximum of P_{cp}	200 mW
π_0	Initial step in DPC algorithm	10 mW
M	Parameter defining initial step π_0	20
I	Maximum number of iterations	30
P_c	Circuit power consumption	10 mW
R	Data rate requirement	1 Mbps
N	Number of clusters	9
L	Packet length	1000 bits

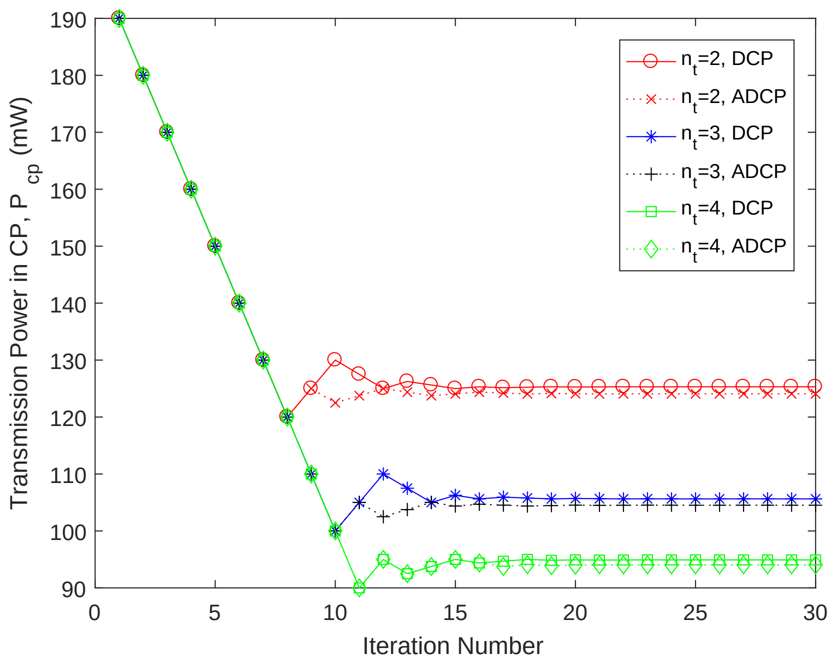

Fig. 3.3 Performance of the DPC and ADPC algorithm with different values of n_t.

ciently small difference in a low number of iterations (e.g., 20 iterations in Fig. 3.3). We also show that the ADPC algorithm has near-optimal performance compared with the DPC algorithm. The cooperation of wireless nodes can provide spatial diversity and channel gain to the receiver which improves the channel quality and thus reduces the transmission power consumption. As we can see in Fig. 3.3, the optimal cooperative transmission power $P^*_{ct|n_t}$ decreases with increasing number of cooperative nodes n_t.

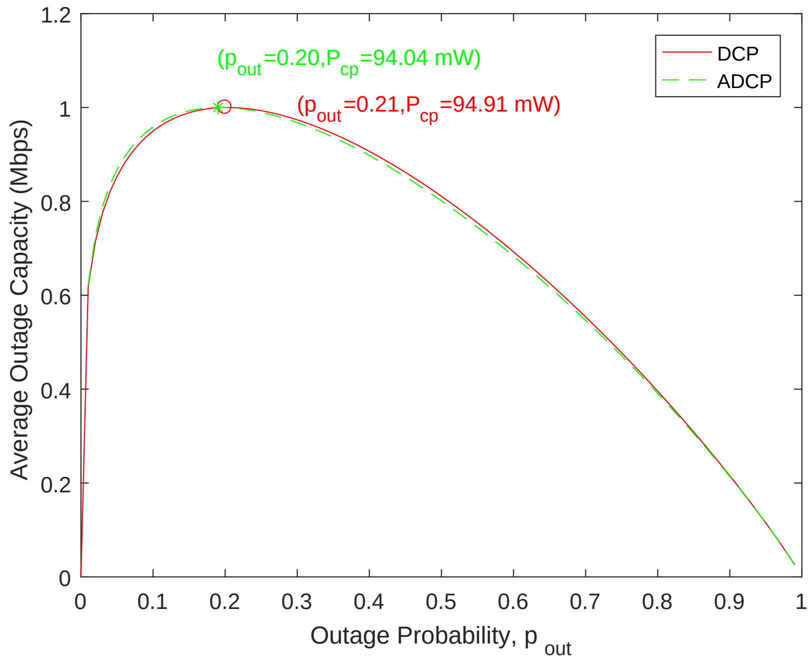

Fig. 3.4 Average outage capacity with different p_{out} for $n_t = 4$.

We then compare the accuracy of the ADPC algorithm with the DPC algorithm. We set the number of cooperative nodes as $n_t = 4$ and the maximum number of iterations as $I = 30$. In Fig. 3.4, we show that under the QoS requirement on the data rate, there exists an optimal outage probability p^*_{out} that can maximize the average outage capacity $\bar{C}_{out}$. In this case, by using the DPC algorithm, we get the optimal average outage capacity $\bar{C}^*_{out} = 1$ Mbps at $p^*_{out} = 0.21$ where $P^*_{ct|n_t} = P_{ct|n_t,I} = 94.91$ mW. On the other hand, the ADPC algorithm finds the optimal approximate average outage capacity $\hat{C}^*_{out} = 1$ Mbps at $p^*_{out} = 0.20$ where $P^*_{ct|n_t} = P_{ct|n_t,I} = 94.04$ mW. Thus we have shown that the ADPC algorithm is a good approximation for the outage channel capacity and gives a near-optimal solution for the power control problem.

We further analyze the relationships between the average outage capacity, the outage probability and the transmission power level. We set the number of cooperative nodes as $n_t = 4$. Fig. 3.5 shows that given any p_{out}, C_{out} increases with P_{cp}. We can also see that

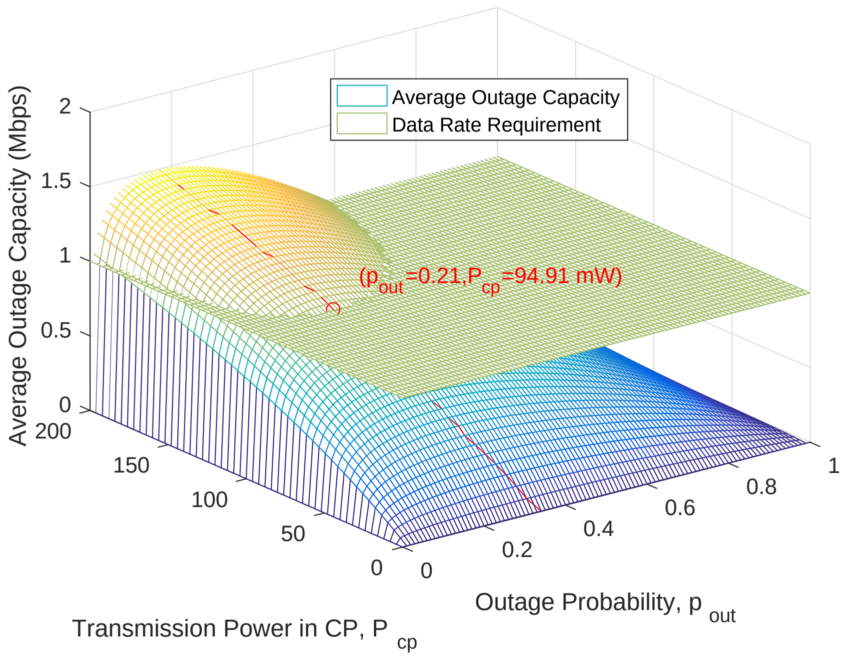

Fig. 3.5 Average outage capacity with different p_{out} and P_{cp} for $n_t = 4$.

given any P_{cp}, there exists a p_{out} that maximizes C_{out}. For every P_{cp}, we mark the maximum $\bar{C}^*_{out}$ as a function of p_{out} and P_{cp} with the red line l_1 in Fig. 3.5. With the QoS requirement (R,D), the optimal P_{cp} is given by the intersection of the average outage capacity surface and the data rate requirement surface. The solution is where l_1 cuts the previously identified P_{cp} locus and has been marked with a red circle. Note that the value of the optimal P_{cp} and other values match with those given previously in Fig. 3.4.

We also show that with the increasing number of cooperative wireless nodes n_t, the optimal outage probability p^*_{out} decreases. The simulation result is shown in Fig. 3.6. Note that for different values of n_t, the optimal outage probability should also fulfill the QoS constraints (R,D), namely $0 < p^*_{out} \leq 1 - \frac{(N-1)L}{RD}$.

The total power consumption of each cluster is given in Fig 3.7. While the transmission power decreases with the increasing number of cooperative nodes, the total circuit power consumption increases with the number of cooperative nodes, consequently, there exists an optimal number of cooperative nodes that minimizes the total power consumption of each cluster. In this case, we show that under the QoS data rate requirement $R = 1$ Mbps, the minimum total power consumption is 109.40 mW with 3 cooperative wireless nodes. Note that the optimal outage probability p^*_{out} should fulfill the QoS constraints (R,D) as discussed in Fig. 3.6. If for $n^*_t = 3$, p^*_{out} is out of range ($p^*_{out} > 1 - \frac{(N-1)L}{RD}$), then the optimal number of cooperative nodes n^*_t should be the smallest n_t that fulfills the QoS requirement.

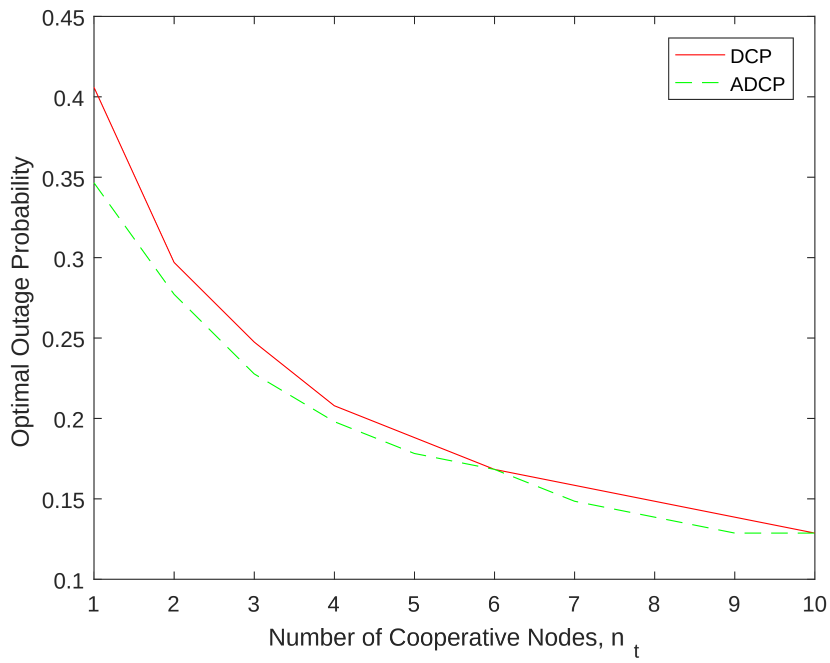

Fig. 3.6 Optimal outage probability with different values of n_t.

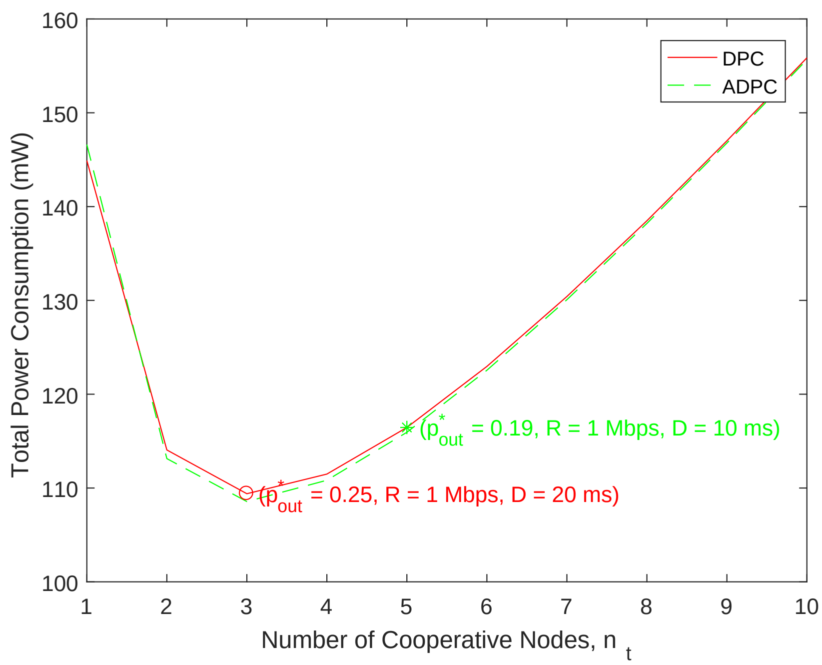

Fig. 3.7 Total power consumption of the DPC and ADPC algorithm with different values of n_t.

From Fig. 3.6, we can see that p^*_{out} decreases with increasing n_t. In this case, we set $N = 9$ and $L = 1000$ bits. For the QoS constraint $R = 1$ Mbps and $D = 20$ ms, we have $1 - \frac{(N-1)L}{RD} = 0.6$ and $p^*_{out}(n_t = 3) = 0.25 < 0.6$. Therefore, $n_t = 3$ is the optimal number of cooperative nodes. For the QoS constraint $R = 1$ Mbps and $D = 10$ ms, since we have $1 - \frac{(N-1)L}{RD} = 0.2$ and $p^*_{out}(n_t = 3) = 0.25 > 0.2$, $n_t = 3$ cannot fulfill the QoS requirement. We find $n_t = 5$ to be the optimal number of cooperative nodes which has the least total power consumption without violating the QoS constraints.

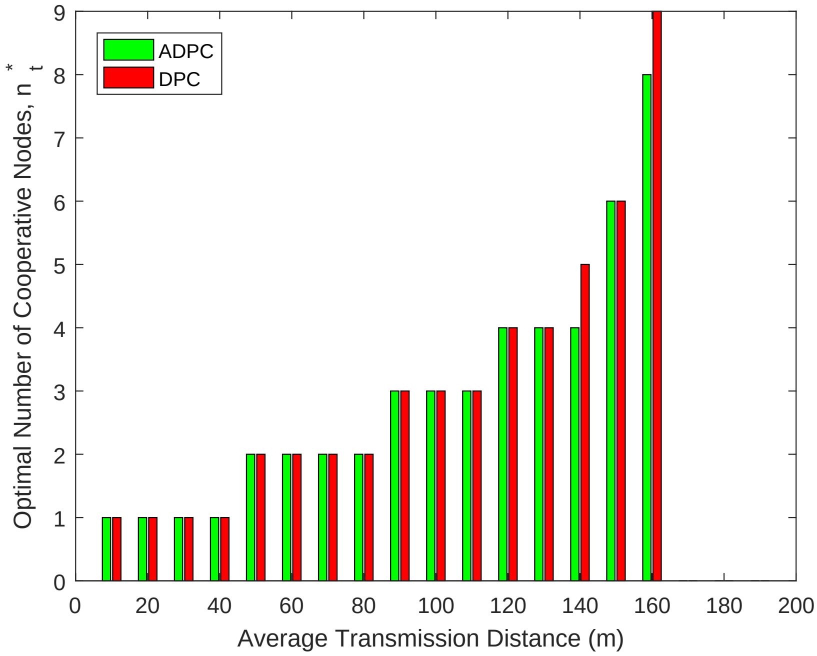

Fig. 3.8 Optimal number of cooperative nodes with different transmission distances.

Then we consider the effects of different transmission distances with QoS constraints and show that long-range communication can benefit from our cooperative transmission scheme. We use the settings given in Table 3.1 and vary the transmission distance d. Fig. 3.8 shows that for short-range cluster-to-cluster communication ($d \leq 40$ m) the SISO transmission scheme outperforms cooperative transmission scheme. As for long-range cluster-to-cluster communication ($d > 40$ m), cooperative transmission scheme is more energy-efficient compared with SISO transmission scheme under QoS constraint $R = 1$ Mbps and $D = 20$ ms. Note that for extra long-range transmission ($d > 160$ m), there is no optimal number of cooperative nodes as no cooperative scheme can fulfill the QoS requirements. The optimal total power consumption with different transmission distances is given in Fig. 3.9. It is clear that the optimal total power consumption increases as the transmission distance increases. Note that the ADPC algorithm can achieve near-optimal results

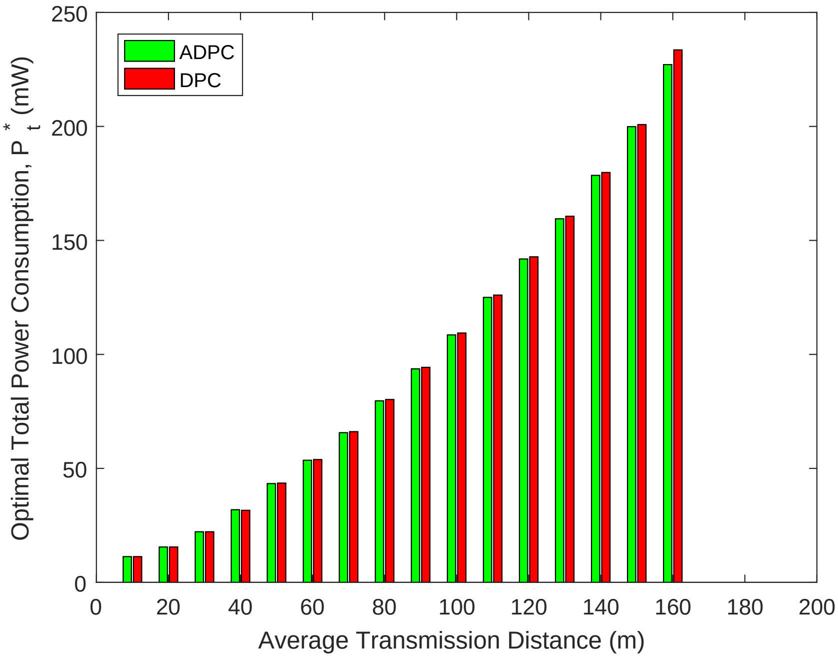

Fig. 3.9 Optimal total power consumption with different transmission distances.

compared with the DPC algorithm for reasonable transmission distance ($d < 120$ m). The performance of the ADPC algorithm degrades as the the transmission distance increases.

Finally, the impact of the time fraction variable α is shown in Fig. 3.10 and Fig. 3.11. We use the simulation parameters in Table 3.1 and vary the time fraction component α. Fig. 3.10 shows that the larger α gets the greater is the number of cooperative nodes required for the optimal performance. This is because that the average outage channel capacity is inversely correlated with α. Therefore, for larger alpha we need more cooperative nodes to achieve the same average data rate. From Fig. 3.11, we notice that there exists an α^* that can minimize the total power consumption. In this case, we have $\alpha^* = 0.15$. If α is smaller than α^*, the total power consumption increases dramatically as α decreases to zero since the cluster head will need a lot of power to broadcast the transmission message in a very limited time. When α is greater than α^*, the cluster head will need more cooperative nodes to achieve the QoS requirements as α increases to one. Note that when α increases beyond 0.55, the cooperative transmission scheme may fail to achieve the QoS requirements due to the limited number of nodes in each cluster.

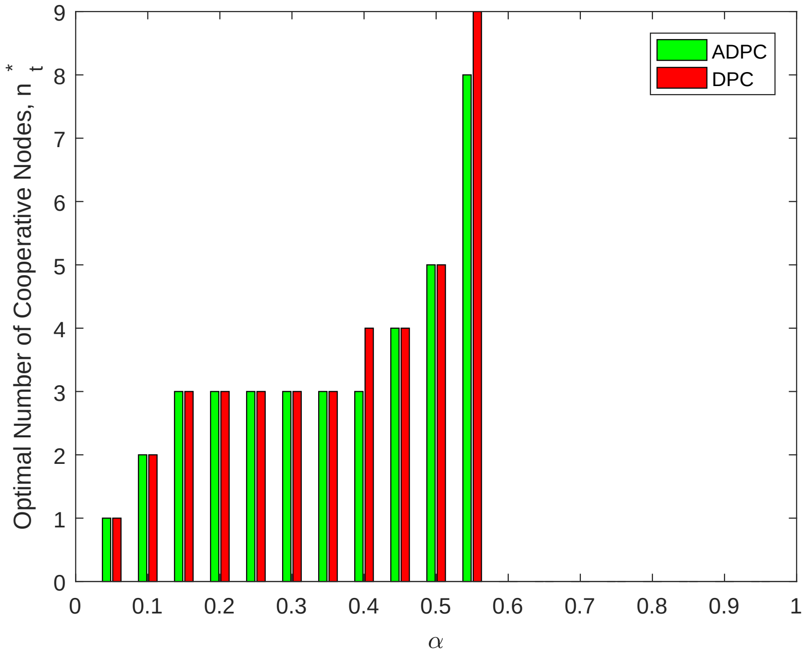

Fig. 3.10 Optimal number of cooperative nodes with different α.

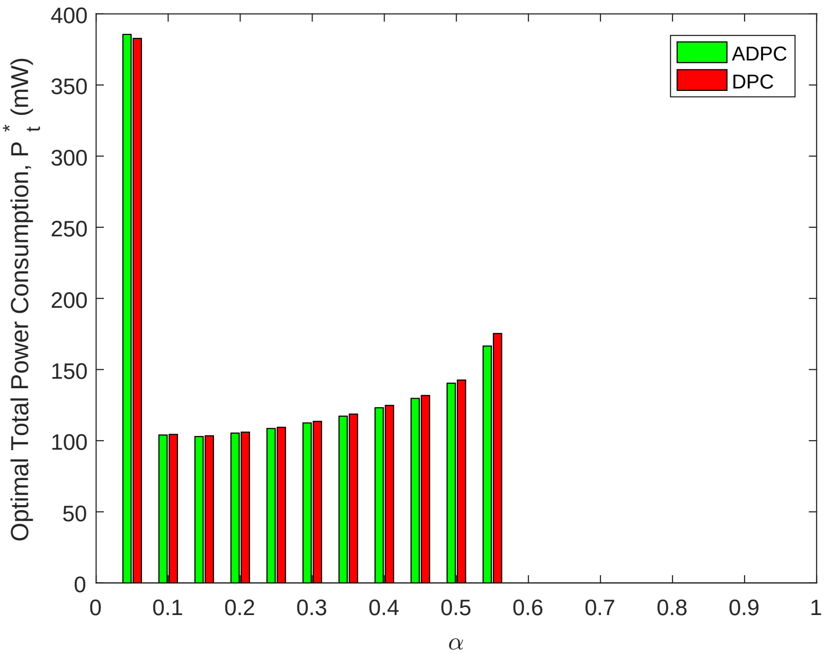

Fig. 3.11 Optimal total power consumption with different α.

3.6 Summary

In this chapter, we considered the power control and optimization problems of a multi-hop cluster-based wireless sensor networks with QoS constraints on average data rate and average delay. We first formulated the power control problem as a dynamic optimization problem. A cooperative transmission scheme was proposed to improve the energy efficiency and minimize the total power consumption of the multi-hop transmission under QoS constraints.

In Section 3.4, the DPC was proposed to solve the power control and optimization problem under certain QoS constraints. We have proved that the DPC algorithm can converge to the optimal solution with sufficiently small difference in $O(1)$ iterations. To reduce the computational complexity of the DPC algorithm, we further proposed an ADPC algorithm that can achieve a near-optimal result. We showed that the ADPC algorithm has a closed-form solution to the power control and optimization problem which significantly reduced the computational complexity and storage cost.

The simulation results are shown in Section 3.5. We first compared and analyzed the performance of DPC and ADPC algorithms in Fig. 3.3. We showed that both DPC and ADPC converge to the optimal and near-optimal power level, respectively. Then we showed that there exists a p_{out} that can maximize the average outage capacity and both DPC and ADPC are able to find the maximum average outage capacity. We also investigated the optimal outage probability and the total power consumption with different number of cooperative nodes in Fig. 3.6 and Fig. 3.7. Finally, the impact of the transmission distance and time fraction variable α were presented in Figs. 3.8 to 3.11.

Chapter 4

Competitive Distributed Spectrum Access for QoS-Constrained Wireless Networks

4.1 Introduction

Cognitive radio has been considered as a method to enhance spectrum efficiency by allowing secondary users (SUs) to utilize the vacant licensed channels of primary users (PUs) without causing severe interference to the PUs [77]. In a large-scale cooperative cognitive radio network (CRN), PUs voluntarily provide their vacant channels to SUs and allocate the channels based on the channel quality and QoS requirements to improve the network throughput. Since it is unlikely to have a central controller to manage the licensed channels in a large-scale CRN, it is important to design efficient distributed dynamic spectrum access methods for both PUs and SUs.

Dynamic spectrum access is an important issue in CRNs and has been studied previously on many occasions [78–80]. In existing work, game-theoretic algorithms have been widely used to address spectrum access problems in wireless communication networks [81–84]. In [82], the authors propose an equilibrium pricing scheme to solve the competitive spectrum access problem for a cognitive radio network. The authors in [83] formulate the dynamic spectrum access problem as a Stackelberg game and solve it by finding the Nash equilibrium. In [84], two local interaction games are proposed to solve the dynamic spectrum access problem. All these classic game theory algorithms require knowledge of actions of all participants and thus are not suitable for practical implementation. Matching theory is considered as a promising method to solve distributed resource allocation problems because some matching algorithms have near-optimal performance and can be implemented in a distributed way [85]. In this chapter, we consider the dynamic spectrum access problem for a QoS-constrained large-scale CRN. Two matching algorithms are proposed that provide near-optimal solutions to dynamic spectrum access problems. We also give distributed implementation of our algorithms and verify their performance via simulations. Most of the results in this chapter are published in the IEEE Global Communications Conference (GLOBECOM) 2016 conference proceedings [15].

The rest of the chapter is organized as follows: In Section 4.2, we describe the system model of a cooperative CRN and express the QoS requirements with a utility function. In Section 4.3, we formulate the dynamic spectrum access problem as a matching problem and give the definition of a stable matching. In Section 4.4, we propose the distributed spectrum access scheme. We give the implementation of the distributed matching algorithm at both the SU and the PU. To reduce the number of message exchanges in the network during the dynamic spectrum access procedure, a fast distributed spectrum access scheme is proposed. We give the simulation results in Section 4.5. Finally, Section 4.6 concludes the chapter.

4.2 System Model and Problem Formulation

We consider a cooperative cognitive radio network with an opportunistic spectrum access model and QoS constraints as shown in Fig. 4.1. In this scenario, SUs are allowed to access vacant channels of the PUs without interfering with the PUs. SUs with assigned vacant channels can communicate with their node receivers under specified QoS constraints. We assume that there are M PUs and N SUs denoted by $\mathbf{PU} = \{PU_1, PU_2, \ldots, PU_M\}$ and $\mathbf{SU} = \{SU_1, SU_2, \ldots, SU_N\}$ respectively. It is also assumed that there are a set of K licensed channels denoted by $\mathbf{CH} = \{CH_1, CH_2, \ldots, CH_K\}$. Each $PU_i \in \mathbf{PU}$ occupies a set of K_i licensed channels denoted by $\mathbf{CH_i}$. Therefore, $\mathbf{CH_1}, \mathbf{CH_2} \ldots, \mathbf{CH_M}$ is a partition of $\mathbf{CH}$ where $\sum_{i=1}^{M} K_i = K$. A time division duplex (TDD) scheme is used by the uplink and downlink communications of all users (both the PUs and the SUs) and their corresponding node receivers. When PUs occupy the licensed channels, all channels are used for their transmission. When the licensed channels are vacant, they can be allocated to different SUs by the idle PUs. Each SU can only access one vacant channel of a PU in a time slot.

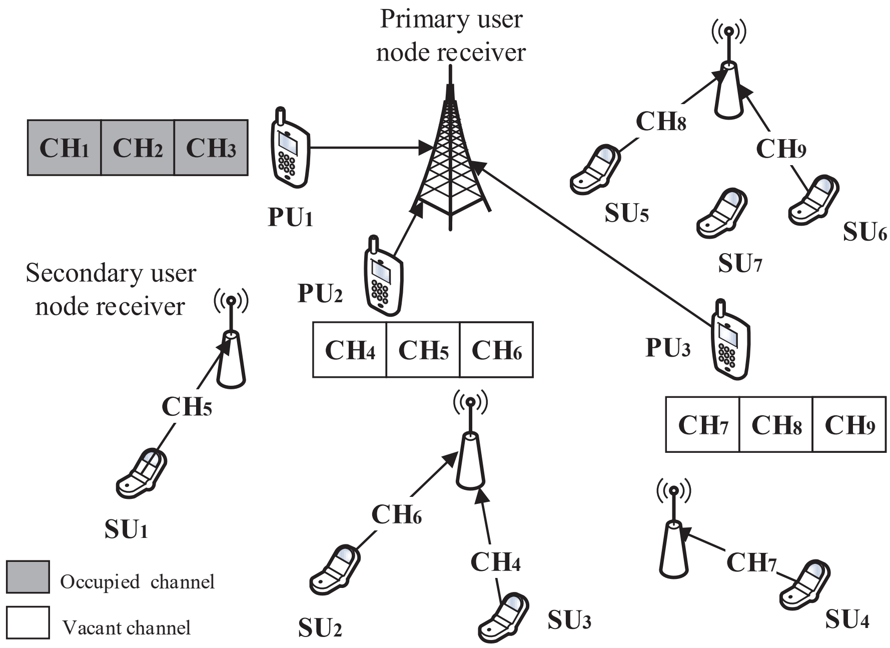

Fig. 4.1 A cooperative cognitive radio network.

4.2.1 QoS Constraints

There are various QoS requirements for different applications. For each $SU_i \in \mathbf{SU}$, let R_i, D_i, ε_i denote the QoS constraints on the average data rate, delay and packet error rate respectively. Consider the transmission between SU_i and its node receiver. Let $C_{i,j}$ be the channel capacity of SU_i on vacant channel CH_j. The channel capacity $C_{i,j}$ is denoted as

$$C_{i,j} = B\log_2\left(1+\gamma_{i,j}\right), \tag{4.1}$$

where B is the channel bandwidth and $\gamma_{i,j}$ is the signal-to-noise ratio (SNR) at SU_i's node receiver. The SNR $\gamma_{i,j}$ is given by

$$\gamma_{i,j} = \frac{P_i\left|h_{i,j}\right|^2}{\beta d_i^{\theta}\sigma^2}, \tag{4.2}$$

where P_i is the transmission power of SU_i, $\left|h_{i,j}\right|^2$ is the instantaneous fading channel gain between SU_i and its node receiver, d_i is the distance between SU_i and its receiver, β is the path loss constant, θ is the path loss exponent and σ^2 is the noise power at the receiver.

We take the average data rate and delay as the two most important factors contributing to the QoS constraints. For SU_i, its QoS constraints are expressed as (R_i, D_i). The vacant channel CH_j is acceptable to SU_i if and only if

$$R_i \leq C_{i,j}, \tag{4.3}$$

and

$$D_i \geq \frac{L}{p_j R_i (1-\varepsilon_i)}, \tag{4.4}$$

where L is the packet length in bits and p_j is the probability that CH_j stays vacant during the transmission. Therefore, we must have

$$C_{i,j} \geq R_i \geq \frac{L}{p_j D_i (1-\varepsilon_i)}, \tag{4.5}$$

for QoS constraints (R_i, D_i). We also know that a channel CH_j is acceptable to SU_i if

$$p_j \geq \frac{L}{R_i D_i (1-\varepsilon_i)} = p_i^*, \tag{4.6}$$

where p_i^* is the threshold of the probability of channel availability.

4.2.2 Utility Function

We further propose a utility function to measure the network performance and QoS constraints. We define the utility function $U_{i,j}$ for SU_i with CH_j as

$$U_{i,j} = C_{i,j} - \lambda R_i, \tag{4.7}$$

where λ is the coefficient to adjust the weighting of the QoS constraints. Setting $\lambda = 1$ denotes a balanced QoS requirement in Equation (4.5). We can decrease λ to relax the QoS requirement or increase it for a stricter QoS requirement. Since we have N SUs and K licensed channels, we use an $N \times K$ matching matrix Π to denote the channel assignment. The matrix element $\pi_{i,j} \in \Pi$ is set to be 1 when CH_j is assigned to SU_i and 0 otherwise.

With QoS constraints (R_i, D_i), we aim to find a spectrum access scheme for the SUs that can maximize their utility without violating their QoS constraints. The optimization problem is thus expressed as:

$$
\begin{aligned}
\Pi^* = &\arg\max_{\Pi} \sum_{SU_i \in \mathbf{SU}} \sum_{CH_j \in \mathbf{CH}} U_{i,j} \\
\text{s.t.} \quad & \sum_{SU_i \in \mathbf{SU}} \pi_{i,j} \leq 1, \ \ \forall j \in \{1, 2, \ldots, K\} \\
& \sum_{CH_j \in \mathbf{CH}} \pi_{i,j} \leq 1, \ \ \forall i \in \{1, 2, \ldots, N\} \\
& \sum_{SU_i \in \mathbf{SU}} \sum_{CH_j \in \mathbf{CH_k}} \pi_{i,j} \leq K_k, \ \ \forall k \in \{1, 2, \ldots, M\}.
\end{aligned}
\tag{4.8}
$$

4.3 Optimal Solution and Matching Theory

4.3.1 Optimal Solution

The optimization problem in Equation (4.8) is a typical assignment problem where the Hungarian algorithm [61] can provide the optimal solution. However, the Hungarian algorithm is a centralized algorithm with $O\left(n^4\right)$ time complexity. For large-scale and densely deployed wireless networks, a distributed algorithm is more practical to handle the distributed access requests. Thus we propose the distributed matching algorithm to solve the assignment problem in Equation (4.8).

4.3.2 Matching Definition

A matching is defined as an allocation between resources and users [85]. In this case, a matching is a solution to the assignment problem in Equation (4.8) where SUs are matched with the licensed channels of PUs. Based on this scenario, we give the definition of a matching as follows:

Definition 4.3.1. We define a matching function $\mathscr{M}$ as: $\mathbf{SU} \rightarrow \mathbf{CH} \cup \{\emptyset\} \times \mathbf{PU} \cup \{\emptyset\}$, $\mathbf{PU} \rightarrow \mathbf{SU} \cup \{\emptyset\}$ and $\mathbf{CH} \rightarrow \mathbf{SU} \cup \{\emptyset\}$, such that for all $SU_i \in \mathbf{SU}$, $CH_j \in \mathbf{CH}$ and $PU_k \in \mathbf{PU}$:

1. $\mathscr{M}(SU_i) = \left(CH_j, PU_k\right) \in \mathbf{CH} \cup \{\emptyset\} \times \mathbf{PU} \cup \{\emptyset\}$, $CH_j \in \mathbf{CH}_k$ and $|\mathscr{M}(SU_i)| \in \{0, 1\}$.

2. $\mathscr{M}\left(CH_j\right) = SU_i \in \mathbf{SU} \cup \{\emptyset\}$, and $\left|\mathscr{M}\left(CH_j\right)\right| \in \{0, 1\}$, where $\mathscr{M}\left(CH_j\right) = SU_i \Leftrightarrow \mathscr{M}(SU_i) = \left(CH_j, PU_k\right), \forall CH_j \in \mathbf{CH_k}$.

3. $\mathscr{M}(PU_k) \subset \mathbf{SU} \cup \{\emptyset\}$, and $|\mathscr{M}(PU_k)| \leq K_k$, where if $\mathscr{M}\left(CH_j\right) = SU_i \in \mathbf{SU}$ and $CH_j \in \mathbf{CH}_k$, then $SU_i \in \mathscr{M}(PU_k), \forall SU_i \in \mathbf{SU}$.

For all $SU_i \in \mathbf{SU}$, $CH_j \in \mathbf{CH_k}$ and $PU_k \in \mathbf{PU}$, if $\mathscr{M}(SU_i) = \left(CH_j, PU_k\right)$ and $|\mathscr{M}(SU_i)| = 1$, we have $\pi_{i,j} = 1$ and we say SU_i is matched with CH_j of PU_k. If $\mathscr{M}\left(CH_j\right) = SU_i \in \mathbf{SU}$

and $\left|\mathscr{M}\left(CH_j\right)\right| = 1$, we have $\pi_{i,j} = 1$ and we say CH_j is matched with SU_i. For $PU_k \in \mathbf{PU}$, $\mathscr{M}\left(PU_k\right)$ is matched with a set of SUs which contains zero, one or multiple SUs. We say PU_k is undersubscribed, full or oversubscribed according to whether $\left|\mathscr{M}\left(PU_k\right)\right| = \sum\limits_{SU_i \in \mathbf{SU}} \sum\limits_{CH_j \in \mathbf{CH_k}} \pi_{i,j}$ is less than, equal to or greater than K_k, respectively.

4.3.3 Stable Matching

We say a matching is stable if it contains no blocking pairs. We define a blocking pair as follows:

Definition 4.3.2. A pair $\left(SU_i, CH_j\right)$ is a blocking pair of matching $\mathscr{M}$ if:

1. CH_j is acceptable to SU_i (i.e., SU_i prefers to be matched with CH_j rather than staying unmatched).

2. Either SU_i is unmatched or SU_i prefers $\left(CH_j, PU_k\right)$ to its matched channel and PU $\mathscr{M}\left(SU_i\right)$.

3. Either CH_j is unmatched, or CH_j is matched and PU_k prefers SU_i to its matched SU $\mathscr{M}\left(CH_j\right)$.

From the above definitions, we know that a matching $\mathscr{M}$ corresponds to a valid matching matrix $\Pi_{\mathscr{M}}$ which is in accordance with the conditions in Equation (4.8). In the next section, we propose a distributed spectrum access scheme that can help the SUs and PUs form a stable matching with reasonable complexity. The distributed spectrum access scheme is based on the idea of a greedy algorithm. Simulation results show that a stable matching corresponds to at least a sub-optimal solution of Equation (4.8).

4.4 Competitive Distributed Spectrum Access

4.4.1 Distributed Spectrum Access Scheme

All SU node receivers monitor the PUs and their licensed channels in its vicinity. If there is a vacant channel detected, the SU node receiver will send a ready for data (RD) message along with the channel state information (CSI) to the corresponding SU through a separate control channel. The CSI is obtained from either the training sequence or historical data. The SU will build a preference list of the vacant channels based on the CSI after it receives the RD message. The SU will wait for $T_{SU} = \frac{T_{\max}}{1+\gamma_{\max}}$ where $T_{\max}$ is the maximum waiting time and $\gamma_{\max}$ is the largest SNR of all available vacant channels. After the waiting period, the SU will send a channel access request (CAR) message to the PU that has the best channel on its preference list. The PU will assign the requested channel to the SU if (i) the channel has not been assigned, or (ii) if the SU has a larger utility than the previous SU holding the channel, i.e., the PU will remove the previous SU from its assignment list and reassign the channel to the new SU. The PU's decisions of acceptance or refusal are sent to the SUs via the acknowledgement of acceptance (ACK-A) and the acknowledgement of refusal (ACK-R) messages respectively. If a channel is assigned to an SU, it will wait until it receives an algorithm termination (AT) message or an ACK-R message. If an SU receives an AT message, it starts its data transmission via the assigned vacant channel. Otherwise, the SU will send a CAR message to the PU that has the next best channel in its preference list. The AT message is sent by any PU if the PU doesn't receive a CAR message for a pre-defined period of time T_{PU}.

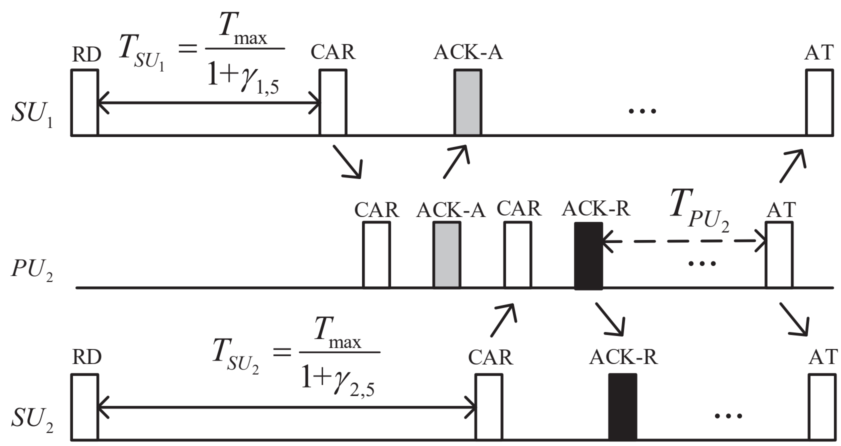

Fig. 4.2 Typical message exchanges of the distributed spectrum access scheme.

Typical message exchanges of the distributed spectrum access scheme is shown in Fig. 4.2. Considering the scenario in Fig. 4.1, we assume that the node receiver of SU_1 and SU_2 monitor the licensed channel of PU_2. When the licensed channels ($CH_4 - CH_6$) become vacant, the node receivers of SU_1 and SU_2 send RD message through a control channel to their corresponding SUs (SU_1 and SU_2) respectively. We assume that both SU_1 and SU_2 apply for CH_5 of PU_2 and we have $\gamma_{1,5} > \gamma_{2,5}$ as well as $U_{1,5} > U_{2,5}$. After receiving RD messages from their node receivers, SU_1 waits for $T_{SU_1} = \frac{T_{\max}}{1+\gamma_{1,5}}$ and SU_2 waits for $T_{SU_2} = \frac{T_{\max}}{1+\gamma_{2,5}}$. Since we assume $\gamma_{1,5} > \gamma_{2,5}$, SU_1 sends its CAR first for CH_5 to PU_2. As this is the first CAR for CH_5, PU_2 sends an ACK-A to SU_1. Then PU_2 receives a CAR for CH_5 from SU_2. Since CH_5 has been assigned to SU_1 and we assume that $U_{1,5} > U_{2,5}$, PU_2 sends an ACK-R to SU_2. After being refused by PU_2, SU_2 keeps sending CARs to PUs for other vacant channels. It will not stop until it receives an ACK-A or AT. After sending the last ACK message (ACK-A or ACK-R), PU_2 will wait for T_{PU_2}. If there is no new CAR sent to PU_2 during that time (T_{PU_2}), PU_2 will send an AT message to all the SUs in its vicinity. Although the waiting period can eliminate most contention among different SUs, we still need to consider the possibility of collisions. If an SU fails to receive an ACK after sending CAR, it assumes that its CAR has collided with other CARs. The SU will wait for a time period based on the binary exponential backoff described in CSMA/CA [86] before retransmitting the CAR.

4.4.2 Distributed Matching Algorithm

We propose the distributed matching (DM) algorithm to implement the distributed spectrum access scheme. The DM algorithm at the SU and the PU are given in Algorithm 4.1 and Algorithm 4.2 respectively.

Algorithm 4.1 Distributed Matching Algorithm at the SU

Initialization for SU_i:
Build SU_i's preference list $list(CH)$ through message exchanges based on the utility function, $state(SU_i) = free$, $state(AT) = false$, $\mathscr{M}(SU_i) = (\emptyset, \emptyset)$.
while $state(AT) = false$ **do**
  if $state(SU_i) = free$ and $list(CH) \neq \emptyset$ **then**
    $CH_j = best(list(CH))$, wait for T_{SU_i},
    $send\left(CAR, SU_i, CH_j\right)$ to PU_k where $CH_j \in \mathbf{CH}_k$.
  else if $get\left(MSG, CH_j, PU_k\right) = true$ **then**
    if $MSG = ACK-A$ **then**
      $\mathscr{M}(SU_i) = \left(CH_j, PU_k\right)$, $state(SU_i) = occupied$.
    else if $MSG = ACK-R$ **then**
      Remove CH_j from $list(CH)$, $\mathscr{M}(SU_i) = (\emptyset, \emptyset)$, $state(SU_i) = free$.
    else if $MSG = AT$ **then**
      $state(AT) = true$.
    end if
  end if
end while

We prove that the DM algorithm always generate a stable matching $\mathscr{M}^*$ that maximizes the total utility among all stable matchings. We first give some lemmas as follows:

Lemma 4.4.1. *With N SUs, M PUs and K licensed channels, the distributed matching algorithm always generates a matching within $O(NK)$ message exchanges.*

Proof. For any $SU_i \in \mathbf{SU}$, it can apply for CH_j at most once as it will remove CH_j from its preference list if it is refused. The total number of CARs SU_i can send is limited by the

Algorithm 4.2 Distributed Matching Algorithm at the PU

Initialization for PU_k:
$state\left(PU_k\right) = free,\ state\left(CH_j \in \mathbf{CH}_k\right) = free,\ \mathscr{M}\left(CH_j \in \mathbf{CH}_k\right) = \emptyset,\ \mathscr{M}\left(PU_k\right) = \emptyset,$
$timer\left(PU_k\right) = T_{PU}$.
while $state\left(PU_k\right) = free$ and $timer\left(PU_k\right) > 0$ **do**
  $timer\left(PU_k\right)$ counts down.
  if $get\left(CAR, SU_i, CH_j\right) = true$ **then**
    $timer\left(PU_k\right) = T_{PU}$.
    if $state\left(CH_j\right) = free$ **then**
      $send\left(ACK-A, CH_j, PU_k\right)$, $state\left(CH_j\right) = occupied$, $\mathscr{M}\left(CH_j\right) = SU_i$, add SU_i to $\mathscr{M}\left(PU_k\right)$.
    else if SU_i has larger utility than $\mathscr{M}\left(CH_j\right)$ **then**
      $send\left(ACK-A, CH_j, PU_k\right)$ to SU_i.
      $send\left(ACK-R, CH_j, PU_k\right)$ to $\mathscr{M}\left(CH_j\right)$.
      Remove $\mathscr{M}\left(CH_j\right)$ from $\mathscr{M}\left(PU_k\right)$, $\mathscr{M}\left(CH_j\right) = SU_i$, add SU_i to $\mathscr{M}\left(PU_k\right)$.
    else
      $send\left(ACK-R, CH_j, PU_k\right)$ to SU_i.
    end if
  end if
end while
$send\left(AT, CH_j \in \mathbf{CH}_k, PU_k\right)$ to all SUs.

length of its preference list. It is obvious that the maximum length of SU_i's preference list is K. If no CAR is received by the PUs, the AT message will be sent by the PUs after the pre-defined time T_{PU}. Based on the Definition 4.3.1, it is obvious that the DM algorithm generates a matching and terminates within $O\left(NK\right)$ message exchanges. □

Lemma 4.4.2. *For any $SU_i \in \mathbf{SU}$, if CH_j is deleted from SU_i's preference list during the distributed matching algorithm, then $\left(SU_i, CH_j\right)$ cannot be a blocking pair of the matching generated by the distributed matching algorithm.*

Proof. We assume that CH_j is deleted from SU_i's preference list and $\left(SU_i, CH_j\right)$ is a blocking pair of the matching generated by the DM algorithm. From Algorithm 4.1 and Algorithm 4.2, we know that CH_j is deleted from SU_i's preference list if and only if PU_k that holds CH_j sends an ACK-R to SU_i. This means that $\mathscr{M}\left(CH_j\right) \neq \emptyset$ and $\mathscr{M}\left(CH_j\right)$ is better than SU_i. The above property holds until the DM algorithm terminates. This property contradicts condition 3 of the definition of blocking pairs since CH_j is matched and PU_k prefers $\mathscr{M}\left(CH_j\right)$ to SU_i. Therefore, our assumption does not hold and $\left(SU_i, CH_j\right)$ cannot be a blocking pair of the matching generated by the DM algorithm. □

The following theorems are proposed based on Lemma 4.4.1 and Lemma 4.4.2.

Theorem 4.4.1. *The DM algorithm always generates a stable matching within $O(NK)$ message exchanges.*

Proof. From Lemma 4.4.1, we know that the DM algorithm always generates a matching within $O(NK)$ message exchanges. Suppose a blocking pair $\left(SU_i, CH_j\right)$ exists in the generated matching. We assume that SU_i is matched with CH_t where $t \neq j$. According to the definition of DM algorithm, CH_t must be the best channel in SU_i's preference list. However, since $\left(SU_i, CH_j\right)$ is a blocking pair, SU_i must prefer CH_j to CH_t according to Definition 4.3.2. Therefore, CH_j has to be deleted from SU_i's preference list, which contradicts Lemma 4.4.2. Therefore, $\left(SU_i, CH_j\right)$ cannot be a blocking pair. Since no blocking pair exists, the generated matching is stable according to the definition of stable matching. □

Theorem 4.4.2. *The DM algorithm generates the optimal stable matching in which each SU is matched with the best channel that it can have in any stable matching.*

Proof. Let $\mathscr{M}$ be the stable matching generated from the DM algorithm where SU_i is matched with CH_j. We assume there exists another stable matching $\mathscr{M}'$ where SU_i is matched with CH_t and prefers CH_t to CH_j. During the DM algorithm, SU_i must be refused by CH_t as it is matched with CH_j in the end. We assume that the refusal is caused by the matching between SU_r and CH_t in $\mathscr{M}$. Then for CH_t, SU_r must have larger utility than SU_i. Without loss of generality, we assume that this is the first refusal during the DM algorithm. Thus, for SU_r there is no channel better than CH_t as SU_r has not been refused before. In the stable matching $\mathscr{M}'$, we know that SU_r prefers CH_t to its matched channel and CH_t prefers SU_r to SU_i. Thus, (SU_r, CH_t) is a blocking pair of $\mathscr{M}'$, which contradicts that $\mathscr{M}'$ is a stable matching. Therefore, no stable matching exists where SU_i is matched with a better channel than the one in $\mathscr{M}$. □

According to the lemmas and theorems, we prove that the DM algorithm always generates an optimal stable matching $\mathscr{M}^*$ that maximizes the total utility.

4.4.3 Fast Distributed Spectrum Access Scheme

Note that although the DM algorithm can generate an optimal stable matching, it still need $O(NK)$ message exchanges. In a highly competitive CRN where $N > K$, the number of message exchanges increases linearly with N given the value of K. We propose a fast distributed matching (FDM) algorithm that can eliminate the impact of K in the algorithm complexity and reduce the total number of message exchanges. In the FDM algorithm, the SU sends a CAR to the PU that has the best average CSI (i.e., highest average utility).The SUs are only matched with PUs instead of specific channels. PUs choose SUs in order to maximize the total utility. If a PU accepts an SU, a vacant channel is randomly assigned to the SU after the FDM algorithm terminates. When a PU is oversubscribed, it refuses the SU with the lowest average utility. In the DM algorithm, an SU can send at most K_k CARs to PU_k where K_k is the number of vacant channels of PU_k. In the FDM algorithm, an SU can send at most one CAR to a PU. Thus the number of CAR messages is greatly reduced. In addition, an SU is refused only if a PU is oversubscribed and it is the 'worst' SU that has the lowest average utility. Therefore, the number of ACK-R messages is also reduced. In general, fewer message exchanges are expected in the FDM algorithm. However, since we only utilize the average utility in the FDM algorithm, we expect suboptimal results compared with the DM algorithm. The FDM algortihm at the SU and the PU are given in Algorithm 4.3 and Algorithm 4.4 respectively.

Algorithm 4.3 Fast Distributed Matching Algorithm at the SU

Initialization for SU_i:
Build SU_i's preference list $list\,(PU)$ through message exchanges based on the utility function, $state\,(SU_i) = free$, $state\,(AT) = false$, $\mathscr{M}\,(SU_i) = (\emptyset,\emptyset)$.
while $state\,(AT) = false$ **do**
  if $state\,(SU_i) = free$ and $list\,(PU) \neq \emptyset$ **then**
    $PU_k = best\,(list\,(PU))$, wait for T_{SU_i},
    $send\,(CAR, SU_i)$ to PU_k.
  else if $get\,(MSG, PU_k) = true$ **then**
    if $MSG = ACK - A$ **then**
      $\mathscr{M}\,(SU_i) = (TBD, PU_k)$, $state\,(SU_i) = occupied$.
    else if $MSG = ACK - R$ **then**
      Remove PU_k from $list\,(PU)$, $\mathscr{M}\,(SU_i) = (\emptyset,\emptyset)$, $state\,(SU_i) = free$.
    else if $MSG = AT$ **then**
      $state\,(AT) = true$.
    end if
  end if
end while

4.5 Simulation Results

In this section, we investigate the performance of the DM and FDM algorithms under various QoS constraints. We assume that the channels are independent identically distributed (i.i.d.) Rayleigh fading channels and do not change over the distributed channel allocation phase. For simplicity, we assume that the transmission power is the same for all SUs. PUs, SUs and the corresponding receivers are randomly distributed in the simulation area

Algorithm 4.4 Fast Distributed Matching Algorithm at the PU

Initialization for PU_k:
$\mathcal{M}(PU_k) = \emptyset$, $timer(PU_k) = T_{PU}$.
while $state(PU_k) = free$ and $timer(PU_k) > 0$ **do**
  $timer(PU_k)$ counts down.
  if $get(CAR, SU_i) = true$ **then**
    $timer(PU_k) = T_{PU}$.
    if $|\mathcal{M}(PU_k)| < K_k$ **then**
      $send(ACK - A, PU_k)$, add SU_i to $\mathcal{M}(PU_k)$.
    else if $|\mathcal{M}(PU_k)| = K_k$ and SU_i has larger utility than $worst(\mathcal{M}(PU_k))$ **then**
      $send(ACK - A, PU_k)$ to SU_i.
      $send(ACK - R, PU_k)$ to $worst(\mathcal{M}(PU_k))$.
      Remove $worst(\mathcal{M}(PU_k))$ from $\mathcal{M}(PU_k)$, add SU_i to $\mathcal{M}(PU_k)$.
    else
      $send(ACK - R, PU_k)$ to SU_i.
    end if
  end if
end while
$send(AT, PU_k)$ to all SUs.

(100×100 m square). We also neglect the effect of message collisions. The detailed simulation parameters are listed in Table 4.1.

Table 4.1 Parameters for simulation

Symbol	Description	Value
β	Path loss constant	1
θ	Path loss exponent	2
B	Channel bandwidth	50 kHz
σ^2	Noise power	5 μW
P	Transmission power of the SU	200 mW

We also assume that there are three types of SUs with various QoS requirements as follows: From Equation (4.6) and the specified value of R, D, L and ε, we give the QoS requirement p^* for different types of SUs in Table 4.2. In the following simulation, we randomly choose p_j of CH_j from a uniform distribution on $[0,1]$.

We first investigate the performance of the DM and FDM algorithms in a small-scale CRN in low competition scenario for channel access. We assume there are $M = 4$ PUs and $N = 8$ SUs randomly distributed in the simulation area (100×100 m square). Each PUs has 3 licensed channels so there are $K = 12$ licensed channels in total. We also assume that all SUs have Type-I QoS requirements and the probability of channel availability can

Table 4.2 QoS requirements of SUs in different type

Type	R [kbps]	D [ms]	L [bit]	ε	p^*
Type-I	144	20	1024	0.05	0.374
Type-II	150	5	512	0.02	0.697
Type-III	200	1	128	0.1	0.711

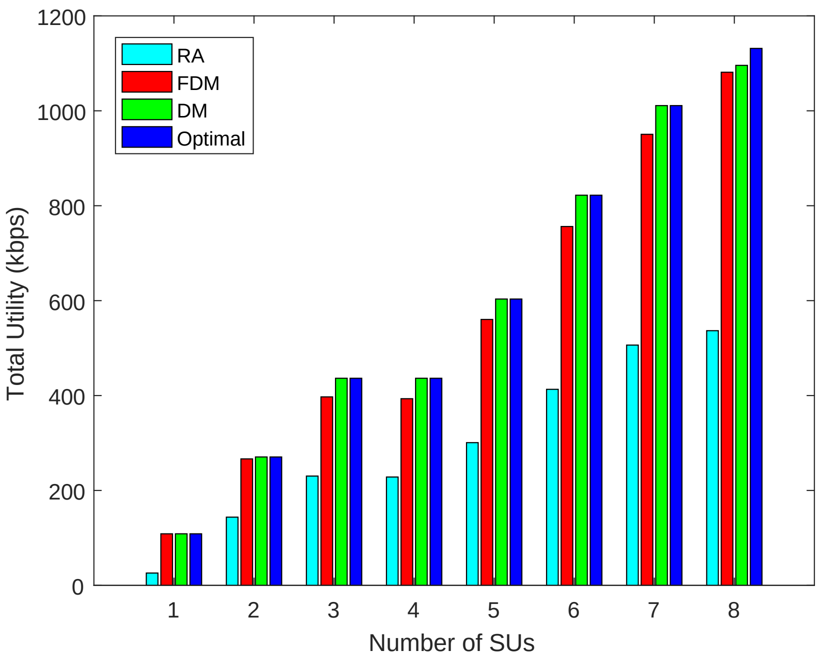

Fig. 4.3 Total utility with different number of active SUs in a small-scale CRN.

fulfill the requirement ($p_j \geq 0.374$, $\forall j \in \{1,2,\ldots,K\}$) in Table 4.2. For comparison, we propose a random access (RA) algorithm. In the RA algorithm, SUs randomly apply for vacant channels and channels are assigned on a first-come-first-serve basis. We also provide the optimal result which is obtained by solving the optimization problem in Equation (4.8) using the Hungarian algorithm. Fig. 4.3 shows the total utility we can achieve using the DM and FDM algorithms with different numbers of active SUs. When the number of available channels are more than the number of active SUs ($K > N$), the DM and the FDM algorithm have near-optimal results. The simulation result also shows that the DM algorithm has a better performance than the FDM algorithm since it utilizes more CSI during the channel allocation process. Both the DM and the FDM algorithms outperform the RA algorithm with different numbers of active SUs.

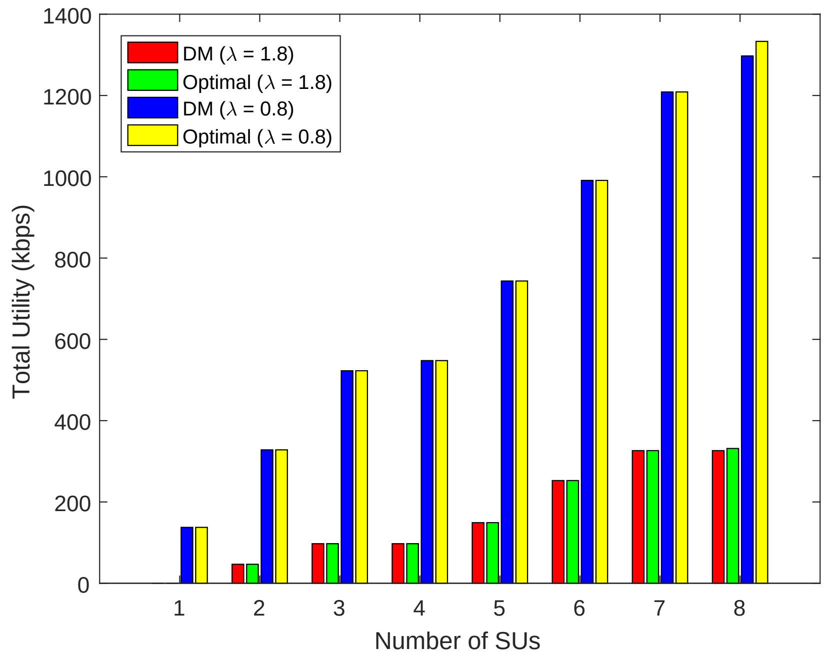

Fig. 4.4 Total utility with various levels of QoS requirements.

We then show that our algorithms can effectively handle various QoS requirements. We use the same settings and assumptions as the ones used to give the results given in Fig. 4.3 and change λ to adjust the weight of QoS requirements in the utility function. The value of λ can express the strictness of the QoS requirements in different scenarios. For wireless channels experiencing frequent deep fades, the applications require strict QoS constraints ($\lambda > 1$). For applications with a high fault tolerance, looser QoS requirements ($\lambda < 1$) may be used. We show the total utility of the DM algorithm for $\lambda = 1.8$ and $\lambda = 0.8$ respectively in Fig. 4.4. Note that SUs only apply for channels with positive utility which means the QoS requirements can be fulfilled through these channels. For strict QoS requirements, the total utility is zero for $N = 1$ which means there is no channel that can fulfill the QoS requirement of that SU.

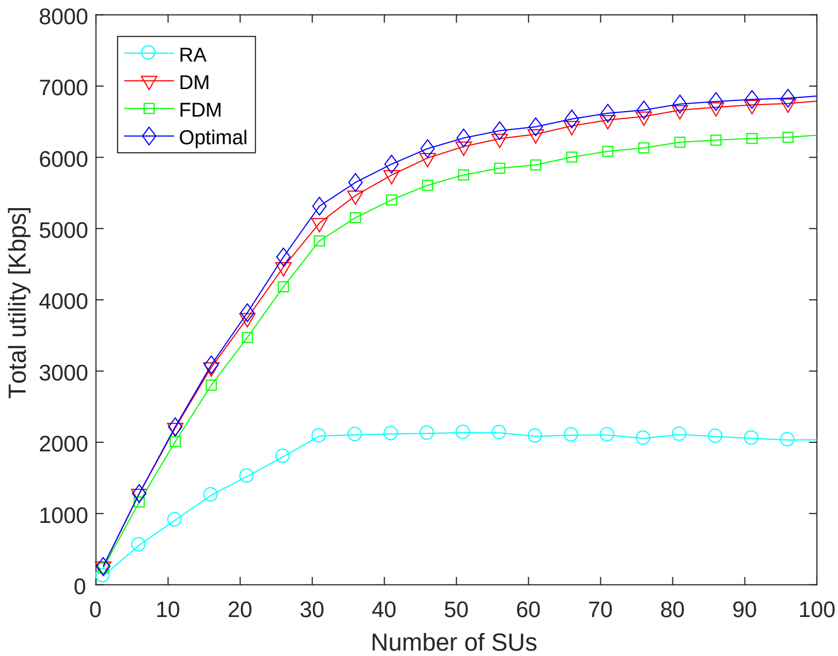

Fig. 4.5 Total utility with different number of active SUs in a large-scale CRN.

In Fig. 4.5, we give the total utility with different number of active SUs in a large-scale CRN. We assume there are $M = 10$ PUs and $N = 100$ SUs randomly distributed in the simulation area (100×100 m square). We also assume that the availability probability of all channels can fulfill the delay requirement in Equation (4.4). Each PU has 3 licensed channels and there are $K = 30$ licensed channels in total. We also assume that there are 30% Type-I, 30% Type-II and 40% Type-III SUs. The simulation result shows that the DM algorithm can achieve in excess of 95% of the optimal total utility while the FDM algorithm can achieve over 90% of the optimal total utility and 100% greater utility compared with the random access (RA) algorithm.

We use the average number of message exchanges per SU as an indication of the algorithm complexity. In Fig. 4.6, we give the average number of message exchanges per SU with different number of active SUs in a large-scale CRN. The settings and assumptions are the same as the ones in Fig. 4.5. We have proved that the DM algorithm terminates within $O(NK)$ message exchanges in Theorem 4.4.1. In a large-scale CRN where $N > K$, the total number of message exchanges for SUs in the DM algorithm is upper bounded by $O\left(N^2\right)$. Thus the average number of message exchanges per SU is upper bounded by $O(N)$. Since

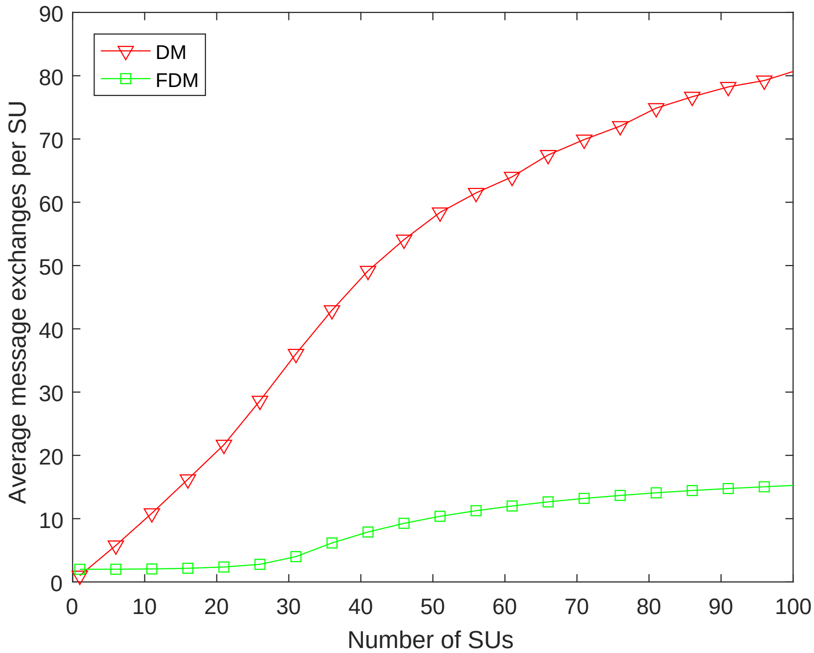

Fig. 4.6 Average message exchanges per SU with different number of active SUs.

the FDM algorithm utilizes the average CSI and matches SUs to PUs instead of vacant channels, it requires far fewer message exchanges compared with the DM algorithm. We also notice that when the number of active SUs is larger than the total number of vacant channels ($N > K$), the average number of message exchanges per SU is much higher for both algorithms as SUs compete for the limited number of vacant channels and thus send more channel access requests. From Fig. 4.5 and Fig. 4.6, we show that the DM algorithm has a better performance than the FDM algorithm. However, for a highly competitive CRN, the FDM algorithm may be a better choice considering the tradeoff of efficiency and algorithm complexity.

We now consider the impact of the probability of channel availability on the total utility. We assume there are $M = 10$ PUs and $N = 30$ SUs with an equal number in the three different categories. Each PU has 3 licensed channels. For simplicity, we also assume that all channels of PUs have the same probability of channel availability. We then vary the probability of channel availability and investigate its impact on total utility. As shown in Equation (4.4) and Equation (4.5), the delay constraints require the channels to have large enough probability of channel availability to fulfill the QoS requirements. The minimum probability of channel availability is given in Table 4.2 for each type of SUs. Fig. 4.7 shows that the total utility is limited by the probability of channel availability of each PU. Since we have three categories of SUs in the CRN, the total utility increases once the probability

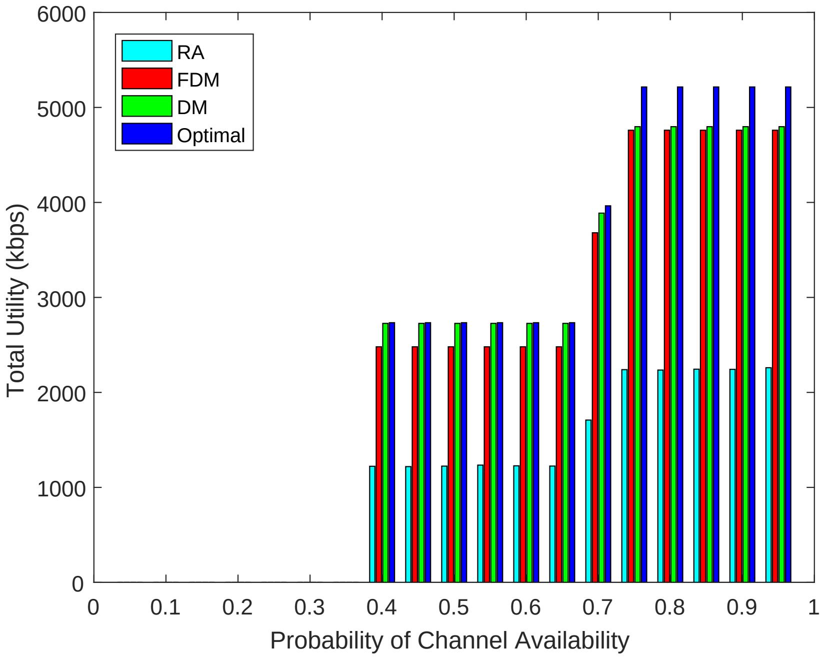

Fig. 4.7 Total utility with various probability of channel availability.

of channel availability gets larger than the probability threshold p^* (i.e., $p^* = 0.374$ for Type-I SUs, $p^* = 0.697$ for Type-II SUs and $p^* = 0.711$ for Type-III SUs). As we can see from Fig. 4.7, both the DM and the FDM algorithms achieve near-optimal results and outperform the RA algorithm with different probability of channel availability.

4.6 Summary

In this chapter, we considered the distributed spectrum access problem in a QoS-constrained cooperative CRN. We formulated the distributed spectrum access problem as an assignment problem. In order to effectively solve the assignment problem in a distributed manner, we further formulated the problem as a matching problem in Section 4.3.

We then proposed the DM algorithm and proved that the DM can always get a stable matching of SUs and channels which corresponds to an optimal assignment solution among all stable matchings. The implementation of the DM algortihm is given in Section 4.4. To further reduce the message exchanges of the DM algorithm, we proposed the FDM algorithm which can achieve a sub-optimal solution and terminates within far fewer message exchanges compared to the DM algorithm.

Simulation results are given in Section 4.5. We first investigated the performance of the DM and FDM algorithms in a small-scale CRN. We showed that both the DM and FDM algorithm achieves near-optimal result in a small-scale CRN and can handle various QoS requirements. Then we gave the performance of both algorithms in a large-scale CRN. We showed that the DM and FDM algorithm can still handle the spectrum access problems in a large-scale CRN. However, the number of message exchanges increases dramatically when there are severe access competitions among SUs for limited vacant channels. Considering the tradeoff of algorithm efficiency and complexity, in large-scale CRN, it may be better to use the FDM algorithm for the competitive distributed spectrum access problem. Finally, the impact of the probability of channel availability on the total utility is analyzed.

Chapter 5

Joint Channel Sensing and Power Control for QoS-Constrained Wireless Networks

5.1 Introduction

Wireless sensors usually operate in the Industrial, Scientific and Medical (ISM) bands and are deployed for applications such as industrial control systems and area monitoring. With the increasing demand placed on unlicensed bands, it is challenging to deploy wireless sensor networks (WSNs) only in unlicensed bands, especially for QoS-constrained applications. Cognitive radio (CR) has been considered as a method to improve spectrum efficiency. However, the primary users (PUs) may not wish to actively allocate their vacant channels to the secondary users (SUs) since the channel allocation process requires extra message exchanges and hence additional power consumption. Therefore, the SUs, such as wireless sensors in a heterogeneous network, are required to monitor the licensed channels and send their data via vacant channels when it is possible. Such a cognitive radio wireless sensor network (CRWSN) [87] is considered in this chapter.

In a CRWSN, wireless sensors are equipped with cognitive radios and usually have a limited energy supply. A wireless sensor can only sense a part of the licensed channel at a time. Therefore, cooperative sensing [88] is needed for joint channel sensing. In addition, the available licensed channels need to be coordinated to avoid collisions on spectrum access requests via control channels. Such licensed channels and control channels may not be available to all sensors due to interference and the dynamic wireless environment. Instead, common channels may exist in a local area [89, 90]. Therefore, a cluster-based heterogenous wireless network is a suitable design for a CRWSN. Sensors in each cluster cooperatively sense licensed channels and report the results to the cluster head via control channels. The cluster head of each cluster can coordinate and allocate available channels to the sensors having data transmission requests.

Channel sensing is an important issue in CR and has been widely investigated. To avoid the message exchanges between PUs and SUs, some previous work has modeled the channel sensing as a learning problem where SUs predict the channel availability from the historical sensing results. In [91], the authors proposed a distributed learning algorithm to minimize the channel allocation regret, which is defined as the transmission loss of SUs due to the imperfect learning of the unknown availability statistics. In [92], the channel sensing and allocation problem is modeled as Markov chain and a restless bandit problem. An algorithm utilizing the regenerative cycle of a Markov chain is proposed to track the best channel that minimizes the learning regret. In [93], the channel sensing and spectrum access problem is formulated as a decentralized multi-armed bandit problem. An algorithm based on the upper confidence bound (UCB) policy [94] is proposed to minimize the online learning regret. All this highlighted work that investigates online learning algorithms only consider the learning regret and do not terminate in a finite time. Therefore, they are not suitable for QoS-constrained WSNs where sensors cannot afford non-stop online learning algorithms and do not necessarily have to access the best channel for data transmission (as long as the QoS requirements are fulfilled).

In this chapter, we consider QoS-constrained applications in a cluster-based CRWSN. For QoS-based applications, it is important that vacant channels are assigned in a timely manner to users in need. Therefore, instead of tracking good channels with high channel availability, sensors in each cluster keep sensing their pre-assigned channels and only stop channel sensing when they have high confidence that the channels are bad channels with low channel availability. We propose three channel sensing algorithms for wireless sensors that can effectively detect licensed channels without message exchanges with the PUs. We prove that the proposed algorithms can terminate in a finite time with a finite error rate. Considering the QoS constraints on delay and data rate, it is reasonable that the sensors transmit their data with the maximum transmission power level. However, since wireless sensors have limited energy supply, it is more energy-efficient for the sensors to transmit their data at a lower power, but not so low that the QoS constraint is violated. We propose a joint channel sensing and power control (JCSPC) scheme that can help sensors find the optimal power level to transmit their data. We show that the total transmitted data is maximized with the JCSPC scheme via simulation results. Some of the results presented in this chapter have been published in the Wireless Days (WD) 2017 conference proceedings [16].

The rest of the chapter is organized as follows: Section 5.2 describes the system model of the cluster-based CRWSN, the channel sensing and power control problems with QoS constraints are described in detail. In Section 5.3, we propose three probably approximately correct (PAC) channel sensing algorithms to classify good channels and bad channels with channel availability constraints. In Section 5.4, the joint channel sensing and power control scheme is proposed to maximize the total number of transmitted bits of each cluster with specified QoS constraints. We provide the simulation results and the performance analyses of the proposed algorithms in Section 5.5. Finally, we conclude the chapter in Section 5.6.

5.2 System Model and Problem Formulation

Consider a cluster-based CRWSN as shown in Fig. 5.1. We assume there are K orthogonal licensed channels allocated to M PUs ($M \leq K$) for time-slotted transmission. For simplicity, we assume that the number of PUs and channels are equal ($M = K$) so that each PU has only one licensed channel. We also assume that each channel has the same bandwidth B and is sensed by an active sensor in each cluster. Therefore, there are K active sensors responsible for channel sensing in each cluster where each sensor monitors a pre-assigned licensed channel. Cognitive radio wireless sensors can send data to their cluster head via vacant licensed channels in each time slot. Let $\mathbf{S} = \{S_1, S_2, \ldots, S_K\}$ and $\mathbf{CH} = \{CH_1, CH_2, \ldots, CH_K\}$ denote the set of sensors and the corresponding licensed channels of one cluster respectively. We use $T = \{T_1, T_2, \ldots\}$ to represent the set of time slots in the network. We assume that all channels are Rayleigh block fading channels where the channel gains stay unchanged over one block. Each block contains a certain number of time slots (e.g., V time slots per fading block). We also assume that there are two phases in each time slot, the channel sensing phase and the data transmission phase. The length of the channel sensing phase and the data transmission phase are αT and $(1-\alpha)T$ respectively, where α is the fraction of time used for channel sensing per time slot and T is the length of a time slot. The block fading channel model and time slot structure are shown in Fig. 5.2, where it can be seen that for each fading block, the channel gains of all channels remain unchanged for V time slots. There are two phases in each time slot. In the channel sensing phase, sensors in each cluster sense their pre-assigned channels availability and report the results along with their transmission requests (if any) to the cluster head via separate control channels. The cluster head then assigns the available channels to the sensors that have sent transmission requests. Note that the channel assigned for transmission is selected from the available channels and does not necessarily have to be the same as the pre-assigned one. In the data transmission phase, sensors with data transmission requests transmit their data via the assigned channels.

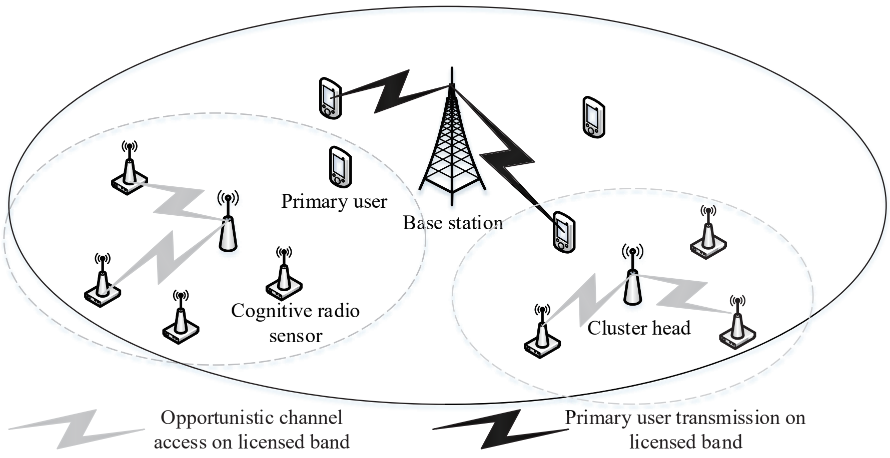

Fig. 5.1 A cluster-based cognitive radio wireless sensor network.

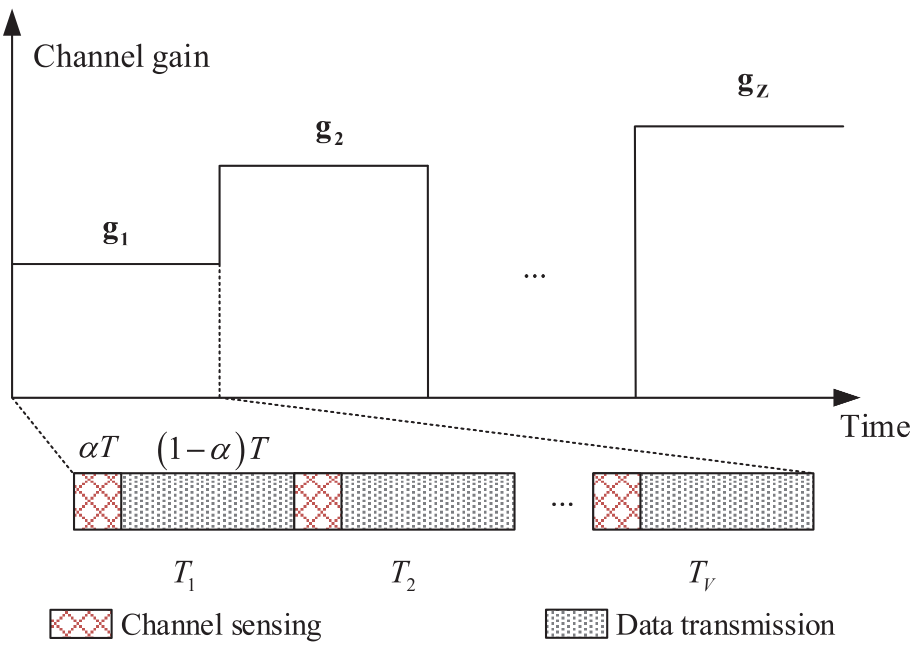

Fig. 5.2 Models for block fading channels and time slots.

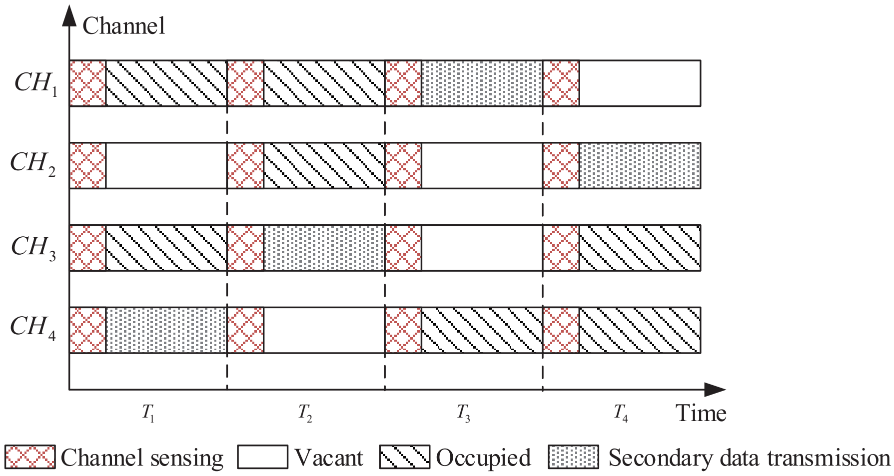

Fig. 5.3 A model for channel sensing and data transmission.

We give an example of how channel sensing and data transmission works in Example 5.2.1 and Fig. 5.3.

Example 5.2.1. *We assume there are $K = 4$ licensed channels allocated to $K = 4$ PUs. In this example, $\{CH_1, CH_2, CH_3, CH_4\}$ are pre-assigned to $\{S_1, S_2, S_3, S_4\}$ for channel sensing. We only consider time slots $\{T_1, T_2, T_3, T_4\}$ and assume that only SU_1 has a data transmission request. In the channel sensing phase, sensors sense their pre-assigned channels and send the sensing results along with their transmission data requests to the cluster head via separate control channels. The cluster head assigns the available channels to the sensors that have data to transmit. In this example, $\{CH_4, CH_3, CH_1, CH_2\}$ are assigned to S_1 for data transmission at time slots $\{T_1, T_2, T_3, T_4\}$ respectively.*

Since the channel gain changes in every fading block, the channel sensing and assignment algorithms shall run in the beginning of each fading block. In the following sections, all of the proposed algorithms and most of the simulation results are discussed at the time scale of one fading block.

5.2.1 Channel Sensing with Availability Constraints

At each time slot, a sensor is only allowed to send its data via a vacant licensed channel. The availability of the licensed channel is completely determined by the behaviour of the PU. For sensor S_i sensing the pre-assigned channel CH_i at time slot T_j, we use a random variable $\theta_{i,j}$ to represent the availability of CH_i. Let $\theta_{i,j} = 1$ denote that CH_i is available and $\theta_{i,j} = 0$ otherwise. Since channel sensing is energy and time consuming, we can reduce the energy consumption and improve the sensing efficiency if we could predict the channel availability by utilizing the channel sensing history. We assume that the availability of all channels follows independent identical Bernoulli distributions over different time slots with parameters $\mathbf{p} = \{p_1, p_2, \ldots p_K\}$ which are the mean values of the Bernoulli distributions. The mean values $\mathbf{p}$ are unknown to the sensors. However, the sensors can get the empirical mean values from the sensing history. We define the empirical mean value of the availability of channel CH_i after the channel sensing in time slot T_n as

$$\hat{p}_{i,n} = \frac{1}{n} \sum_{j=1}^{n} \theta_{i,j}. \tag{5.1}$$

It is obvious that the availability of channels affects the delay of the data transmission since sensors cannot transmit their data consistently when the licensed channels are frequently occupied. Therefore, the QoS delay requirements of applications can also be expressed in terms of the channel availability requirements. For applications with specified QoS delay constraints, we aim at finding 'good' channels that can fulfill the channel availability requirements (i.e., satisfy the delay QoS constraints). Assuming that all channels have the same availability requirement p^*, we define the set of good channels as $\mathbf{C_G} = \{CH_i \in \mathbf{CH} : p \geq p^*\}$ and the set of bad channels as $\mathbf{C_B} = \{CH_i \in \mathbf{CH} : p < p^*\}$ respectively. Note that the sensors do not know the mean values $\mathbf{p}$ but they can estimate the mean values from Equation (5.1). Channel sensing algorithm starts in the beginning of each fading block. Let E_i be the energy of sensor S_i that can be used in one fading block and η_i be the maximum fraction of energy used for channel sensing. We use $\eta_i E_i$ to denote the energy constraint of sensor S_i for channel sensing in each fading block. For simplicity and without loss of generality, we assume that all sensors have the same value of E and η. The relationship between η and other network parameters is given in Equation (5.18) and will be detailed presently. To classify the channels into empirical good and bad channels, we assume that we have a set of algorithms Ω. Assuming that the sensing energy constraint is ηE and an arbitrary algorithm $\omega \in \Omega$ is used to classify the channels, we use $\hat{\mathbf{C}}_\mathbf{G}(\omega, \eta)$ and $\hat{\mathbf{C}}_\mathbf{B}(\omega, \eta)$ to represent the set of empirical good channels and bad channels respectively. The set of misclassified channels with algorithm ω and energy constraint ηE is defined as

$$\mathbf{C}_\varepsilon(\omega, \eta) = \left\{CH_i \in \hat{\mathbf{C}}_\mathbf{G} : p_i < p^*\right\}. \tag{5.2}$$

We also defined the classification error rate as

$$\varepsilon = \frac{|\mathbf{C}_\varepsilon(\omega, \eta)|}{|\mathbf{CH}|} = \frac{|\mathbf{C}_\varepsilon(\omega, \eta)|}{K}. \tag{5.3}$$

With constraints on the channel availability and energy, we define the optimal algorithm $\omega^* \in \Omega$ as the algorithm that can classify the good and bad channels with high confidence and the minimum error rate in Ω. The optimal algorithm is given by

$$\begin{aligned} &\omega^* = \arg\min_{\omega\in\Omega} \varepsilon(\omega,\eta) = \arg\min_{\omega\in\Omega} \left(\tfrac{|\mathbf{C}_\varepsilon(\omega,\eta)|}{K}\right), \\ &\text{s.t.} \quad \alpha T\left(P_{i,s}+P_{i,c}\right)N_{i,\max} \le \eta E, \forall i \in \{1,2,\ldots,K\} \end{aligned} \tag{5.4}$$

where $P_{i,s}$ is the channel sensing power consumption of sensor S_i, $P_{i,c}$ is the circuit power consumption of sensor S_i and $N_{i,\max}$ is the maximum number of time slots that S_i can spend on channel sensing in one fading block. We define the maximum number of time slots N used for channel sensing of each cluster in one fading block as

$$N = \min_i N_{i,\max} = \min_i \left(\left\lfloor \frac{\eta E}{\alpha T\left(P_{i,s}+P_{i,c}\right)} \right\rfloor\right). \tag{5.5}$$

5.2.2 Power Control with Rate Constraints

Apart from saving energy required for the channel sensing phase, we also need to consider the energy efficiency of the data transmission phase in the long run. Although increasing the transmission power level generally increases the data rate, it also increases the energy consumption and thus decreases the lifetime of the sensor node. In order to improve the energy efficiency of the CRWSN, we aim at finding the optimal transmission power that can maximize the total number of transmitted bits under the data rate QoS constraints.

We assume that for any sensor S_i, its transmission power $P_{i,t}$ can only take on discrete power levels. We also assume that all sensors have the same set of transmission power levels denoted by $\mathbf{P} = \{P_1, P_2, \ldots, P_M\}$ where M is the number of power levels. Without loss of generality, we assume that $\mathbf{P}$ is in increasing order and $0 \le P_1 < P_2 < \cdots < P_M$. Let $R_{i,j,k} = f\left(S_i, P_j, CH_k\right)$ denote the maximum data rate of sensor S_i with transmission power $P_{i,t} = P_j$ on channel CH_k. For simplicity, we define $R_{i,j,k}$ as

$$R_{i,j,k} = f\left(S_i, P_j, CH_k\right) = B\log_2\left(1+P_j g_{i,k}\right), \tag{5.6}$$

where B is the channel bandwidth of CH_k and $g_{i,k}$ is the instantaneous channel power gain to noise ratio of CH_k for S_i. We then define the number of transmitted bits of S_i with transmission power P_j on channel CH_k as

$$L_{i,j,k} = \frac{(1-\eta)ER_{i,j,k}}{P_{i,t}+P_{i,c}} = \frac{(1-\eta)EB\log_2\left(1+P_j g_{i,k}\right)}{P_j+P_{i,c}}. \tag{5.7}$$

Let R_i^* be the minimum data rate requirement of S_i and η^* be the minimum fraction of energy used for channel sensing. The optimal transmission power of S_i on channel CH_k is defined as

$$\begin{aligned} &P_{i,k}^* = \arg\max_{P_{i,t}\in\mathbf{P}} L_{i,j,k} = \arg\max_{P_{i,t}\in\mathbf{P}} \left(\tfrac{(1-\eta)ER_{i,j,k}}{P_{i,t}+P_{i,c}}\right), \\ &\text{s.t.} \quad R_{i,j,k} \geq R_i^*, \forall S_i \in \mathbf{S}, CH_k \in \mathbf{CH}; \quad \eta \geq \eta^*. \end{aligned} \tag{5.8}$$

Let $L_{i,k}^*$ denote the maximum total number of transmitted bits of S_i on channel CH_k. The definition of $L_{i,k}^*$ is given as

$$\begin{aligned} &L_{i,k}^* = \max_{P_{i,t}\in\mathbf{P}} L_{i,j,k} = \max_{P_{i,t}\in\mathbf{P}} \left(\tfrac{(1-\eta)ER_{i,j,k}}{P_{i,t}+P_{i,c}}\right), \\ &\text{s.t.} \quad R_{i,j,k} \geq R_i^*, \forall S_i \in \mathbf{S}, CH_k \in \mathbf{CH}; \quad \eta \geq \eta^*. \end{aligned} \tag{5.9}$$

We use a $K \times K$ matrix Π to denote the channel assignment where the matrix element $\pi_{i,j}$ is set to be 1 if CH_j is assigned to S_i and 0 otherwise. The maximum total number of transmitted bits in each cluster is given as

$$\begin{aligned} &L^* = \max \sum_{i=1}^{K} \sum_{k=1}^{K} \pi_{i,k} L_{i,k}^* \\ &\text{s.t.} \quad \sum_{k=1}^{K} \pi_{i,k} \leq 1, \forall i \in \{1,2,\ldots,K\} \\ &\qquad \sum_{i=1}^{K} \pi_{i,k} \leq 1, \forall k \in \{1,2,\ldots,K\}. \end{aligned} \tag{5.10}$$

5.3 Probably Approximately Correct Channel Sensing Algorithms

In this section, we propose three probably approximately correct (PAC) algorithms [95, 96] to classify the good channels and bad channels with channel availability constraints. An algorithm is an ε-PAC algorithm if it gets the correct result with probability at least $1-\varepsilon$. We first give two passive rejection (PR) algorithms that can identify bad channels with high probability and low error rate. In order to improve the efficiency of the channel sensing and classification process, an active elimination (AE) algorithm is also proposed. We prove that the AE algorithm can identify numbers of good channels with a finite time horizon and low error rate.

5.3.1 Passive Rejection Algorithm

We first propose two PR algorithms. With a PR algorithm, a sensor S_i keeps sensing its pre-assigned channel CH_i in each time slot until it has high confidence that p_i is less than the minimum channel availability requirement p^*. We prove that both PR algorithms are ε-PAC algorithms.

The fist PR algorithm is called the simple reject (SR) algorithm and is denoted by ω_{SR}. The details of the SR algorithm are given in Algorithm 5.1.

Algorithm 5.1 Simple Reject (SR) Algorithm

Input the value of p^*, η and T. Calculate N based on Equation (5.5).
Initialization: $\hat{\mathbf{C}}_{\mathbf{G}}(\omega_{SR},\eta) \leftarrow \mathbf{CH}$, $\hat{\mathbf{C}}_{\mathbf{B}}(\omega_{SR},\eta) \leftarrow 0$.
for $1 \le n \le N$ **do**
  for each $CH_i \in \hat{\mathbf{C}}_{\mathbf{G}}$ **do**
    Calculate $\hat{p}_{i,n}$ based on (5.1).
    if $\gamma_{i,n} = p^* - \hat{p}_{i,n} \ge \sqrt{\frac{1}{2n}\ln\left(\frac{1}{\varepsilon}\right)}$ **then**
      $\hat{\mathbf{C}}_{\mathbf{G}} \leftarrow \hat{\mathbf{C}}_{\mathbf{G}} - \{CH_i\}$, $\hat{\mathbf{C}}_{\mathbf{B}} \leftarrow \hat{\mathbf{C}}_{\mathbf{B}} \cup \{CH_i\}$.
    end if
  end for
end for
Output $\hat{\mathbf{C}}_{\mathbf{G}}(\omega_{SR},\eta)$.

We prove that SR algorithm is an ε-PAC algorithm as follows:

Theorem 5.3.1. *The SR algorithm is an ε-PAC algorithm that can correctly identify a bad channel with a probability that is at least $1-\varepsilon$.*

Proof. For any p_i in $\mathbf{p}$, we have $p_i \in [0,1]$. According to Hoeffding's inequality [97], we have

$$\Pr\left(p_i \ge p^* \middle| CH_i \in \hat{\mathbf{C}}_{\mathbf{B}}\right) = \Pr\left(p_i - \hat{p}_{i,n} \ge p^* - \hat{p}_{i,n} \ge \sqrt{\frac{1}{2n}\ln\left(\frac{1}{\varepsilon}\right)}\right) \le e^{-2n\gamma_{i,n}}. \quad (5.11)$$

Let ε denote the error rate of the SR algorithm. For S_i sensing CH_i at T_n, if $\gamma_{i,n} = p^* - \hat{p}_{i,n} \ge \sqrt{\frac{1}{2n}\ln\left(\frac{1}{\varepsilon}\right)}$, then we have $\Pr\left(p_i \ge p^* \middle| CH_i \in \hat{\mathbf{C}}_{\mathbf{B}}(\omega_{SR},\eta)\right) \le e^{-2n\gamma_{i,n}} \le \varepsilon$. Therefore, the probability that CH_i is correctly identified as a bad channel is expressed as

$$\Pr\left(CH_i \in \mathbf{C}_{\mathbf{B}} \middle| CH_i \in \hat{\mathbf{C}}_{\mathbf{B}}\right) = \Pr\left(p_i < p^* \middle| CH_i \in \hat{\mathbf{C}}_{\mathbf{B}}\right) > 1-\varepsilon. \quad (5.12)$$

□

The second PR algorithm is called the improved reject (IR) algorithm and is denoted by ω_{IR}. The details of the IR algorithm are given in Algorithm 5.2.

Algorithm 5.2 Improved Reject (IR) Algorithm

Input the value of p^*, η and T. Calculate N based on Equation (5.5). Let $B_\varepsilon(n,p)$ denote the quantile of order ε for the binomial distribution with parameter n and p.
Initialization: $\hat{\mathbf{C}}_\mathbf{G}(\omega_{IR},\eta) \leftarrow \mathbf{CH}$, $\hat{\mathbf{C}}_\mathbf{B}(\omega_{IR},\eta) \leftarrow 0$.
for $1 \le n \le N$ **do**
  for each $CH_i \in \hat{\mathbf{C}}_\mathbf{G}$ **do**
    Calculate $\hat{p}_{i,n}$ based on (5.1).
    if $n\hat{p}_{i,n} \le B_\varepsilon(n,p^*)$ **then**
      $\hat{\mathbf{C}}_\mathbf{G} \leftarrow \hat{\mathbf{C}}_\mathbf{G} - \{CH_i\}$, $\hat{\mathbf{C}}_\mathbf{B} \leftarrow \hat{\mathbf{C}}_\mathbf{B} \cup \{CH_i\}$.
    end if
  end for
end for
Output $\hat{\mathbf{C}}_\mathbf{G}(\omega_{IR},\eta)$.

We prove that IR algorithm is an ε-PAC algorithm as follows:

Theorem 5.3.2. *The IR algorithm is an ε-PAC algorithm that can correctly identify a bad channel with a probability that is at least* $1-\varepsilon$

Proof. For S_i sensing CH_i at T_n, we have defined the channel availability $\theta_{i,n}$ as a random variable having a Bernoulli distribution with parameter p_i. Therefore, $n\hat{p}_{i,n}$ is a random variable of a binomial distribution with parameters n and p_i. We use $n\hat{p}_{i,n}$ as a test statistic for hypothesis tests about the value of p_i. We reject the null hypothesis $H_0 : p_i \ge p^*$ and accept the alternative hypothesis $H_1 : p_i < p^*$ if and only if $n\hat{p}_{i,n} \le B_\varepsilon(n,p^*)$ where $B_\varepsilon(n,p^*)$ is the quantile of order ε for the binomial distribution with parameters n and p^*. According to the definition of binomial hypothesis test, the IR algorithm can correctly identify a bad channel with probability at least $1-\varepsilon$. □

We prove that both SR and IR algorithm can correctly identify a bad channel with a probability that is at least $1-\varepsilon$. However, it is still non-trivial for the PR algorithms to classify the channels with mean values close to p^*. It is also not energy-efficient to keep all sensors sensing their pre-assigned channels when only a small number of sensors have data transmission requests. In order to improve the energy efficiency of channel sensing, we propose an active elimination (AE) algorithm that can identify the m best channels in **CH** with a finite time horizon and low error rate.

5.3.2 Active Elimination Algorithm

We first introduce some definitions before proposing the active elimination (AE) algorithm. Without loss of generality, we assume that the mean values $\mathbf{p}$ are in strict increasing order such that $p_1 < p_2 < \ldots < p_K$. To find the m best channels, we set $p^* = p_m$. We use $\Delta_{i,j} = p_j - p_i$ to denote the gap between p_i and p_j. For the m best channels, we further define Δ_i^m as

$$\Delta_i^m = \begin{cases} \Delta_{i,m+1}, & 1 \le i \le m \\ \Delta_{m,i}, & m+1 \le i \le K. \end{cases} \tag{5.13}$$

Note that according to the definition in Equation (5.13), we have $\Delta_m^m = \Delta_{m+1}^m = \min\limits_i \Delta_i^m = p_{m+1} - p_m$.

Let $\hat{\mathbf{C}}_{\mathbf{G},\mathbf{i}}$ denote the set of empirical good channels in round i. The AE algorithm denoted by ω_{AE} is given as follows:

Algorithm 5.3 Active Elimination (AE) Algorithm

Input the value of p^*, η, m and T. Calculate N based on Equation (5.5).
Initialization: $\hat{\mathbf{C}}_{\mathbf{G},\mathbf{0}} \leftarrow \mathbf{CH}$.
for $1 \le i \le \lceil \log_2 (K/m) \rceil$ **do**
  Sensing each channel $CH_j \in \hat{\mathbf{C}}_{\mathbf{G},\mathbf{i-1}}$ for $t = \left\lfloor \frac{N}{\lceil \log_2 \left(\frac{K}{m}\right) \rceil} \right\rfloor$ time slots. Let $\hat{\mathbf{C}}_{\mathbf{G},\mathbf{i}}$ be the set of $\left\lceil \frac{|\hat{\mathbf{C}}_{G,i-1}|}{2} \right\rceil$ channels in $\hat{\mathbf{C}}_{\mathbf{G},\mathbf{i-1}}$ with largest empirical mean value.
end for
Output $\hat{\mathbf{C}}_{\mathbf{G}} (\omega_{AE}, \eta) \leftarrow \hat{\mathbf{C}}_{\mathbf{G},\lceil \log_\mathbf{2} (\mathbf{K}/\mathbf{m}) \rceil}$.

To prove that the AE algorithm is a ε-PAC algorithm, we first give a lemma as follows:

Lemma 5.3.1. *In the AE algorithm, the probability that a good channel $CH_k \in \mathbf{C_G}$ is eliminated in round i is at most* $6\exp\left(-\frac{(\Delta_m^m)^2}{2} t\right)$ *where* $t = \left\lfloor \frac{N}{\lceil \log_2 \left(\frac{K}{m}\right) \rceil} \right\rfloor$.

Proof. Initially, we assume that all channels are empirical good channels and let $\hat{\mathbf{C}}_{\mathbf{G},\mathbf{0}} = \mathbf{CH}$. In round i, the set of empirical good channels in the previous round is denoted by $\hat{\mathbf{C}}_{\mathbf{G},\mathbf{i-1}}$. Let $\mathbf{G_{i-1}}$ be the set of $\frac{3}{4} \left| \hat{\mathbf{C}}_{\mathbf{G},\mathbf{i-1}} \right|$ channels that have the lowest empirical mean values in $\hat{\mathbf{C}}_{\mathbf{G},\mathbf{i-1}}$. If $CH_k \in \mathbf{C_G}$ is eliminated in round i, then at least half of the channels in $\hat{\mathbf{C}}_{\mathbf{G},\mathbf{i-1}}$ have larger empirical mean values than CH_k. By the definition of $\mathbf{G_{i-1}}$, at least $\frac{1}{3} |\mathbf{G_{i-1}}|$ channels in $\mathbf{G_{i-1}}$ have larger empirical mean values than CH_k. Let X_i be the number of channels in $\mathbf{G_{i-1}}$ that have larger empirical mean values than CH_k. According to Hoeffding's inequality [97] and the union bound theory [98] we have

$$\begin{aligned}
\mathrm{E}[X_i] &= \sum_{CH_j \in \mathbf{G_{i-1}}} \Pr\left(\hat{p}_{k,t} < \hat{p}_{j,t}\right) \\
&= \sum_{CH_j \in \mathbf{G_{i-1}}} \Pr\left(\hat{p}_{j,t} - p_j + p_k - \hat{p}_{k,t} > \Delta_{k,j}\right) \\
&\leq \sum_{CH_j \in \mathbf{G_{i-1}}} \Pr\left(\hat{p}_{j,t} - p_j > \frac{\Delta_{k,j}}{2}\right) + \sum_{CH_j \in \mathbf{G_{i-1}}} \Pr\left(p_k - \hat{p}_{k,t} > \frac{\Delta_{k,j}}{2}\right) \\
&\leq \sum_{CH_j \in \mathbf{G_{i-1}}} 2\exp\left(-\frac{\Delta_{k,j}^2}{2}t\right) \\
&\leq 2\left|\mathbf{G_{i-1}}\right| \max_{CH_j \in \mathbf{G_{i-1}}} \exp\left(-\frac{\Delta_{k,j}^2}{2}t\right) \\
&\leq 2\left|\mathbf{G_{i-1}}\right| \exp\left(-\frac{(\Delta_m^m)^2}{2}t\right)
\end{aligned} \tag{5.14}$$

where the last inequality holds because of the fact that $\Delta_m^m = \Delta_{m+1}^m = \min_i \Delta_i^m = p_{m+1} - p_m$. From the definition of the AE algorithm, we know that $CH_k \in \mathbf{C_G}$ is eliminated in round i if and only if $X_i > \frac{1}{3}|G_{i-1}|$. We further apply Markov's inequality on Equation (5.14) and have

$$\Pr\left(X_i > \frac{1}{3}|G_{i-1}|\right) \leq \frac{3\mathrm{E}[X_i]}{|G_{i-1}|} \leq 6\exp\left(-\frac{(\Delta_m^m)^2}{2}t\right), \tag{5.15}$$

which proves the lemma. □

An example of the AE algorithm in operation is given in Example 5.3.1, supported by Fig. 5.4.

Example 5.3.1. *We assume that there are $K = 8$ channels with the mean values $\mathbf{p}$ in strict increasing order. We aim at finding the $m = 2$ best channels (i.e., CH_1 and CH_2) in $N = 100$ time slots. According to the definition in Algorithm 5.3, there are two rounds in this example. Each round contains $t = \left\lfloor \frac{N}{\lceil \log_2(\frac{K}{m}) \rceil} \right\rfloor = 50$ time slots. In round 1, sensors sensing channel $CH_j \in \hat{\mathbf{C}}_{\mathbf{G},\mathbf{0}}$ for $t = 50$ time slots. At the end of round 1, we assume that channels in $\hat{\mathbf{C}}_{\mathbf{G},\mathbf{0}}$ and $\mathbf{G_0}$ are in strict ascending order according to their empirical mean values. Suppose that the good channel CH_2 is eliminated. From Fig. 5.4, we show that at least half of the channels in $\hat{\mathbf{C}}_{\mathbf{G},\mathbf{0}}$ have larger empirical mean values than CH_2 (i.e., CH_1, CH_3, CH_4 and CH_5). In addition, at least $\frac{1}{3}|\mathbf{G_0}| = 2$ channels in $\mathbf{G_0}$ have larger empirical mean values*

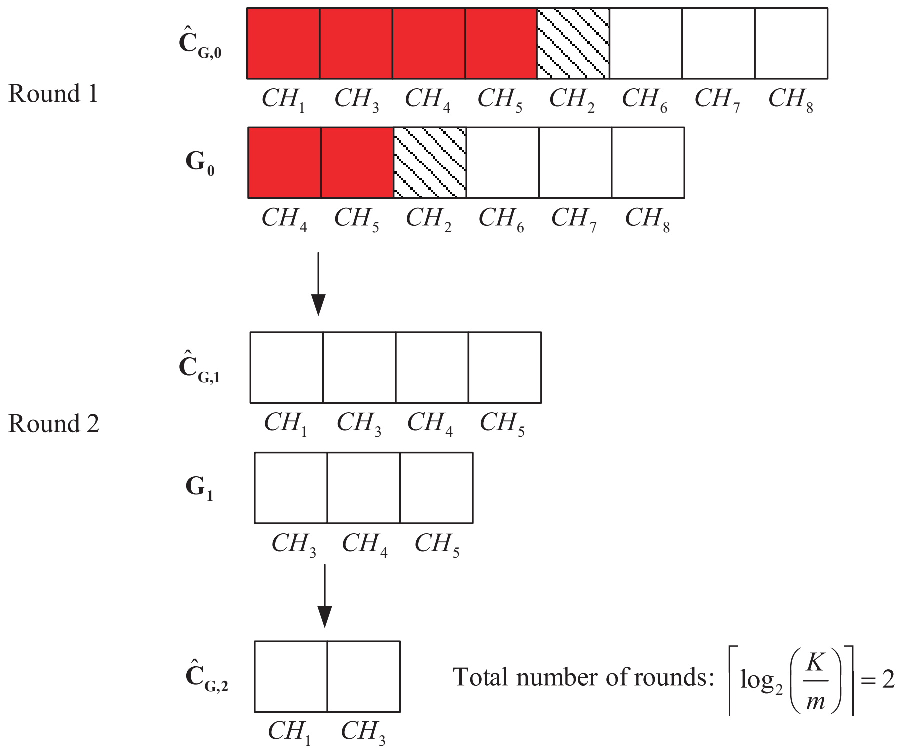

Fig. 5.4 An example of the AE algorithm.

than CH_2 (i.e., CH_4 and CH_5). Half of the channels with the smallest empirical mean values in $\hat{\mathbf{C}}_{\mathbf{G},\mathbf{0}}$ are eliminated at the end of round 1 including the good channel CH_2. Let $\hat{\mathbf{C}}_{\mathbf{G},\mathbf{1}}$ be the remaining channels for channel sensing in round 2. We have a similar channel sensing and elimination process in the next rounds as shown in Fig. 5.4. Finally, the AE outputs $\hat{\mathbf{C}}_{\mathbf{G},\mathbf{2}} = \{CH_1, CH_3\}$ as the final result.

We then prove that the AE algorithm is a ε-PAC algorithm as follows:

Theorem 5.3.3. *The AE algorithm is an ε-PAC algorithm that can correctly identify m best channels with a probability that is at least $1-\varepsilon$ where $\varepsilon = \frac{6mN}{t}\exp\left(-\frac{(\Delta_m^m)^2}{2}t\right)$.*

Proof. From Lemma 5.3.1, we know the probability that $CH_k \in \mathbf{C}_\mathbf{G}$ is eliminated during the AE algorithm is expressed as

$$\sum_{i=1}^{\lceil \log_2(K/m)\rceil} \Pr\left(X_i > \frac{1}{3}|G_{i-1}|\right) = 6\sum_{i=1}^{\lceil \log_2(K/m)\rceil} \exp\left(-\frac{(\Delta_m^m)^2}{2}t\right) \le \frac{6N}{t}\exp\left(-\frac{(\Delta_m^m)^2}{2}t\right), \tag{5.16}$$

where $t = \left\lfloor \frac{N}{\lceil \log_2(K/m) \rceil} \right\rfloor$. According to the union bound theory, the probability of incorrectly identifying the m best channels is at most $\sum_{i=1}^{m} \frac{6N}{t} \exp\left(-\frac{(\Delta_m^m)^2}{2} t\right) = \frac{6mN}{t} \exp\left(-\frac{(\Delta_m^m)^2}{2} t\right)$ which proves the theorem. □

Note that $\varepsilon = \frac{6mN}{t} \exp\left(-\frac{(\Delta_m^m)^2}{2} t\right)$ is only an upper-bound of the error rate of the AE algorithm. In practice, the error rate of the AE algorithm is much lower as shown in the simulation results.

In this section, we propose two PR algorithms and one AE algorithm. With the availability constraint p^*, all of the algorithms are proved to be ε-PAC algorithms that can identify good and bad channels with a finite time horizon and low error rate.

5.4 Joint Channel Sensing and Power Control Scheme

In this section, we propose a joint channel sensing and power control (JCSPC) scheme that can maximize the total number of transmitted bits of each cluster under channel availability and data rate constraints. We use the AE algorithm for the channel sensing phase to find the m best channels for n sensors ($n \leq m \leq K$) to regularly transmit their data. Let ε^* be the maximum error rate of the AE algorithm and $t = \frac{N}{\log_2\left(\frac{K}{m}\right)}$ for simplicity. According to Theorem 5.3.3, we know that $\varepsilon = \frac{6mN}{t} \exp\left(-\frac{(\Delta_m^m)^2}{2} t\right) \leq \varepsilon^*$. Therefore, we have

$$N \geq \frac{2\log_2\left(\frac{K}{m}\right)}{(\Delta_m^m)^2} \ln\left(\frac{6m\log_2\left(\frac{K}{m}\right)}{\varepsilon^*}\right). \tag{5.17}$$

We also assume that all sensors have the same sensing power consumption P_s and circuit power consumption P_c. Therefore, according to Equation (5.5) and Equation (5.17), the minimum fraction of energy used for channel sensing η^* is given by

$$\eta \geq \frac{\alpha NT\,(P_c + P_s)}{E} \geq \frac{2\alpha T\,(P_c + P_s)\log_2\left(\frac{K}{m}\right)}{(\Delta_m^m)^2 E} \ln\left(\frac{6m\log_2\left(\frac{K}{m}\right)}{\varepsilon^*}\right) = \eta^*. \tag{5.18}$$

Next we prove that for sensor S_i on channel CH_k, there exists a $P_{i,k}^*$ that maximizes the total number of transmitted bits. For sensor S_i with transmission power P_j on channel CH_k we take the limits of $L_{i,j,k}$ in Equation (5.9) and have

$$\lim_{P_j \to 0} L_{i,j,k} = \lim_{P_j \to 0} \frac{(1-\eta)\,EB\log_2\left(1 + P_j g_{i,k}\right)}{P_j + P_c} = 0, \tag{5.19}$$

and

$$\lim_{P_j \to P_M} L_{i,j,k} = \lim_{P_j \to P_M} \frac{(1-\eta)EB\log_2\left(1+P_j g_{i,k}\right)}{P_j+P_c} = \frac{(1-\eta)EB\log_2\left(1+P_M g_{i,k}\right)}{P_M+P_c} > 0. \tag{5.20}$$

Since we have $\lim_{P_j \to P_M} L_{i,j,k} > \lim_{P_j \to 0} L_{i,j,k} = 0$ and $L_{i,j,k}$ in Equation (5.9) is finite for any $P_j \in \mathbf{P}$, according to the extreme value theorem, there exists a $P^*_{i,k}$ that maximizes the total number of transmitted bits.

The JCSPC scheme is given in Algorithm 5.4, where the Hungarian algorithm is used to solve the assignment problem in Equation (5.10). Although the Hungarian algorithm has $O\left(n^4\right)$ complexity, this is usually not a problem in practice, since in the cluster-based CRWSN, the number of sensors with data transmission requests in each cluster is often not high, for example less than 10% of sensors are active in a cluster with 100 sensor nodes.

Algorithm 5.4 Joint Channel Sensing and Power Control Scheme

Input the value of n, m, K, T, Δ^m_m and ε^*.
Initialization: Find the m best channels using the AE algorithm. Calculate η^* according to Equation (5.18).
for $1 \le i \le n$ **do**
  for $1 \le k \le m$ **do**
    Calculate $P^*_{i,k}$ and $L^*_{i,k}$ based on Equation (5.8) and Equation (5.9).
    $L \leftarrow L^*_{i,k}$.
  end for
end for
Solve Equation (5.10) using the Hungarian algorithm [61].
Output Π^* and L^*, where Π^* is the $K \times K$ matrix with element $\pi^*_{i,k}$ that maximizes L^* in Equation (5.10).

Note that for the AE algorithm, we need to know Δ^m_m for calculating N and η^*. However, this is not usually a problem in practice since we can set Δ^m_m to a small value δ (e.g., $\delta = 0.05$). If the actual Δ^m_m is larger than δ, we will only have a tighter lower bound for N and η^* which will not violate the QoS constraints. If the actual Δ^m_m is smaller than δ, the difference of p_m and p_{m+1} is so small that it is not helpful to identify which channel is better. In other words, either CH_m and CH_{m+1} can be identified as a good channel when $\Delta^m_m < \delta$.

5.5 Simulation Results

In this section, we provide simulation results to show the performance of our channel sensing algorithms and the JCSPC scheme. We assume that the channels are Rayleigh block fading channels. The channel state information (CSI) is assumed to be known by both the transmitter and receiver. For CH_k assigned to S_i, the normalized channel gain $g_{i,k}$ is randomly generated from an exponential distribution in each fading block. The transmission power ranges from 0 to 100 mW and is equally divide into $M = 10$ power levels. The parameters of used in the simulation are given in Table 5.1

Table 5.1 Parameters for simulation

Symbol	Description	Value
P_c	Circuit power consumption	20 mW
P_s	Sensing power consumption	30 mW
T	Length of each time slot	1 s
α	Fraction of time for channel sensing	0.1
E	Total energy spent in one fading block	10 J
B	Channel bandwidth	200 kHz
M	Number of transmission power levels	10
R^*	Minimum data rate requirement	100 kbps

We first show the performance of channel sensing algorithms. We assume that there are $K = 8$ licensed channels and each channel is sensed by an active sensor per cluster. The mean values of channel availability $\mathbf{p} = \{p_1, p_2, \dots p_K\}$ are in increasing order and equally spaced in the interval [0.05, 0.95]. We set the channel availability constraint as $p^* = 0.8$ and the fraction of energy used for channel sensing as $\eta = 0.05$. We have $N = 100$ according to Equation (5.5) and we aim at finding $m = 2$ best channels within N time slots. For performance comparison, we propose a threshold detection (TD) algorithm. In the TD algorithm, the channel CH_k is identified as a bad channel at any time slot T_n once we have $\hat{p}_{k,n} < p^*$.

The simulation results of the channel sensing algorithms are averaged over 500 simulation runs. In the beginning, all channels are assumed to be good channels. The SR and IR algorithms gradually identify bad channels and eliminate them from the good channels with high confidence. Unlike the SR and IR algorithms, the AE algorithm keeps sensing the channels until it has a confidence high enough to eliminate at most half of the current channels and keep the rest as good channels. In this example, according to the definition in Algorithm 5.3, the channel sensing of the AE algorithm contains $\lceil \log_2 (K/m) \rceil = 2$ rounds and each round contains $t = \left\lfloor \frac{N}{\lceil \log_2 (\frac{K}{m}) \rceil} \right\rfloor = 50$ time slots. The AE algorithm keeps sensing

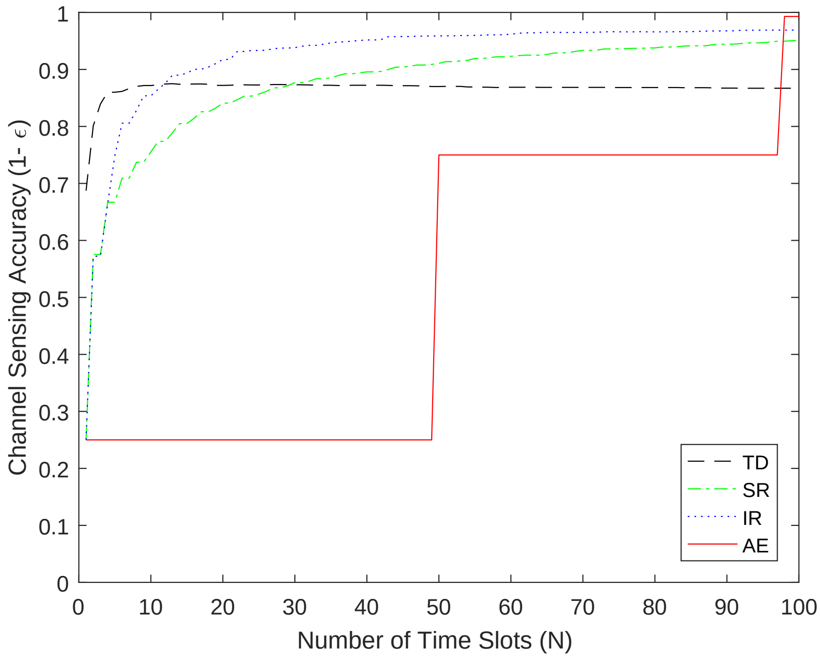

Fig. 5.5 Channel sensing accuracy $(1-\varepsilon)$ of various channel sensing algorithms.

8 channels for 50 time slots (round 1). It eliminates 4 channels with the smallest empirical mean value after the first round. Then in the second round, the AE algorithm keeps sensing the remaining 4 channels for 50 time slots. It eliminates 2 channels with the smallest empirical mean value after the second round and outputs the $m = 2$ best channels.

The channel identification accuracy of the channel sensing algorithms are given in Fig. 5.5. We show that the three proposed algorithms achieve higher channel sensing accuracy (above 95%) than the TD algorithm which achieves 86% accuracy. For the final error rate, we have $\varepsilon(\omega_{TD},\eta) > \varepsilon(\omega_{SR},\eta) > \varepsilon(\omega_{IR},\eta) > \varepsilon(\omega_{AE},\eta)$. We also find that for any algorithm the error rate decreases with an increasing number of time slots (N). Eventually, the AE algorithm achieves the highest channel sensing accuracy and the lowest error rate.

We then investigate the impact of $\Delta_{i,j}$ on the error rate ε. Specifically, we choose Δ_m^m as a variable of the simulation. According to Equation (5.13), we have $\Delta_m^m = \Delta_{m+1}^m = \min_i \Delta_i^m = p_{m+1} - p_m$. In this simulation, we assume that we have $K = 16$ licensed channels and each channel is sensed by an active sensor per cluster. We aim at finding the $m = 5$ best channels within $N = 30$ time slots. The variable Δ_m^m is varied from 0.05 to 0.45. In Fig. 5.6, we show that the error rate of our proposed algorithms decrease with increasing Δ_m^m. On the other hand, the value of Δ_m^m has little impact on the performance of the TD algorithm. For the same value of Δ_m^m, the AE algorithm always achieves the lowest error rate. We also notice

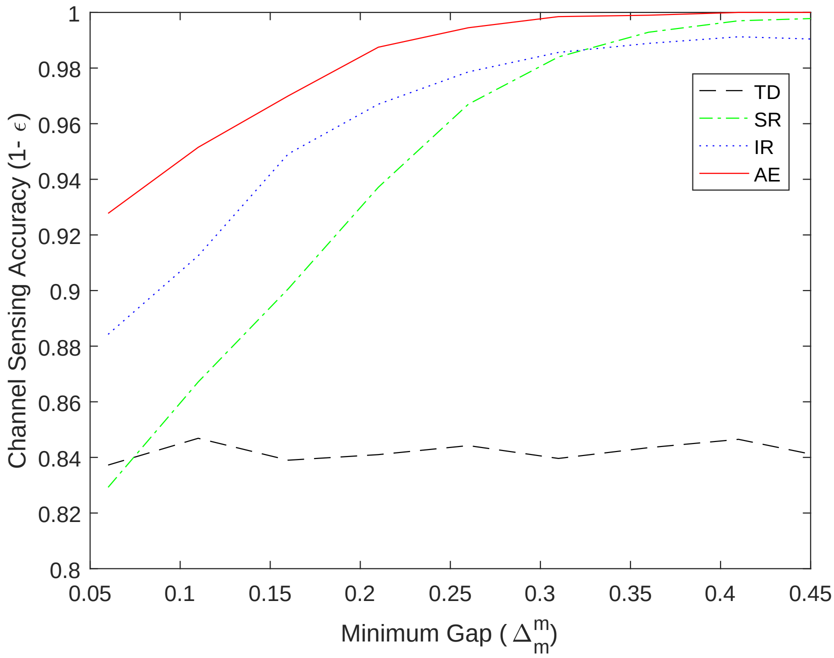

Fig. 5.6 Channel sensing accuracy $(1-\varepsilon)$ with various minimum channel availability gap (Δ_m^m).

that the SR algorithm has a lower error rate than the IR algorithm when Δ_m^m is sufficiently large $(\Delta_m^m > 0.32)$.

We consider the efficiency of the JCSPC scheme in one fading block. For performance comparison, we propose a random channel access (RCA) scheme which randomly allocates available channels to sensors having data transmission requests. We also give the optimal channel access scheme by solving the optimization problem in Equation (5.10) using the Hungarian algorithm, given that the channel availability information $\mathbf{p}$ is perfectly known. We assume that we have $K = 8$ licensed channels and each channel is sensed by an active sensor per cluster. We set the other parameters as $N = 10$, $m = 4$, $\varepsilon^* = 0.1$, $\Delta_m^m = 0.1$ and $p^* = 0.5$. We vary the number of sensors with data transmission requests (n) from 1 to 4 and compare the performance of JCSPC scheme with the optimal solution and the RCA scheme. For each fading block, the normalized channel gains $\mathbf{g_i}$ are randomly generated based on the Rayleigh fading channel models. An example of the mean values of channel availability $\mathbf{p}$ and the normalized channel gains for one fading block (e.g., $\mathbf{g_1}$ in Fig. 5.2) are given in Table 5.2.

The simulation result based on the channel availability $\mathbf{p}$ and the normalized channel gains in Table 5.2 is given in Fig. 5.7. We first consider the JCSPC scheme. According to Algorithm 5.4, the JCSPC scheme utilizes the AE algorithm for channel sensing and the

Table 5.2 The normalized channel gain

	CH_1	CH_2	CH_3	CH_4	CH_5	CH_6	CH_7	CH_8
p	0.05	0.18	0.31	0.44	0.56	0.69	0.82	0.95
S_1	22.81	30.60	14.78	4.93	27.49	1.31	17.97	5.09
S_2	1.51	0.34	15.79	28.46	18.76	9.30	9.88	29.83
S_3	22.31	38.19	18.70	71.28	51.15	1.59	4.39	20.41
S_4	2.02	34.86	6.35	28.62	41.05	46.56	0.99	15.12

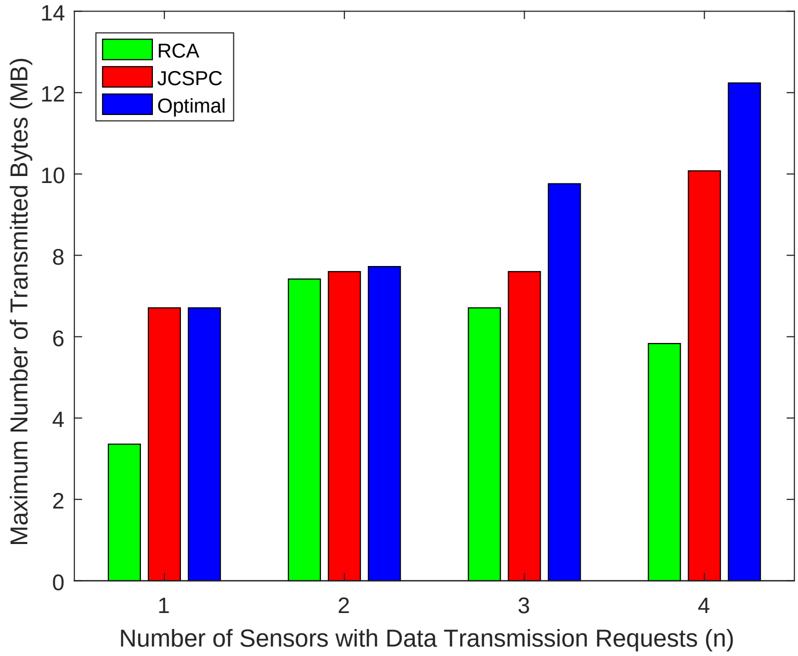

Fig. 5.7 Maximum transmitted bytes in the cluster vs. various numbers of sensors with data transmission requests, for one fading block.

Hungarian algorithm for power control and channel assignment. The Hungarian algorithm is an optimization algorithm that can solve the assignment problem in polynomial time [61]. Therefore, the performance of the JCSPC scheme relies heavily on the performance of the AE algorithm. As the AE algorithm cannot perfectly identify the 'good' channels that satisfy the channel availability constraints, the JCSPC scheme can only achieve near-optimal results. We provide the optimal transmission power and the maximum number of transmitted bytes given by the JCSPC scheme for $n = 4$ in Table 5.3 and Table 5.4 respectively where n/a means that the channel availability requirement ($p^* = 0.5$) or the data rate requirement ($R^* = 100$ kbps) is not fulfilled on that channel. We identify the channel assignment of the JCSPC scheme using red backgrounds. The corresponding optimal transmission power and the maximum number of transmitted bytes are marked with grey backgrounds in Table 5.3 and Table 5.4 respectively. In this example, for $n = 4$ channel $\{CH_8, CH_7, CH_6\}$ is assigned to $\{S_1, S_2, S_4\}$ respectively by the JCSPC scheme. Note that no channel is assigned to S_3 as no channel can fulfill the channel availability or the data rate constraints.

Table 5.3 The optimal transmission power given by the JCSPC scheme

	CH_1	CH_2	CH_3	CH_4	CH_5	CH_6	CH_7	CH_8
S_1	n/a	n/a	n/a	n/a	n/a	20 mW	n/a	20 mW
S_2	n/a	n/a	n/a	n/a	n/a	70 mW	60 mW	30 mW
S_3	n/a	n/a	n/a	n/a	n/a	n/a	n/a	30 mW
S_4	n/a	n/a	n/a	n/a	n/a	20 mW	n/a	40 mW

Table 5.4 The maximum number of transmitted bytes given by the JCSPC scheme

	CH_1	CH_2	CH_3	CH_4	CH_5	CH_6	CH_7	CH_8
S_1	n/a	n/a	n/a	n/a	n/a	3.36 MB	n/a	6.71 MB
S_2	n/a	n/a	n/a	n/a	n/a	0.71 MB	0.89 MB	2.47 MB
S_3	n/a	n/a	n/a	n/a	n/a	n/a	n/a	1.85 MB
S_4	n/a	n/a	n/a	n/a	n/a	2.48 MB	n/a	1.46 MB

For comparison, the optimal transmission power and the maximum number of transmitted bytes given by the optimal solution is provided in Table 5.5 and Table 5.6 respectively. In Table 5.5 and Table 5.6, we mark the channels that fulfill the channel availability requirements with yellow backgrounds. The corresponding optimal transmission power and the maximum number of transmitted bytes of the optimal solution are identified with green backgrounds. In this example, for $n = 4$ channel $\{CH_8, CH_7, CH_5, CH_6\}$ is assigned to $\{S_1, S_2, S_3, S_4\}$ respectively by the optimal solution. From Table 5.4 and Table 5.6, we see that the loss of the number of transmitted data in the JCSPC scheme is due to the misidentification of CH_4 as a good channel and CH_5 as a bad channel compared with the optimal solution. The performance of the JCSPC scheme relies heavily on the performance of the channel sensing algorithm (i.e., the AE algorithm).

Table 5.5 The optimal transmission power given by the optimal solution

	CH_1	CH_2	CH_3	CH_4	CH_5	CH_6	CH_7	CH_8
S_1	n/a	n/a	n/a	n/a	n/a	20 mW	n/a	20 mW
S_2	n/a	n/a	n/a	n/a	50 mW	70 mW	60 mW	30 mW
S_3	n/a	n/a	n/a	n/a	20 mW	n/a	n/a	30 mW
S_4	n/a	n/a	n/a	n/a	30 mW	20 mW	n/a	40 mW

Table 5.6 The maximum number of transmitted bytes given by the optimal solution

	CH_1	CH_2	CH_3	CH_4	CH_5	CH_6	CH_7	CH_8
S_1	n/a	n/a	n/a	n/a	n/a	3.36 MB	n/a	6.71 MB
S_2	n/a	n/a	n/a	n/a	1.01 MB	0.71 MB	0.89 MB	2.47 MB
S_3	n/a	n/a	n/a	n/a	2.16 MB	n/a	n/a	1.85 MB
S_4	n/a	n/a	n/a	n/a	1.85 MB	2.48 MB	n/a	1.46 MB

We then consider the performance of the JCSPC scheme over several fading blocks. In each fading block, the normalized channel power gain is randomly generated from the same Rayleigh fading channel model. The maximum transmitted bytes in each cluster that is averaged over 1000 fading blocks (e.g., from $\mathbf{g_1}$ to $\mathbf{g_Z}$ where $Z = 1000$ in Fig. 5.2) is given in Fig. 5.8. The simulation result shows that the JCSPC scheme achieves near-optimal results and outperforms the RCA scheme for various values of n in the long run.

Finally, we investigate the impact of N on the performance of the JCSPC scheme, where N is defined as the maximum number of time slots for channel sensing of each cluster. We assume that the value of P_c, P_s, T, α and E are the same as the ones used to yield the results given in Fig. 5.7. We vary N and give the performance of the JCSPC scheme in Fig. 5.9. The simulation result is averaged by 1000 simulation runs and shows that the performance of the JCSPC converges to the optimal solution with increasing N. Clearly the performance of the JCSPC scheme relies heavily on the accuracy of the AE channel sensing algorithm. According to the definition of the AE algorithm in Algorithm 5.3, the channel sensing and elimination process is divided into $\lceil \log_2 (K/m) \rceil$ rounds and each round contains $t = \left\lfloor \frac{N}{\lceil \log_2 (\frac{K}{m}) \rceil} \right\rfloor$ time slots. The AE algorithm will have more historical data to identify and so better eliminate the 'bad' channels in each round as N increases. Thus the accuracy of the AE algorithm increases with N which positively affects the performance of the JCSPC scheme.

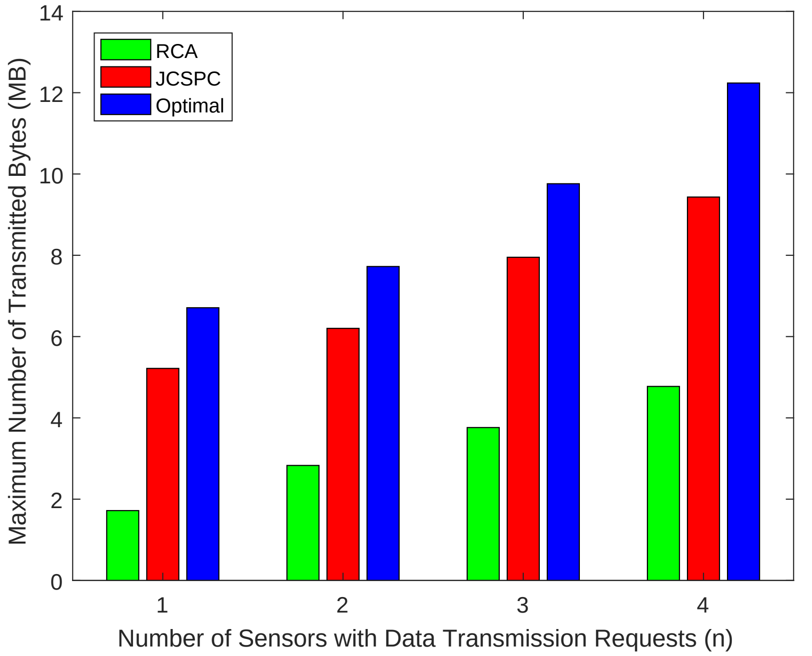

Fig. 5.8 Maximum transmitted bytes in the cluster vs. different number of sensors with data transmission requests, averaged over 1000 fading blocks.

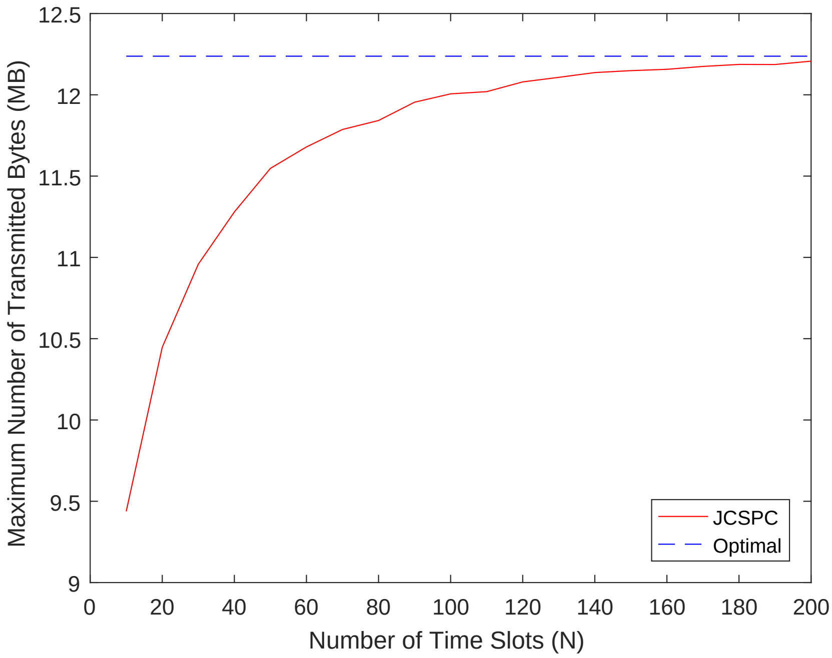

Fig. 5.9 Maximum transmitted bytes in the cluster vs. different N.

5.6 Summary

In this chapter, we considered a cluster-based CRWSN. Unlike the scenarios where PUs voluntarily allocate their vacant channels to SUs, in the CRWSN, the sensors with cognitive radios must sense the vacant channels and find the good channels that are available and can fulfill their QoS requirements on delay and data rate.

We first proposed three cluster-based channel sensing algorithms that can identify good channels with high accuracy. We proved that given specified channel availability constraints, all of the three algorithms are ε-PAC algorithms that terminate in a finite time with a finite error rate. We then considered the transmission power and data transmission via the good channels. A joint channel sensing and power control (JCSPC) scheme is proposed to maximize the total number of transmitted bits in each cluster.

We provided the simulation results in Section 5.5. We first considered the performance of the proposed channel sensing algorithms. The simulation results showed that the AE algorithm outperformed the other algorithms and achieved the highest channel sensing accuracy. We then investigated the impact of the minimum channel availability gap (Δ_m^m) on the error rate. The AE algorithm outperformed the other algorithms given the same simulation settings. Finally, we showed that the JCSPC scheme can achieve near-optimal performance compared to the optimal solution. The performance of the JCSPC scheme relies heavily on the accuracy of the channel sensing algorithm, namely the AE algorithm.

Chapter 6

Conclusions and Future Work

6.1 Conclusions

This dissertation has focused on the power control and optimal resource allocation strategies in cooperative communication networks and cognitive radio networks with QoS constraints. In various scenarios, QoS-constrained efficient power control and resource allocation schemes were proposed. Both the theoretical and simulation results are provided in this dissertation.

In Chapter 1, we introduced the motivation and topics of our research. In Chapter 2, we gave some background information on the wireless channel capacity, the end-to-end delay and various QoS metrics such as delay, data rate and packet error rate. We also introduced some power control and resource allocation methods that are used in our research.

We first investigated the power control and optimization problem of a cooperative communication network. A cluster-based wireless sensor network was considered in Chapter 3, where a cooperative transmission scheme for WSNs was presented. In this scenario, sensors in each cluster cooperatively transmit data to the neighboring cluster [14]. With specified QoS constraints on delay and data rate, we proposed a dynamic power control algorithm that can minimize the total power consumption of the transmitters in each cluster. We also gave an approximate algorithm that has a closed-form and near-optimal solution to the power control and optimization problem.

In Chapter 4, we investigated the competitive spectrum access problem in a cooperative cognitive radio network [15]. In this scenario, we assumed that the primary users are willing to allocate their vacant licensed channels to secondary users for secondary transmissions. The channel access problem was formulated as an assignment problem and further can be expressed as a matching problem. We proposed a distributed matching algorithm that can give near-optimal results to the assignment problem. Specifically, we gave the implementation of the matching algorithms at the SU and the PU. We also developed a fast distributed matching algorithm that achieves sub-optimal results with far fewer message exchanges compared with the distributed matching algorithm.

Finally, channel sensing and power control in a cluster-based cognitive radio wireless sensor network are analyzed in Chapter 5 [16]. In this scenario, the primary users do not voluntarily allocate their vacant channels to the secondary users. As secondary users, wireless sensors with cognitive radios cooperatively sense the whole spectrum and periodically report the sensing result to the cluster head. To facilitate the channel sensing process, we proposed three probably approximately correct algorithms that utilize the historical sensing data to predict the availability of the licensed channels. Based on the channel sensing algorithms, we further developed a joint channels sensing and power control (JCSPC) scheme to maximize the total number of transmitted bits in each cluster.

All of the power control and resource allocation algorithms in different scenarios are designed under specified QoS constraints. We provided extensive theoretical proofs and simulation results to establish the performance of our proposed algorithms.

6.2 Future Work

In this section, we point out several future research directions and possible extensions of our work.

6.2.1 Dynamic Power Control for Virtual MIMO Wireless Networks

In Chapter 1, we have considered the dynamic power control problem under a cooperative transmission scheme. The cooperative transmission scheme can be viewed as a virtual multiple-input single-output (MISO) scheme where the the sensors in the transmitter cluster achieve the diversity gain via cooperative transmission. To improve the cooperative transmission performance, we can extend the virtual MISO scheme to a virtual MIMO scheme. The diversity gain of the receiver cluster can be achieved by diversity combining techniques such as selection combining [99] and max ratio combing [100]. More specifically, the cluster head of the receiver cluster can enhance the SNR of the received message by selecting or combining the received message of other sensors in the cluster. A new cooperation framework and power control scheme would need to be developed for the virtual MIMO network.

6.2.2 Efficient Distributed Spectrum Access

Although the distributed spectrum access algorithms achieve near-optimal results in Chapter 4, it is still interesting to investigate whether the message exchanges in the spectrum access process can be further reduced. One possible approach is to set the maximum length of the preference list [101] of each secondary user or the maximum number of times it can send the channel access requests. Another approach is that secondary users having data transmission requests can jointly apply for a group of channels and take turns to send their data. Efficient algorithms for group formation of secondary users require further investigation.

6.2.3 Optimal Channel Tracking

The channel sensing algorithms proposed in Chapter 5 can be used in various scenarios. For example, although it is important to select the channels with large values of channel power gain for data transmission, it is difficult track the 'good' channels in a fading environment. Although the proposed channel sensing algorithms cannot predict the channel power gain in every fading block, they can gradually find out the mean value of the channel power gain of each channel, regardless of what distribution the channel power gain may follow. However, the PAC algorithm cannot find accurate mean values with only a limited quantity of channel feedback (i.e., the channel power gain in previous fading blocks), so it has to transmit through each channel and get as much channel feedback as possible. On the other hand, it cannot efficiently track and utilize the 'good' channels if it only focuses on collecting channel feedback. Thus, there is an exploration vs. exploitation tradeoff for any PAC channel sensing algorithm [102] and it is interesting to develop an efficient algorithm that can expend the minimum number of explorations to find the best channel for data transmission.

6.2.4 Applications in Other Scenarios

In addition to the applications in WSNs, cooperative communication can also improve the performance of other wireless networks with QoS constraints such as the device-to-device (D2D) communication networks [103] and mobile ad-hoc networks [104] where wireless devices are usually equipped with single antennas and have a limited energy supply. To consider the power control and resource allocation problems in these scenarios, different channel models involving user mobility need to be considered. Besides, cooperative communication can do more than just provide transmission diversity. Control and other channel information can also be shared via cooperation of different users in the wireless networks.

The power control and resource allocation problems in scenarios such as cooperative spectrum sensing, cooperative routing and cooperative localization are worth investigating in the future. Some of the possible research topics could be optimal cooperative spectrum sensing with energy constraints, delay-tolerant cooperative routing and power management for cooperative localization.

References

[1] J. N. Laneman, “Cooperative communications in mobile ad hoc networks,” *IEEE Signal Processing Magazine*, vol. 1053, no. 5888/06, 2006.

[2] Y. C. Liang, K. C. Chen, G. Y. Li, and P. Mahonen, “Cognitive radio networking and communications: an overview,” *IEEE Transactions on Vehicular Technology*, vol. 60, pp. 3386–3407, Sept 2011.

[3] A. Paulraj, R. Nabar, and D. Gore, *Introduction to space-time wireless communications*. Cambridge university press, 2003.

[4] A. Nosratinia, T. E. Hunter, and A. Hedayat, “Cooperative communication in wireless networks,” *IEEE communications Magazine*, vol. 42, no. 10, pp. 74–80, 2004.

[5] Y. Yuan, Z. He, and M. Chen, “Virtual MIMO-based cross-layer design for wireless sensor networks,” *IEEE Transactions on Vehicular Technology*, vol. 55, pp. 856–864, May 2006.

[6] A. Del Coso, S. Savazzi, U. Spagnolini, and C. Ibars, “Virtual MIMO channels in cooperative multi-hop wireless sensor networks,” in *Information Sciences and Systems, 2006 40th Annual Conference on*, pp. 75–80, IEEE, 2006.

[7] S. H. Lee, D. R. Shin, H. W. Jeong, and Y. H. Kim, “Distributed bargaining strategy for downlink virtual MIMO with device-to-device communication,” *IEEE Transactions on Communications*, vol. 64, pp. 1503–1516, April 2016.

[8] P. Kolodzy and I. Avoidance, “Spectrum policy task force,” *Federal Commun. Comm., Washington, DC, Rep. ET Docket*, no. 02-135, 2002.

[9] M. H. Islam, C. L. Koh, S. W. Oh, X. Qing, Y. Y. Lai, C. Wang, Y.-C. Liang, B. E. Toh, F. Chin, G. L. Tan, *et al.*, “Spectrum survey in singapore: occupancy measurements and analyses,” in *Cognitive Radio Oriented Wireless Networks and Communications, 2008. CrownCom 2008. 3rd International Conference on*, pp. 1–7, IEEE, 2008.

[10] A. Goldsmith, S. A. Jafar, I. Maric, and S. Srinivasa, “Breaking spectrum gridlock with cognitive radios: an information theoretic perspective,” *Proceedings of the IEEE*, vol. 97, no. 5, pp. 894–914, 2009.

[11] S. Srinivasa and S. A. Jafar, “Cognitive radios for dynamic spectrum access - the throughput potential of cognitive radio: a theoretical perspective,” *IEEE Communications Magazine*, vol. 45, pp. 73–79, May 2007.

[12] R. Tandra, S. M. Mishra, and A. Sahai, "What is a spectrum hole and what does it take to recognize one?," *Proceedings of the IEEE*, vol. 97, no. 5, pp. 824–848, 2009.

[13] S. Huang, X. Liu, and Z. Ding, "Opportunistic spectrum access in cognitive radio networks," in *INFOCOM 2008. The 27th Conference on Computer Communications. IEEE*, pp. 1427–1435, IEEE, 2008.

[14] Z. Feng and I. Wassell, "Dynamic power control and optimization scheme for QoS-constrained cooperative wireless sensor networks," in *2016 IEEE International Conference on Communications (ICC)*, pp. 1–6, May 2016.

[15] Z. Feng and I. Wassell, "Competitive distributed spectrum access in QoS-constrained cognitive radio networks," in *2016 IEEE Global Communications Conference (GLOBECOM)*, pp. 1–6, Dec 2016.

[16] Z. Feng and I. Wassell, "Joint channel sensing and power control scheme for cognitive radio wireless sensor networks," in *2017 Wireless Days*, pp. 180–183, March 2017.

[17] A. Goldsmith, *Wireless communications*. Cambridge university press, 2005.

[18] A. J. Goldsmith and P. P. Varaiya, "Capacity of fading channels with channel side information," *IEEE Transactions on Information Theory*, vol. 43, no. 6, pp. 1986–1992, 1997.

[19] C. E. Shannon, "A mathematical theory of communication," *ACM SIGMOBILE Mobile Computing and Communications Review*, vol. 5, no. 1, pp. 3–55, 2001.

[20] R. McEliece and W. Stark, "Channels with block interference," *IEEE Transactions on Information Theory*, vol. 30, pp. 44–53, Jan 1984.

[21] S. Jin, M. R. McKay, C. Zhong, and K. K. Wong, "Ergodic capacity analysis of amplify-and-forward MIMO dual-hop systems," *IEEE Transactions on Information Theory*, vol. 56, pp. 2204–2224, May 2010.

[22] L. Li and A. J. Goldsmith, "Capacity and optimal resource allocation for fading broadcast channels - part I: ergodic capacity," *IEEE Transactions on Information Theory*, vol. 47, pp. 1083–1102, Mar 2001.

[23] L. Li and A. J. Goldsmith, "Capacity and optimal resource allocation for fading broadcast channels - part II: outage capacity," *IEEE Transactions on Information Theory*, vol. 47, pp. 1103–1127, Mar 2001.

[24] X. Kang, Y. C. Liang, A. Nallanathan, H. K. Garg, and R. Zhang, "Optimal power allocation for fading channels in cognitive radio networks: ergodic capacity and outage capacity," *IEEE Transactions on Wireless Communications*, vol. 8, pp. 940–950, Feb 2009.

[25] J. Chen, *Resource allocation for delay constrained wireless communications*. PhD thesis, University College London, 2010.

[26] D. Tse and P. Viswanath, *Fundamentals of wireless communication*. Cambridge university press, 2005.

[27] A. Goldsmith, S. A. Jafar, N. Jindal, and S. Vishwanath, "Capacity limits of MIMO channels," *IEEE Journal on Selected Areas in Communications*, vol. 21, pp. 684–702, June 2003.

[28] E. Telatar, "Capacity of multi-antenna gaussian channels," *European transactions on telecommunications*, vol. 10, no. 6, pp. 585–595, 1999.

[29] G. J. Foschini and M. J. Gans, "On limits of wireless communications in a fading environment when using multiple antennas," *Wireless personal communications*, vol. 6, no. 3, pp. 311–335, 1998.

[30] D. P. Bertsekas, R. G. Gallager, and P. Humblet, *Data networks*, vol. 2. Prentice-Hall International New Jersey, 1992.

[31] D. Gross, *Fundamentals of queueing theory*. John Wiley & Sons, 2008.

[32] U. N. Bhat, *An introduction to queueing theory: modeling and analysis in applications*. Birkhäuser, 2015.

[33] D. G. Kendall, "Stochastic processes occurring in the theory of queues and their analysis by the method of the imbedded markov chain," *The Annals of Mathematical Statistics*, pp. 338–354, 1953.

[34] F. Pollaczek, "Über eine aufgabe der wahrscheinlichkeitstheorie. I," *Mathematische Zeitschrift*, vol. 32, no. 1, pp. 64–100, 1930.

[35] A. Y. Khinchin, "The mathematical theory of a stationary queue," tech. rep., DTIC Document, 1967.

[36] D. Wu, "QoS provisioning in wireless networks," *Wireless communications and mobile computing*, vol. 5, no. 8, pp. 957–969, 2005.

[37] S. Cui, A. J. Goldsmith, and A. Bahai, "Energy-efficiency of MIMO and cooperative MIMO techniques in sensor networks," *IEEE Journal on selected areas in communications*, vol. 22, no. 6, pp. 1089–1098, 2004.

[38] T. H. Lee, *The design of CMOS radio-frequency integrated circuits*. Cambridge university press, 2003.

[39] S. H. Han and J. H. Lee, "An overview of peak-to-average power ratio reduction techniques for multicarrier transmission," *IEEE wireless communications*, vol. 12, no. 2, pp. 56–65, 2005.

[40] G. Miao, N. Himayat, Y. G. Li, and A. Swami, "Cross-layer optimization for energy-efficient wireless communications: a survey," *Wireless Communications and Mobile Computing*, vol. 9, no. 4, pp. 529–542, 2009.

[41] D. Feng, C. Jiang, G. Lim, L. J. Cimini, G. Feng, and G. Y. Li, "A survey of energy-efficient wireless communications," *IEEE Communications Surveys & Tutorials*, vol. 15, no. 1, pp. 167–178, 2013.

[42] S. K. Jayaweera, "Virtual MIMO-based cooperative communication for energy-constrained wireless sensor networks," *IEEE Transactions on wireless communications*, vol. 5, no. 5, pp. 984–989, 2006.

[43] T. D. Nguyen, O. Berder, and O. Sentieys, "Cooperative MIMO schemes optimal selection for wireless sensor networks," in *2007 IEEE 65th Vehicular Technology Conference - VTC2007-Spring*, pp. 85–89, April 2007.

[44] W. Yu, W. Rhee, S. Boyd, and J. M. Cioffi, "Iterative water-filling for gaussian vector multiple-access channels," *IEEE Transactions on Information Theory*, vol. 50, no. 1, pp. 145–152, 2004.

[45] O. Ozel, K. Tutuncuoglu, J. Yang, S. Ulukus, and A. Yener, "Transmission with energy harvesting nodes in fading wireless channels: optimal policies," *IEEE Journal on Selected Areas in Communications*, vol. 29, pp. 1732–1743, September 2011.

[46] F. Wang, M. Krunz, and S. Cui, "Price-based spectrum management in cognitive radio networks," *IEEE Journal of Selected Topics in Signal Processing*, vol. 2, pp. 74–87, Feb 2008.

[47] S. Weber, J. G. Andrews, and N. Jindal, "The effect of fading, channel inversion, and threshold scheduling on ad hoc networks," *IEEE Transactions on Information Theory*, vol. 53, no. 11, pp. 4127–4149, 2007.

[48] T. Haustein, C. Von Helmolt, E. Jorswieck, V. Jungnickel, and V. Pohl, "Performance of MIMO systems with channel inversion," in *Vehicular Technology Conference, 2002. VTC Spring 2002. IEEE 55th*, vol. 1, pp. 35–39, IEEE, 2002.

[49] H. Sung, S.-R. Lee, and I. Lee, "Generalized channel inversion methods for multiuser MIMO systems," *IEEE Transactions on Communications*, vol. 57, no. 11, 2009.

[50] A. J. Goldsmith and P. P. Varaiya, "Capacity of fading channels with channel side information," *IEEE Transactions on Information Theory*, vol. 43, pp. 1986–1992, Nov 1997.

[51] H. A. Suraweera, P. J. Smith, and M. Shafi, "Capacity limits and performance analysis of cognitive radio with imperfect channel knowledge," *IEEE Transactions on Vehicular Technology*, vol. 59, pp. 1811–1822, May 2010.

[52] A. Pascual-Iserte, D. P. Palomar, A. I. Perez-Neira, and M. A. Lagunas, "A robust maximin approach for MIMO communications with imperfect channel state information based on convex optimization," *IEEE Transactions on Signal Processing*, vol. 54, pp. 346–360, Jan 2006.

[53] Y. Chen, G. Yu, Z. Zhang, H. h. Chen, and P. Qiu, "On cognitive radio networks with opportunistic power control strategies in fading channels," *IEEE Transactions on Wireless Communications*, vol. 7, pp. 2752–2761, July 2008.

[54] J. G. Andrews and T. H. Meng, "Optimum power control for successive interference cancellation with imperfect channel estimation," *IEEE Transactions on Wireless Communications*, vol. 2, pp. 375–383, Mar 2003.

[55] A. Das and P. Narayan, “Capacities of time-varying multiple-access channels with side information,” *IEEE Transactions on Information Theory*, vol. 48, pp. 4–25, Jan 2002.

[56] J. Munkres, “Algorithms for the assignment and transportation problems,” *Journal of the society for industrial and applied mathematics*, vol. 5, no. 1, pp. 32–38, 1957.

[57] S. Mallick, R. Devarajan, R. A. Loodaricheh, and V. K. Bhargava, “Robust resource optimization for cooperative cognitive radio networks with imperfect CSI,” *IEEE Transactions on Wireless Communications*, vol. 14, pp. 907–920, Feb 2015.

[58] L. Lu, D. He, X. Yu, and G. Y. Li, “Energy-efficient resource allocation for cognitive radio networks,” in *2013 IEEE Global Communications Conference (GLOBECOM)*, pp. 1026–1031, Dec 2013.

[59] S. Aslam, A. Shahid, and K. G. Lee, “IMS: interference minimization scheme for cognitive radio networks using hungarian algorithm,” in *The First International Conference on Future Generation Communication Technologies*, pp. 17–21, Dec 2012.

[60] R. Burkard, M. Dell’Amico, and S. Martello, *Assignment problems: revised reprint*. SIAM, 2012.

[61] H. W. Kuhn, “The hungarian method for the assignment problem,” *Naval research logistics quarterly*, vol. 2, no. 1-2, pp. 83–97, 1955.

[62] Z. Ding, S. M. Perlaza, I. Esnaola, and H. V. Poor, “Power allocation strategies in energy harvesting wireless cooperative networks,” *IEEE Transactions on Wireless Communications*, vol. 13, pp. 846–860, February 2014.

[63] J. Huang, Z. Han, M. Chiang, and H. V. Poor, “Auction-based resource allocation for cooperative communications,” *IEEE Journal on Selected Areas in Communications*, vol. 26, pp. 1226–1237, September 2008.

[64] S. Gandhi, C. Buragohain, L. Cao, H. Zheng, and S. Suri, “A general framework for wireless spectrum auctions,” in *2007 2nd IEEE International Symposium on New Frontiers in Dynamic Spectrum Access Networks*, pp. 22–33, April 2007.

[65] A. E. Roth and M. A. O. Sotomayor, “Two-sided matching: a study in game-theoretic modeling and analysis,” no. 18, 1992.

[66] A. Abdulkadiroglu and T. Sönmez, “Matching markets: theory and practice,” *Advances in Economics and Econometrics*, vol. 1, pp. 3–47, 2013.

[67] D. Gale and L. S. Shapley, “College admissions and the stability of marriage,” *The American Mathematical Monthly*, vol. 69, no. 1, pp. 9–15, 1962.

[68] I. F. Akyildiz, W. Su, Y. Sankarasubramaniam, and E. Cayirci, “A survey on sensor networks,” *IEEE Communications Magazine*, vol. 40, pp. 102–114, Aug 2002.

[69] V. C. Gungor and G. P. Hancke, “Industrial wireless sensor networks: challenges, design principles, and technical approaches,” *IEEE Transactions on industrial electronics*, vol. 56, no. 10, pp. 4258–4265, 2009.

[70] A. Nosratinia, T. E. Hunter, and A. Hedayat, "Cooperative communication in wireless networks," *IEEE Communications Magazine*, vol. 42, pp. 74–80, Oct 2004.

[71] A. D. Coso, U. Spagnolini, and C. Ibars, "Cooperative distributed MIMO channels in wireless sensor networks," *IEEE Journal on Selected Areas in Communications*, vol. 25, pp. 402–414, February 2007.

[72] S. Farahani, *ZigBee wireless networks and transceivers*. newnes, 2011.

[73] O. Younis and S. Fahmy, "Heed: a hybrid, energy-efficient, distributed clustering approach for ad hoc sensor networks," *IEEE Transactions on mobile computing*, vol. 3, no. 4, pp. 366–379, 2004.

[74] W. R. Heinzelman, A. Chandrakasan, and H. Balakrishnan, "Energy-efficient communication protocol for wireless microsensor networks," in *System sciences, 2000. Proceedings of the 33rd annual Hawaii international conference on*, pp. 10–pp, IEEE, 2000.

[75] G. Fairhurst and L. Wood, "Advice to link designers on link automatic repeat request (ARQ)," 2002.

[76] J. Pérez, J. Ibánez, L. Vielva, and I. Santamaria, "Closed-form approximation for the outage capacity of orthogonal STBC," *IEEE Communications Letters*, vol. 9, no. 11, pp. 961–963, 2005.

[77] S. Haykin, "Cognitive radio: brain-empowered wireless communications," *IEEE Journal on Selected Areas in Communications*, vol. 23, pp. 201–220, Feb 2005.

[78] Q. Zhao and B. M. Sadler, "A survey of dynamic spectrum access," *IEEE Signal Processing Magazine*, vol. 24, pp. 79–89, May 2007.

[79] T. Yucek and H. Arslan, "A survey of spectrum sensing algorithms for cognitive radio applications," *IEEE Communications Surveys Tutorials*, vol. 11, pp. 116–130, First 2009.

[80] I. F. Akyildiz, W. y. Lee, M. C. Vuran, and S. Mohanty, "A survey on spectrum management in cognitive radio networks," *IEEE Communications Magazine*, vol. 46, pp. 40–48, April 2008.

[81] Z. Ji and K. J. R. Liu, "Cognitive radios for dynamic spectrum access - dynamic spectrum sharing: a game theoretical overview," *IEEE Communications Magazine*, vol. 45, pp. 88–94, May 2007.

[82] D. Niyato and E. Hossain, "Competitive pricing for spectrum sharing in cognitive radio networks: dynamic game, inefficiency of nash equilibrium, and collusion," *IEEE Journal on Selected Areas in Communications*, vol. 26, pp. 192–202, Jan 2008.

[83] O. Simeone, I. Stanojev, S. Savazzi, Y. Bar-Ness, U. Spagnolini, and R. Pickholtz, "Spectrum leasing to cooperating secondary ad hoc networks," *IEEE Journal on Selected Areas in Communications*, vol. 26, pp. 203–213, Jan 2008.

[84] Y. Xu, J. Wang, Q. Wu, A. Anpalagan, and Y. D. Yao, "Opportunistic spectrum access in cognitive radio networks: global optimization using local interaction games," *IEEE Journal of Selected Topics in Signal Processing*, vol. 6, pp. 180–194, April 2012.

[85] Y. Gu, W. Saad, M. Bennis, M. Debbah, and Z. Han, "Matching theory for future wireless networks: fundamentals and applications," *IEEE Communications Magazine*, vol. 53, pp. 52–59, May 2015.

[86] G. Bianchi, L. Fratta, and M. Oliveri, "Performance evaluation and enhancement of the CSMA/CA MAC protocol for 802.11 wireless LANs," in *Personal, Indoor and Mobile Radio Communications, 1996. PIMRC'96., Seventh IEEE International Symposium on*, vol. 2, pp. 392–396 vol.2, Oct 1996.

[87] O. B. Akan, O. B. Karli, and O. Ergul, "Cognitive radio sensor networks," *IEEE Network*, vol. 23, pp. 34–40, July 2009.

[88] S. M. Mishra, A. Sahai, and R. W. Brodersen, "Cooperative sensing among cognitive radios," in *2006 IEEE International Conference on Communications*, vol. 4, pp. 1658–1663, June 2006.

[89] T. Chen, H. Zhang, G. M. Maggio, and I. Chlamtac, "CogMesh: a cluster-based cognitive radio network," in *2007 2nd IEEE International Symposium on New Frontiers in Dynamic Spectrum Access Networks*, pp. 168–178, April 2007.

[90] J. Zhao, H. Zheng, and G.-H. Yang, "Distributed coordination in dynamic spectrum allocation networks," in *First IEEE International Symposium on New Frontiers in Dynamic Spectrum Access Networks, 2005. DySPAN 2005.*, pp. 259–268, Nov 2005.

[91] A. Anandkumar, N. Michael, A. K. Tang, and A. Swami, "Distributed algorithms for learning and cognitive medium access with logarithmic regret," *IEEE Journal on Selected Areas in Communications*, vol. 29, pp. 731–745, April 2011.

[92] C. Tekin and M. Liu, "Online learning in opportunistic spectrum access: a restless bandit approach," in *2011 Proceedings IEEE INFOCOM*, pp. 2462–2470, April 2011.

[93] Y. Gai and B. Krishnamachari, "Decentralized online learning algorithms for opportunistic spectrum access," in *Global Telecommunications Conference (GLOBECOM 2011), 2011 IEEE*, pp. 1–6, IEEE, 2011.

[94] P. Auer, N. Cesa-Bianchi, and P. Fischer, "Finite-time analysis of the multiarmed bandit problem," *Machine learning*, vol. 47, no. 2, pp. 235–256, 2002.

[95] D. Haussler, *Probably approximately correct learning*. University of California, Santa Cruz, Computer Research Laboratory, 1990.

[96] D. Haussler and M. Warmuth, "The probably approximately correct (PAC) and other learning models,"

[97] W. Hoeffding, "Probability inequalities for sums of bounded random variables," *Journal of the American statistical association*, vol. 58, no. 301, pp. 13–30, 1963.

[98] G. Casella and R. L. Berger, *Statistical inference*, vol. 2. Duxbury Pacific Grove, CA, 2002.

[99] N. Kong and L. B. Milstein, "Average SNR of a generalized diversity selection combining scheme," *IEEE Communications Letters*, vol. 3, no. 3, pp. 57–59, 1999.

[100] T. Eng, N. Kong, and L. B. Milstein, "Comparison of diversity combining techniques for rayleigh-fading channels," *IEEE Transactions on communications*, vol. 44, no. 9, pp. 1117–1129, 1996.

[101] K. Iwama, D. Manlove, S. Miyazaki, and Y. Morita, "Stable marriage with incomplete lists and ties," in *ICALP*, vol. 99, pp. 443–452, Springer, 1999.

[102] H. Valizadegan, R. Jin, and S. Wang, "Learning to trade off between exploration and exploitation in multiclass bandit prediction," in *Proceedings of the 17th ACM SIGKDD international conference on Knowledge discovery and data mining*, pp. 204–212, ACM, 2011.

[103] B. Zhou, H. Hu, S. Q. Huang, and H. H. Chen, "Intracluster device-to-device relay algorithm with optimal resource utilization," *IEEE Transactions on Vehicular Technology*, vol. 62, pp. 2315–2326, Jun 2013.

[104] A. Scaglione, D. L. Goeckel, and J. N. Laneman, "Cooperative communications in mobile ad hoc networks," *IEEE Signal Processing Magazine*, vol. 23, pp. 18–29, Sept 2006.